

**Mechanism of carbon monoxide oxidation
at the active site [Ni-4Fe-5S] cluster of
carbon monoxide dehydrogenase from
*Carboxydotherrnus hydrogenoformans***

Dissertation

zur Erlangung des akademischen Grades
Doktor der Naturwissenschaften
- Dr. rer. nat. -
der Fakultät Biologie, Chemie und Geowissenschaften
der Universität Bayreuth

vorgelegt von
Dipl. Ing.
Seung-Wook Ha
aus Uiryeong, Süd-Korea

Bayreuth 2008

Die vorliegende Arbeit wurde am Lehrstuhl für Mikrobiologie der Universität Bayreuth unter der Leitung von PD Dr. Vitali Svetlitchnyi in der Zeit von November 2004 bis September 2008 angefertigt und von der Deutschen Forschungsgemeinschaft gefördert (DFG) (Förderkennzeichen SV10/1-1 and SV10/1-2).

Vollständiger Abdruck der von der Fakultät Biologie, Chemie und Geowissenschaften der Universität Bayreuth genehmigten Dissertation zur Erlangung des Grades eines Doktors der Naturwissenschaften (Dr. rer. nat.).

Promotionsgesuch eingereicht am: 28.10.2008

Tag des wissenschaftlichen Kolloquiums: 04.05.2009

Erster Gutachter: Prof. Dr. Ortwin Meyer

Zweiter Gutachter: Prof. Dr. Stephan Clemens

Voritzender: Prof. Dr. Harold Drake

Dr. Franz X. Schmit

Dr. Paul Rösch

This dissertation is submitted as a “**Cumulative Thesis**” that based on three publications; one printed article and two manuscripts for the submission to international peer-reviewed journals.

In order to clarify the publications, they are listed below.

Chapter 5:

Ha, S.-W., Korbas, M., Klepsch, M., Meyer-Klaucke, W., Meyer, O., and Svetlitchnyi, V. 2007. Interaction of potassium cyanide with the [Ni-4Fe-5S] active site cluster of CO dehydrogenase from *Carboxydothemus hydrogenoformans*. Journal of Biological Chemistry Vol. 282, Issue 14, 10639-10646.

Chapter 6:

Ha, S.-W., Bourenkov, G., M., Meyer-Klaucke, W., Meyer, O., and Svetlitchnyi, V. The [Ni-4Fe-5S] cluster of *Carboxydothemus hydrogenoformans* CO dehydrogenase is biologically relevant.

Manuscript is prepared for the submission to Science.

Chapter 7:

Ha, S.-W., Meyer, O., and Svetlitchnyi, V. Cyanide-induced decomposition of the active site [Ni-4Fe-5S] cluster of CO dehydrogenase from *Carboxydothemus hydrogenoformans* and its functional reconstitution.

Manuscript is prepared for the submission to the Journal of Biological Chemistry.

Declaration of the self-contribution of research articles

This thesis is compiled with three research articles in international peer-reviewed journals. Most of the research work in this thesis was carried out at the Department of Microbiology, University of Bayreuth under the supervision of PD Dr. Vitali Svetlitchnyi (~ Jun 2008) and Prof. Dr. Ortwin Meyer. They contributed support and supervision in all stages of the research, discussion of results and critical comment on the manuscripts. The research was designed by Dr. Svetlitchnyi and myself.

Contribution to the chapter 6:

Most of the research experiments were carried out by myself, including sample preparation for x-ray absorption spectroscopy (XAS) measurement that was done by Dr. Meyer-Klaucke and Dr. Korbas (European Molecular Biology Laboratory (EMBL), Hamburg at Deutsches Elektronen-Synchrotron). I did substantially contribute to the discussion and to the drafting the manuscript. My contribution in this chapter was about 60 %. Miss Mirjam Klepsch, a former diploma student, joined a small experiment under my direct supervision.

Contribution to the chapter 7:

I participated in most part of experiments, including sample preparation for XAS and production of enzyme crystals. XAS and x-ray crystallographic work were done by Dr. Meyer-Klaucke and Dr. Bourenkov (EMBL, Hamburg at Deutsches Elektronen-Synchrotron). I did substantially contribute to the discussion and to the drafting the manuscript. My contribution in this chapter was about 60 %.

Contribution to the chapter 8:

The research was designed by Dr. Svetlitchnyi and myself. I substantially participated in experiments and wrote most part of manuscripts. Miss Mirjam Klepsch, a former diploma student, joined some experiments under my direct supervision. My contribution in this chapter would be about 70 %.

ACKNOWLEDGMENTS

This thesis would have been possible with the help of many people, so I wish to express my gratitude to all of them.

First of all, I would like to thank **Dr. Vitali Svetlitchnyi**, Department of Microbiology, University of Bayreuth, Germany (presently in Moscow), for giving me the opportunity to work out this research. He shared with me a lot of his technical know-how and research insight. Without his ideas, passion, patience, and confidence in me, I would never have accomplished my object.

I want to thank **Prof. Dr. Ortwin Meyer**, Department of Microbiology, University of Bayreuth, for his kind support and for many beneficial discussions. His passion to tackle scientific questions taught me what a scientist could do.

I am grateful to **Dr. Wolfram Meyer-Klaucke**, **Dr. Malgorzata Korbas** and **Dr. Gleb Bourenkov**, EMBL Hamburg at Deutsches Elektronen-Synchrotron, for their excellent joined experimental work, preparation of manuscripts, and friendly cooperation.

I would like to thank all present and former lab members who build up a wonderful and friendly working atmosphere and a help in many aspects: **Astrid Pelzmann**, **Dr. Dilip Gadkari**, **Prof. Franz Meußdoerffer**, **Helga Castorph**, **Dr. Ingo Schmidt**, **Prof. Mikhail Ravinovich**, **Mirjam Klepsch**, **Oliver Kress**, **Stefan Gilch**, **Sven Arnold**, **Tobias Maisel**, and **Ulrike Brandauer**.

A special thanks to **Sven Arnold** and to **Oliver Kress** for great help in German translation and to **Viola Khodaverdi** (Technical University of Berlin) for English corrections.

Further, I thank all my friends and country-mates for inestimable friendship: **Ho-Bin**, **Hyun-Jeong**, **Family Mader**, **Family Otto**, **Family Park**, and **Yang-Min Kim**.

I gratefully thank to German Research funding (DFG) for the generous financial support.

Finally, my special thanks are given to my parents, **Bok-Sik Ha** and **Jeong-Soon Nam**, and my wife, **Eon-Ryeong An**, and my daughters, **Ye-Ji** and **Ye-Chan**, for their understanding, support, and endless and inestimable love.

Many many thanks!!!!

Seung-Wook Ha

Bayreuth, October 2008

CONTENTS

I Detailed Summary

1 Summary	2
1 Zusammenfassung	4
2 Introduction	7
2.1 Life of microbes with carbon monoxide and carbon dioxide	7
2.2 The bacterium <i>Carboxydotherrnus hydrogenoformans</i>	10
2.2.1 General characteristics	10
2.2.2 CODH and ACS in <i>C. hydrogenoformans</i>	10
2.3 Carbon monoxide dehydrogenases (CODHs)	13
2.3.1 Molecular structure of NiFe-CODH _{Ch} from <i>C. hydrogenoformans</i>	13
2.3.2 Molecular structure of CuMo-CODH from <i>Oligotropha carboxidovorans</i>	18
2.4 Modeling of CO oxidation mechanism based on the crystal structure of CODH _{Ch}	20
2.5 Objectives of this research work	23
3 Synopsis	25
3.1 The [Ni-4Fe-5S] cluster C containing bimetallic Ni-(μ_2 S)-Fe1 subsite is the functional active site of native CODH _{Ch}	25
3.2 Interaction of potassium cyanide with cluster C of native CODH _{Ch}	26
3.2.1 Potassium cyanide is a competitive inhibitor of the reduced CODH _{Ch}	26
3.2.2 Cyanide provokes a chemical decomposition of cluster C under oxidizing conditions	29
3.2.3 The inhibition of reduced CODH _{Ch} by cyanide is fully reversible	30
3.2.4 Potassium cyanide interacts with Ni of cluster C	31
3.2.5 Crystal structure of reversibly inhibited CODH _{Ch} confirms the Ni-CN complex in equatorial plane	32
3.3 Sulfide-dependent reformation of the bimetallic Ni-(μ_2 S)-Fe1 subcluster	34
3.4 The fate of μ_2 S in cyanide-induced inhibition and CO oxidation	36

3.5	Why does native CODHII _{Ch} contain the bridging μ_2 S in [Ni-4Fe-5S] cluster C?	37
3.5.1	The μ_2 S enhances the rate of CO oxidation	37
3.5.2	The μ_2 S stabilizes cluster C at high temperature	40
3.5.3	The bridging μ_2 S diminishes the CO ₂ reduction activity	41
3.6	Mechanism of CO oxidation in cluster C of native CODHII _{Ch}	44
3.7	Conclusions	46
4	References	48

II Publications

5	Interaction of potassium cyanide with the [Ni-4Fe-5S] active site cluster of CO dehydrogenase from <i>Carboxydothemus hydrogenoformans</i>	60
6	The [Ni-4Fe-5S] cluster of <i>Carboxydothemus hydrogenoformans</i> CO dehydrogenase is biologically relevant	82
7	Cyanide-induced decomposition of the active site [Ni-4Fe-5S] cluster of CO dehydrogenase from <i>Carboxydothemus hydrogenoformans</i> and its functional reconstitution	114
8	Erklärung	135

I Detailed Summary

1 SUMMARY

The carbon monoxide (CO) metabolism relies on CO-dehydrogenase (CODH) that oxidizes CO with H₂O to CO₂. The crystal structures of the native Ni-Fe CODH_{Ch} from the CO-grown thermophilic hydrogenogenic anaerobic bacterium *Carboxydotherrnus hydrogenoformans* reveal the active site as a [Ni-4Fe-5S] cluster C, carrying a bimetallic Ni-(μ₂S)-Fe1 subsite with a bridging μ₂S. This is the assumed site, where the oxidation of CO occurs. However, cluster C in other catalytically active Ni-Fe CODHs, from *Rhodospirillum rubrum*, *Moorella thermoacetica*, and recombinant CODH_{Ch} expressed in *Escherichia coli*, for example, lack the μ₂S bridging Ni and Fe and contain a [Ni-4Fe-4S] form of a cluster C. The CO oxidation mechanism proposed based on crystallographical and biochemical studies involved the apical binding of CO at the nickel ion and the activation of water at the Fe1 ion of the cluster. In order to understand how CO interacts with the active site of native CODH_{Ch} and what function does the bridging μ₂S ligand fulfill in the enzyme, this research work focuses (i) on the interaction of cluster C with CO analogue potassium cyanide and analysis of the resulting type of nickel coordination and (ii) on the effect of sodium sulfide on the enzymatic activities of the native CODH_{Ch}.

Under catalytic conditions, cyanide acts as a competitive inhibitor of CODH_{Ch} with respect to CO. Under N₂ gas phase without electron acceptor (non-catalytic conditions), cyanide inhibits CODH_{Ch} at highly reduced state (low redox-potentials ~ -500 mV), not at oxidized and slightly reduced (~ -320 mV) states. Cyanide is not able to inhibit CODH_{Ch} at reduced conditions (-500 mV) when CO is present in the atmosphere. Therefore, the interaction of cyanide with reduced active site is expected to mimic the substrate.

The binding of cyanide to the nickel ion has been discovered by x-ray absorption spectroscopy and confirmed by x-ray crystallography at the atomic resolution. This structure comprises an intermediate state of cluster C with CO in NiFe-CODH_{Ch}. In this reaction, cyanide displaces the μ₂S ligand giving rise to square-planar Ni with three S and one CN ligands. Cluster C and its protein environment undergo significant conformational changes induced by the binding of cyanide. Remarkably, Fe1 is

displaced by 1.1 Å, which reduces the Fe1 to Ni distance by 0.1 Å. Electron densities of the CN ligand estimate an occupancy of 80 % and N atom of cyanide is in hydrogen bonding distance to His⁹³ and Lys⁵⁶³, which are involved in proton transfer network.

The binding of cyanide eliminates the bridging $\mu_2\text{S}$ from the cluster C yielding H_2S , whereas the Ni-($\mu_2\text{S}$)-Fe1 bridge is reformed after the catalytic cycle. It is likely that the high rate of CO oxidation (K_{cat}/K_m of $1.7 \cdot 10^9 \text{ M}^{-1} \text{ s}^{-1}$ at 70 °C) and subsequent rebinding of $\mu_2\text{S}$ would prevent the release of this ion from the protein by diffusion-controlled process (10^8 to $10^9 \text{ M}^{-1} \text{ s}^{-1}$).

Cyanide-inhibited reduced CODHII_{Ch} is fully reactivated after the release of cyanide upon incubation at 70 °C in the presence of low-potential reductants. The square-planar NiS₄-coordinated cluster C is recovered by reactivation with sulfide, resulting in fully active enzyme, which includes the reformation of the Ni-($\mu_2\text{S}$)-Fe1 bridge. Reactivation in the absence of sulfide generates the NiS₃-coordination, lacking the $\mu_2\text{S}$ ligand, and results in partially active enzyme.

NiS₃-coordinated cluster C is readily converted to NiS₄-conformation by incorporation of sulfide. This conversion results in an increase of CO oxidation activity and a stabilization of cluster C at growth temperatures of the bacterium. In addition, the NiS₄-conformation displays better catalytic efficiency (K_{cat}/K_m) than NiS₃ under low concentrations of CO. Inhibition of CO₂ reduction activity by sulfide and higher CO₂ reduction activity of NiS₃-conformation suggest that the $\mu_2\text{S}$ ligand retards the binding of CO₂ to Ni. The crystal structure of CO₂ loaded NiS₃-cluster further convinces this assumption.

The $\mu_2\text{S}$ ligand accelerates the physiologically relevant CO oxidation, prevents inhibition by the product CO₂, and inhibits a non-physiological CO₂ reduction. These functions of the bridging $\mu_2\text{S}$ are of physiological importance for the metabolism of *C. hydrogenoformans* in highly reducing, CO-limited, and CO₂-rich volcanic environments. Thus, it is concluded that the [Ni-4Fe-5S]-form of cluster C is the biologically relevant species in CODHII_{Ch}.

A CO oxidation mechanism developed in this thesis is based on the structures of cyanide-bound intermediated state and CO₂-bound state, as well as on the kinetic data on the reactivity of the enzyme with CO, potassium cyanide and sodium sulfide.

1 ZUSAMMENFASSUNG

Der Kohlenstoffmetabolismus ist angewiesen auf Kohlenmonoxid (CO)–Dehydrogenasen (CODH), welche die Oxidation von CO mit H₂O zu CO₂ katalysieren. Die Kristallstruktur der Ni–Fe CODH_{Ch}, isoliert aus CO gewachsenen Zellen des thermophilen hydrogenogenen anaeroben Bakteriums *Carboxydotherrnus hydrogeniformans*, besitzt ein [Ni-4Fe-5S]–Cluster C im aktiven Zentrum, welches während der Oxidation von CO eine bimetallische Ni-(μ₂S)-FeI Form annimmt. Dem Cluster C anderer aktiver Ni–Fe CODH's, z.B. aus *Rhodospirillum rubrum* (CODH_{Rr}), *Moorella thermoacetica* (CODH_{Mt}), und rekombinanter, in *Escherichia coli* exprimierter CODH_{Ch}, fehlt der Ni und Fe überbrückende μ₂S, so dass das aktive Zentrum als [Ni-4Fe-4S]–Cluster C vorliegt. Die auf der Basis von Analysen der Kristallstruktur und biochemischen Studien vorgeschlagenen Mechanismen der CO Oxidation beinhalten die apikale Bindung von CO am Ni Ion und die Aktivierung von Wasser am FeI Ion des Clusters.

Um zu verstehen, wie CO mit dem aktiven Zentrum der nativen CODH_{Ch} interagiert und welche Funktion der verbrückende μ₂S Ligand im Enzym erfüllt, konzentriert sich die vorliegende Studie (i) auf die Interaktion von Cluster C mit dem CO Analogon Cyanid und der Analyse der daraus resultierenden Koordination des Nickels und (ii) auf die Auswirkung von Natriumsulfid auf die enzymatische Aktivität der nativen CODH_{Ch}.

Unter katalytischen Bedingungen reagiert Cyanid als ein kompetitiver Inhibitor von CO in CODH_{Ch}. Bei stark niedrigem Redoxpotential (–500 mV, N₂-Atmosphäre ohne Elektronenakzeptor: nicht-katalytische Bedingungen) inhibiert Cyanid die CODH_{Ch}. Cyanid wirkt unter oxidierenden oder leicht reduzierenden Bedingungen (~ –320 mV) nicht als Inhibitor. Bei stark niedrigem Redoxpotential (–500 mV) kann Cyanid die CODH_{Ch} nicht inhibieren, wenn gleichzeitig CO vorhanden ist. Hieraus lässt sich ableiten, dass Cyanid das Substrat nachahmt, wenn es mit dem reduzierten aktiven Zentrum interagiert.

Die Bindung von Cyanid am Ni Ion wurde durch den Einsatz Röntgenabsorptionsspektroskopie aufgeklärt und durch Röntgenkristallographie bei

atomarer Auflösung bestätigt. Die Struktur zeigt einen intermediären Zustand von Cluster C mit CO in NiFe-CODHII_{Ch}. In dieser Reaktion ersetzt Cyanid den μ_2 S Ligand, was zu einem quadratisch-planaren Nickel mit drei S und einem CN Liganden führt. Cluster C und seine Proteinumgebung werden durch die Bindung von Cyanid signifikant verändert. Bemerkenswert ist, dass sich Fe1 um 1,1 Å verlagert, was den Abstand von Nickel zu Fe1 um 0,1 Å verkürzt. Die Elektronendichte am CN Liganden lässt eine 80 %ige Besetzung vermuten und das N Atom von CN befindet sich Wasserstoffbrückenbindungsdistanz zu His⁹³ und Lys⁵⁶³, welche im Protonentransfernetzwerk involviert sind.

Die Bindung von Cyanid entfernt den verbrückenden μ_2 S vom Cluster C und es entsteht H₂S, wobei die Ni-(μ_2 S)-Fe1 Brücke nach dem katalytischem Zyklus wieder hergestellt wird. Es ist wahrscheinlich, dass die hohe CO Oxidationsrate (K_{cat}/K_m von $1.7 \cdot 10^9 \text{ M}^{-1} \text{ s}^{-1}$ bei 70 °C) und die Bindung des μ_2 S den Verlust von Sulfid durch Kontrolle des Diffusionsprozesses (10^8 to $10^9 \text{ M}^{-1} \text{ s}^{-1}$) verhindern.

Die Inhibition von reduzierter CODHII_{Ch} wird durch die Freisetzung von Cyanid bei 70 °C in der Gegenwart von schwachen Reduktionsmitteln vollständig aufgehoben. Das quadratisch-planare NiS₄-koordinierte Cluster C wird durch die Reaktivierung mit Sulfid wieder vollständig hergestellt. Die Wiederherstellung der Ni-(μ_2 S)-Fe1 Brücke führt zu einem vollständig aktiven Enzym. Im Falle des Verlusts von einem Schwefelatom wird eine NiS₃-Koordination und damit ein teilweise aktives Enzym generiert.

Ein NiS₃-koordiniertes Cluster C wird durch Inkorporation von Sulfid leicht in eine NiS₄-Koordination überführt. Dies führt zu einer Aktivierung der CO Oxidationsaktivität und zur Stabilisierung des Clusters. Zusätzlich zeigt das NiS₄-Cluster C bei niedrigen CO Konzentrationen eine höhere katalytische Effizienz (K_{cat}/K_m) als das NiS₃-Cluster C. Die Inhibition der CO₂ Reduktionsaktivität (Rückreaktion) durch Sulfid und die höhere CO₂ Reduktionsaktivität der NiS₃-Konformation lassen vermuten, dass die Bindung von CO₂ am Ni durch den μ_2 S Ligand gestört wird. Diese Vermutung wird die Kristallstruktur des CO₂ gebundenen NiS₃-Cluster C bestätigt.

Der μ_2 S Ligand beschleunigt die physiologisch relevante CO Oxidation, verhindert die Inhibition durch das Produkt CO₂ und inhibiert damit die nicht

physiologische CO₂ Reduktion. Diese Funktionen des verbrückenden $\mu_2\text{S}$ ist für den Stoffwechsel von *C. hydrogenoformans* in einer stark reduzierten, CO limitierten und CO₂ reichen vulkanischen Umgebung physiologisch wichtig. Daraus kann abgeleitet werden, dass die [Ni-4Fe-5S]-Form von Cluster C die biologisch relevante Form von CODHII_{Ch} darstellt.

Ein im Rahmen dieser Arbeit entwickelter Mechanismus der CO Oxidation basiert auf der Struktur des Cyanid und des CO₂ gebundenen Zustands von Cluster C sowie auf kinetischen Daten.

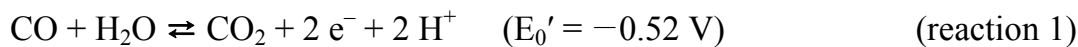
2 INTRODUCTION

2.1 Life of microbes with carbon monoxide and carbon dioxide

The energy is the most important matter in all organisms to do work and to sustain life. In chemotrophs, energy is generated by oxidation of energy-rich inorganic and organic compounds and the energy generation process involves the transfer of electrons produced by oxidation to a suitable electron acceptor, e.g. oxygen, carbon dioxide, nitrate, protons, etc.

Carbon monoxide (CO) is one of the energy-conserving carbon matters and it can be produced from incomplete combustion of carbon containing organic material under limited oxygen supply. CO is an extremely toxic, tasteless, odorless, and colorless gas (Omaye 2002). In terms of chemistry, CO is characterized by both a π acceptor and a σ donor for transition metals in lower oxidation states due to a small dipole moment with its negative end on the carbon atom (Ragsdale 2004; Crabtree 1988). CO, thus, can form a strong ligand to metal centers in metalloproteins, e.g. hemoglobin and myoglobin (Alonso et al. 2002; Haldane 1895; Omaye 2002). Nevertheless, the utilization and interconversion of CO is a central metabolic feature of some specialized groups of microorganisms, especially aerobic carboxidotrophic bacteria and anaerobic hydrogenogenic, acetogenic, methanogenic, sulfidogenic, phototrophic bacteria and archaea (Ferry 1995; Lindahl 2002; Meyer *et al.* 2000; Mörsdorf *et al.* 1992; Ragsdale 2004; Yagi and Tamiya 1962). Most of the 10^9 tons of CO entering the atmosphere of the Earth per year originate from human activities (Khalil and Rasmussen 1984) and every year approximately 10^8 tons of CO is eliminated from the lower atmosphere of the Earth by microbial CO metabolism (Bartholomew and Alexander 1979). Notably, the aerobic carboxidotrophic microbes are suited for lowering the concentration of CO in the atmosphere and maintain this toxic gas at a subhazardous level because they a high propensity for CO uptake with a very low K_m values (as low as 0.6 μM) (Meyer *et al.* 1993).

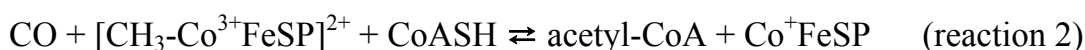
The oxidation of CO with H₂O is catalyzed by CO dehydrogenase (CODH), yielding CO₂, 2e⁻, and 2H⁺ according to the reaction:



Anaerobic CODH also carries out the reverse reaction of CO₂ reduction with the formation of CO (Kumar *et al.* 1994; Lindahl *et al.* 1990A).

CO₂ is a greenhouse gas that directly relates to global warming and is present in the largest amount among the carbon-containing atmospheric gases (Ragsdale 2007). It is normally emitted as a product of aerobic metabolism from all animals, plants and microorganisms. A nearly equal amount of produced CO₂ is consumed by plants and microbes again, called CO₂-fixation (approx. 10¹¹ tons of CO₂ every year) (Ragsdale 2007). There are four different pathways to incorporate CO₂ into organic compounds: Calvin-Benson-Bassham cycle (also termed Calvin cycle) (Bassham *et al.* 1950), reductive TCA cycle (tricarboxylic acid cycle) (Evans *et al.* 1966; Shiba *et al.* 1985), 3-hydroxypropionate cycle (Holo 1989; Klatt *et al.* 2007; Strauss and Fuchs 1993), and reductive acetyl-CoA pathway (Fig. 1) (also termed Wood-Ljungdahl pathway) (Ljungdahl 1986, 1994; Ragsdale 1997).

The Calvin-Benson-Bassham cycle is known as major pathway for CO₂ fixation, especially in plants. The Calvin cycle is also adopted for the CO₂ fixation in CO-utilizing carboxidotrophic bacteria (Mörsdorf *et al.* 1992; Meyer *et al.* 1993) and in CO-dependent hydrogenogenic phototrophs (Ferry 1995), whereas anaerobic bacteria and archaea such as acetogens and methanogens employ the reductive acetyl-CoA pathway. In autotrophic microorganisms employing the reductive acetyl-CoA pathway, synthesis of acetyl-CoA from CO, a methyl group and coenzyme A (CoA) is catalyzed by acetyl-CoA synthase (ACS) according to the reaction (Ragsdale and Wood 1985):



Here, CO is delivered either from the reduction of CO₂ by CODH (reaction 1) or from external CO supplied as the growth substrate. CH₃-CoFeSP indicates a methylated corrinoid Fe-S protein, which donates a methyl group to ACS (Poston *et al.* 1964;

Ljungdahl *et al.* 1965). Thus, the biological activities of these microorganisms play a crucial role in the global carbon cycle (Ferry 1995; Lindahl 2002; Meyer *et al.* 2000; Mörsdorf *et al.* 1992; Ragsdale 2004).

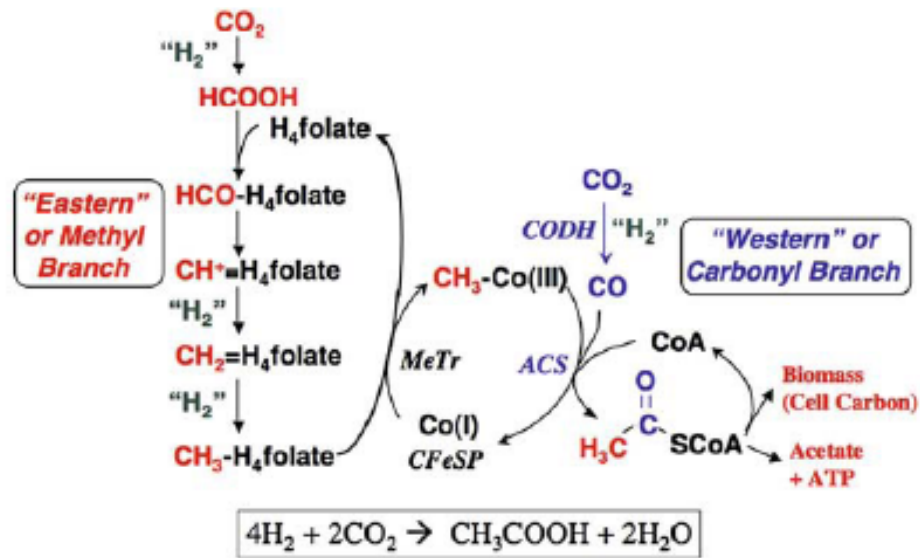


Fig. 1. Wood-Ljungdahl pathway for CO₂ fixation in acetogenic bacteria (Ragsdale and Pierce 2008). The carbonyl branch is operated by CODH in a complex of CODH/ACS and [Co] Protein indicates corrinoid Fe-S protein that donates methyl group to ACS. In the case of *Carboxydotherrmus hydrogenoformans*, this reductive acetyl-Co A pathway is operated without carbonyl branch when the cells are grown under excess of CO (Svetlichnyi *et al.* 2001; Arnold 2006).

2.2 The bacterium *Carboxydothemus hydrogenoformans*

2.2.1 General characteristics

The CO-utilizing bacterium “*Carboxydothemus hydrogenoformans* Z-2901” (DSM 6008) was isolated from volcanic habitats of Kunashir Island (Russian Federation) and the terms of “hydrogenogenic,” “hydrogenogens,” and “hydrogenogenesis” reflect the type of metabolism, the physiological group, and the H₂ formation process of this bacterium, respectively (Svetlitchnyi *et al.* 1991; 2001).

C. hydrogenoformans is a Gram-positive, strictly anaerobic, and thermophilic bacterium with a growth optimum at 70–72 °C (Svetlitchnyi *et al.* 1991A, B). The bacterium is able to grow chemolithoautotrophically on CO as the sole source of carbon and energy with the production of equimolar quantities of H₂ as ultimate fermentation product (Svetlitchnyi *et al.* 1991A, B).

C. hydrogenoformans does not possess complete sets of genes encoding sugar-compound degradation pathways and sugar phosphotransferase systems (PTS) in the genome (size of 2.4 Mbp), suggesting features related to an autotrophic lifestyle (Wu *et al.* 2005). However, *C. hydrogenoformans* is able to grow on pyruvate under anaerobic conditions without CO, producing H₂, CO₂, and acetate (Svetlitchnyi *et al.* 1994). It is also able to grow on formate, lactate, glycerol, and H₂ but only in the presence of 9,10-anthraquinone-2,6-disulfonate (AQDS) as electron acceptor (Henstra *et al.* 2004), which agrees with the predictions about heterotrophic capabilities of *C. hydrogenoformans* (Wu *et al.* 2005).

2.2.2 CODH and ACS in *C. hydrogenoformans*

Nearly one third of all known enzymes are metalloenzymes that require the presence of metal ions, most commonly transition metal ions like Fe^{2+/3+}, Cu²⁺, Zn²⁺, or Ni²⁺, for the catalytic activity (Ragsdale 2006; Voet and Voet 1995). The metal ions participate in a variety of catalytic processes and promote the reactions, including mediation of oxidation-reduction reactions e.g. electron transfer through reversible

changes of the metal ion's oxidation state, charge shielding, radical chemistry, etc (Ragsdale 2006; Voet and Voet 1995).

In *C. hydrogenoformans* two essential metalloenzymes, nickel containing CODH_{Ch} and ACS_{Ch}, allow the bacterium to utilize and interconvert CO (Svetlitchnyi *et al.* 2001, 2004). The oxidation of CO (reaction 1) in the bacterium is coupled to the reduction of protons to H₂ ($E_0' = -0.41$ V) in energy-conserving reaction $\text{CO} + \text{H}_2\text{O} \rightarrow \text{CO}_2 + \text{H}_2$ ($\Delta G^{0'} = -20$ kJ mol⁻¹) (Svetlitchnyi *et al.* 1991A, B).

ACS_{Ch} plays a crucial role in carbon assimilation to cell materials under autotrophic growth condition with CO (Svetlitchnyi *et al.* 2004). Under CO limitation, ACS_{Ch} is found as a complex with CODHIII_{Ch}, which mainly catalyzes reduction of CO₂ to provide CO for acetyl-CoA synthesis (Svetlitchnyi *et al.* 2004). In contrast, ACS_{Ch} does not form a complex with CODHIII_{Ch} and is expressed as a monomer when sufficient CO is supplied (Svetlitchnyi *et al.* 2004).

The complete genome sequence indicates that *C. hydrogenoformans* possesses five distinct genes coding for CODHs which are referred to as CODHI-V_{Ch} (Wu *et al.* 2005). It is expected that CODHI_{Ch} is involved in energy conservation because the genes coding for CODHI_{Ch}, a ferredoxin-like electron acceptor protein called CooF, and a proton-reducing energy-conserving hydrogenase are clustered on the genome. CODHII_{Ch} plays a role in NADPH generation and the genes codes for CODHII_{Ch} and CooF are independently located from the gene cluster of hydrogenase. CODHIII_{Ch} participates in carbon fixation process since the gene cluster contains both, the CODHIII_{Ch} and the ACS_{Ch} encoding gene. CODHIV_{Ch} is proposed to respond oxidative stress and a function of CODHV_{Ch} is not yet known (Wu *et al.* 2005).

CODHI_{Ch} and CODHII_{Ch} have been purified and their biochemical characteristics have been documented precisely (Svetlitchnyi *et al.* 2001). Both enzymes catalyze the same reaction of reversible CO oxidation with similar catalytic activities. They are membrane associated proteins, have the same isoelectric point of 5.5, and display identical UV-visible absorption and electron paramagnetic resonance (EPR) spectra. Both CODHs, however, differ slightly in the molecular masses of their subunits, CODH I (holoenzyme, 137.0kDa; protein subunit, 67.5kD) and CODH II (holoenzyme, 136.6kD; protein subunit, 67.3kD), primary sequences peptide maps, and

immunological reactivity (Svetlitchnyi *et al.* 2001). During CO oxidation, CODHI_{Ch} generates electrons that are subsequently transferred via the ferredoxin-like electron acceptor protein CooF to a membrane-bound complex I-related H₂ evolving hydrogenase that is the suggested site where protons are reduced to H₂. Accordingly, the catalytic action of CODHI_{Ch} is coupled to the energy conservation (Fig. 2) (Gerhardt *et al.* 1991; Svetlitchnyi *et al.* 1991; Svetlitchnyi *et al.* 2001; Soboh *et al.* 2002). In agreement with CO-dependent reduction of NADP⁺ to NADPH/H⁺ in acetogenic bacteria (Hugenholtz *et al.* 1989; Ragsdale *et al.* 1983), it is likely that CODHII_{Ch} participates in carbon assimilation with generation of reducing power, NADPH, in the presence of cytoplasmic coupling factor X⁺/XH that could be a ferredoxin:NADP⁺ oxidoreductase (Fig. 2) (Svetlitchnyi *et al.* 2001).

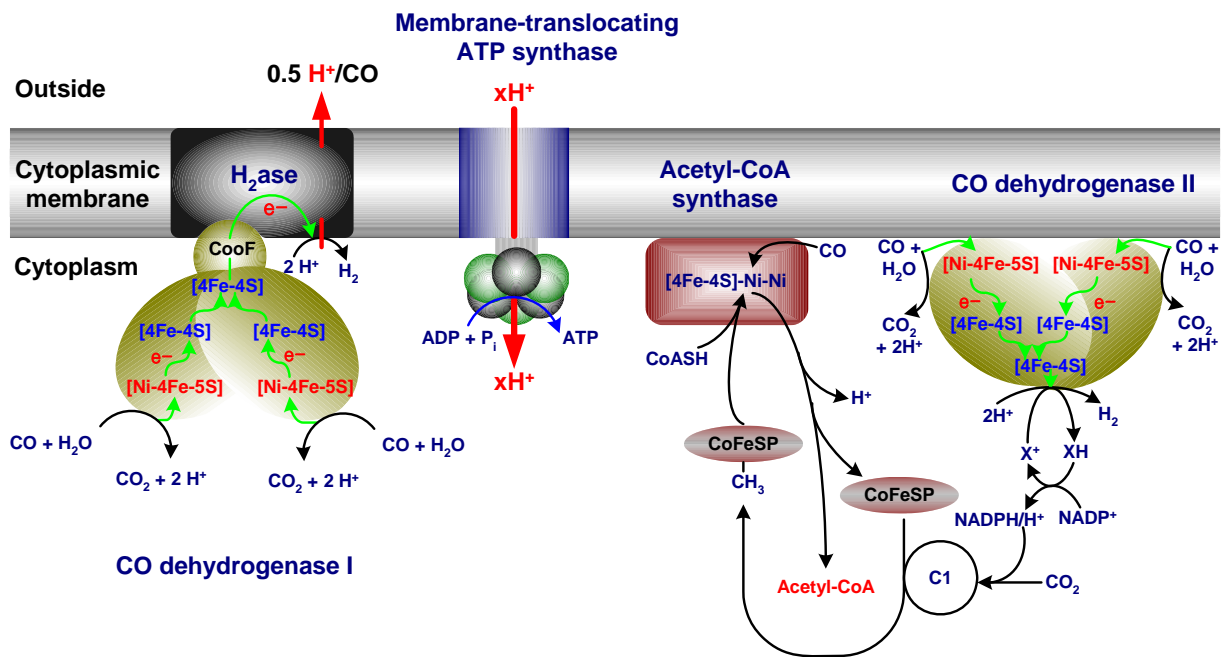


Fig. 2. Schematic representation of the functions of CODHI_{Ch}, CODHII_{Ch} and the monomeric acetyl-CoA synthase in CO-dependent hydrogenogenesis of *C. hydrogeniformans*. CooF, ferredoxin-like protein; H₂ase, membrane-bound complex I-related hydrogenase; CoFeSP, corrinoid iron-sulfur protein; C1, methyl branch of the reductive acetyl-CoA pathway (modified from Svetlitchnyi *et al.* 2001; 2004).

2.3 Carbon monoxide dehydrogenases

2.3.1 Molecular structure of NiFe-CODH_{Ch} from *C. hydrogenoformans*

Oxygen sensitive CODH that contain Ni and Fe ions in their active site was obtained in 1980 from the anaerobic acetogenic bacterium *Moorella thermoacetica* (Drake *et al.* 1980).

Based on the catalytic activities and metabolic functions, two types of NiFe-CODHs have been reported so far. First type is a heterotetrameric ($\alpha_2\beta_2$) bifunctional CODH employed in methanogens, acetogens, and sulfidogens (Drake *et al.* 1980; Grahame and Stadtman 1987; Ragsdale 2004). The bifunctional CODH is naturally found as a tight complex with ACS and catalyzes the reduction of CO₂ to CO rather than oxidation of CO for autotrophic carbon assimilation (Ferry 1995; Lindahl 2002; Ragsdale and Kumar 1996; Ragsdale 2004). Second type is a homodimeric (α_2) monofunctional CODH, which is found in the hydrogenogenic bacterium *C. hydrogenoformans* (Svetlitchnyi *et al.* 2001) and phototrophic bacterium *Rhodospirillum rubrum* (Bonam *et al.* 1984). In contrast to bifunctional CODH in the complex, monofunctional CODH mainly catalyzes the oxidation of CO to CO₂ and is involved in energy conservation.

The first crystal structure of anaerobic NiFe-CODH_{Ch} from *C. hydrogenoformans* was solved in 2001 (Fig. 3) (Dobbek *et al.* 2001).

Overall structure

The CODH_{Ch} is a mushroom-shaped homodimer containing five metal clusters (Fig. 3A and C) and each subunit (67.3 kDa) contains an asymmetrical [Ni-4Fe-5S] cluster C representing the active site along with a conventional cubane-type [4Fe-4S] cluster B. Each [Ni-4Fe-5S] cluster C contains an inorganic μ_2 S bridge between Ni and Fe1 forming a heterobimetallic Ni-(μ_2 S)-Fe1 subcluster. Additional cubane-type [4Fe-4S] cluster D is bound at the subunit interface and covalently links the two subunits (Dobbek *et al.* 2001). Additional crystal structures of the monofunctional CODH_{Rt} from *R. rubrum* (Drennan *et al.* 2001) as well as of the bifunctional ACS_{Mt}/CODH_{Mt}

from *M. thermoacetica* (Doukov *et al.* 2002; Darnault *et al.* 2003) reveal an equivalent structure of CODHII_{Ch} with a [Ni-4Fe-4S] cluster C lacking the bridging μ_2 S (Fig. 4).

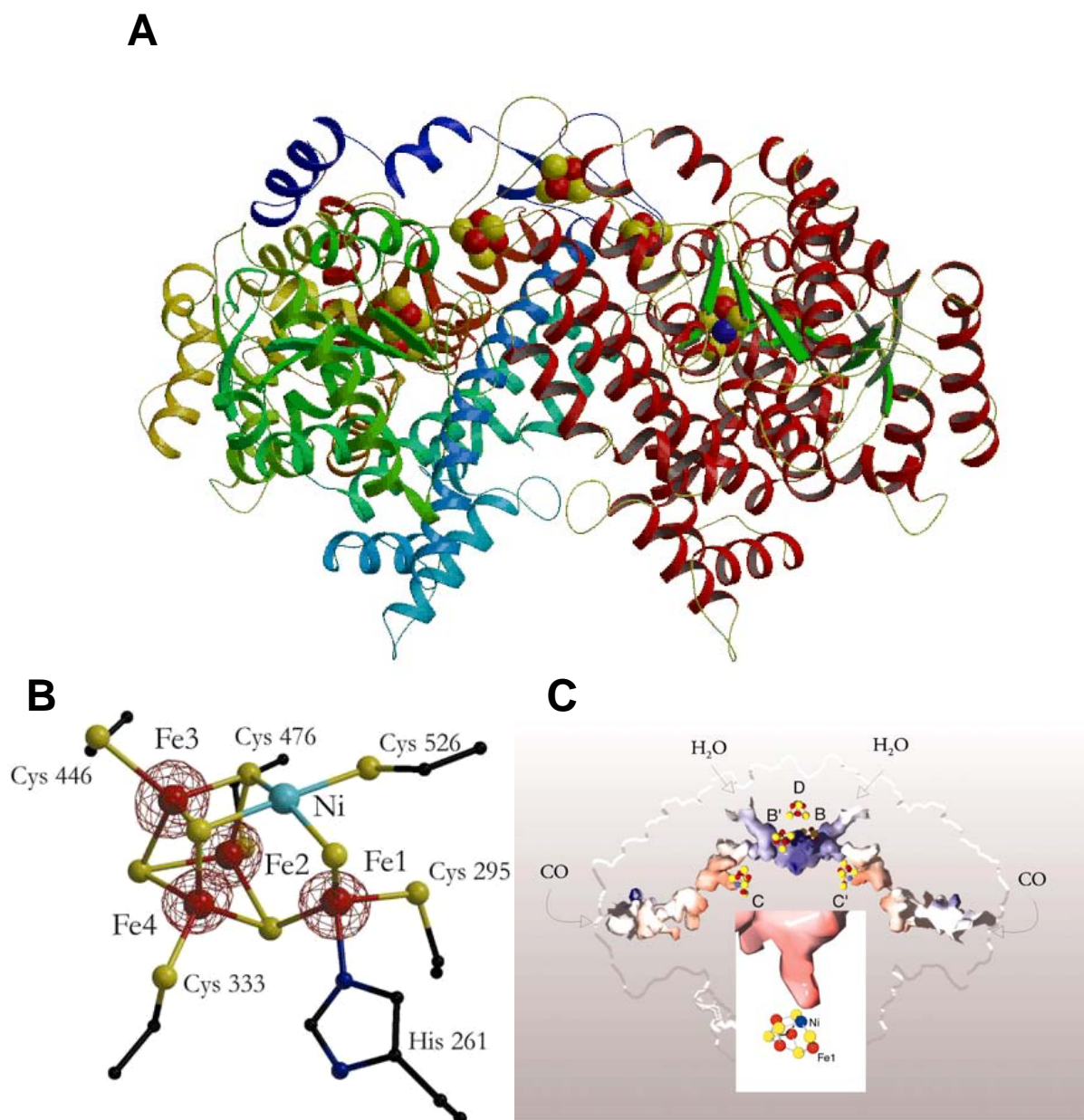


Fig. 3. Crystal structure of the CODHII_{Ch} from *C. hydrogeniformans* (Dobbek *et al.* 2001). (A) Overall structure of dimer. The subunit is colored from blue at the NH₂-terminus via green through yellow to red at its COOH-terminus and is colored with red for α helices and green for β sheets. (B) Structure of active site cluster C. Fe atom colored in red, S atom in yellow, Ni atom in cyan, N atom in blue, and C atom in black. (C) Putative substrate and water channel ranging through the dimer of CODHII_{Ch}. A branch of the channel depicted in the inset ends at cluster C directly above the apical coordination site of the Ni ion. Arrows mark the potential entrances for the substrates CO and H₂O.

Active site cluster C

Cluster C of NiFe-CODHs had been already proposed as the reaction center of CO oxidation based on extensive biochemical studies and various spectroscopic techniques (Kumar *et al.* 1993; Tan *et al.* 1992; Lindahl *et al.* 1990; DeRose *et al.* 1998). Initially, the cluster C was considered to be a cubane-type [4Fe-4S] cluster linked to a Ni ion that was predicted to be five-coordinate through a single bridging atom (Hu *et al.* 1996; Ragsdale and Kumar 1996). However, the structure of cluster C (Fig. 3B) was rather unexpected (Dobbek *et al.* 2001) because it had no precedent in either biology or chemistry. Cluster C contains one Ni atom, four Fe atoms, and five (CODH_{Ch}) or four (CODH_{Rr} and CODH_{Mt}) labile sulfur atoms which are arranged as an asymmetrical heteronuclear [Ni-4Fe-5S] cluster or [Ni-4Fe-4S] cluster (Fig. 4) (Darnault *et al.* 2003; Dobbek *et al.* 2001; Doukov *et al.* 2002; Drennan *et al.* 2001).

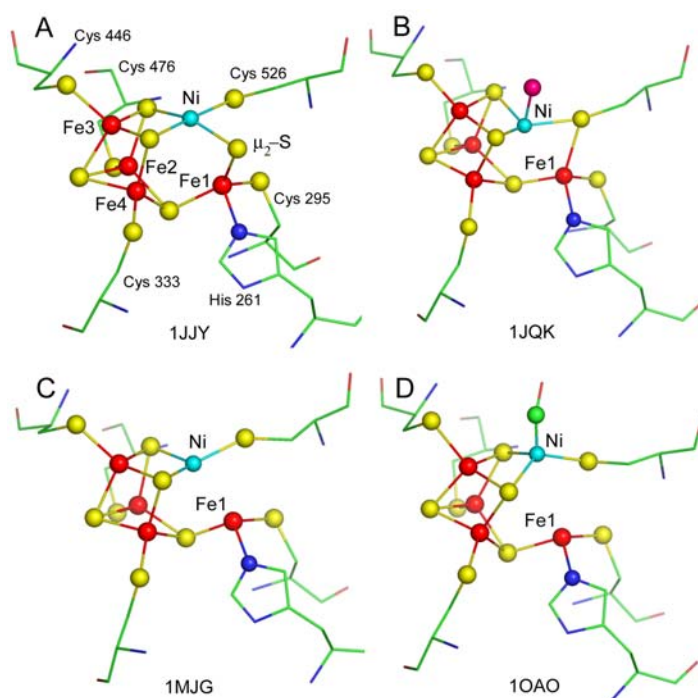


Fig. 4. Four models, which have been proposed for cluster C (Dobbek *et al.* 2004). (A) The [Ni-4Fe-5S] cluster of CODH_{Ch} at a resolution of 1.63 Å. (B) The 2.8 Å structure of cluster C in the CODH_{Rr}, interpreted as an [Ni-4Fe-4S] cluster. An additional ligand of unknown nature has been modeled in the apical coordination site at the Ni ion. (C) Cluster C in the 2.2 Å structure of CODH_{Mt}. (D) Cluster C in the 1.9 Å structure of CODH_{Mt} with a CO ligand modeled in the apical coordination site of Ni. Ni atom colored in cyan, Fe atom in red, S atom in yellow, and N atom in blue.

The metal ions of the cluster are covalently bound to the protein by five cysteine residues (Cys²⁹⁵, Cys³³³, Cys⁴⁴⁶, Cys⁴⁷⁶, Cys⁵²⁶; numbering is based on the CODHII_{Ch} sequence) and one histidine residue (His²⁶¹) (Dobbek *et al.* 2001).

The Ni-ion is coordinated by four sulfur atoms including one labile μ_2 S which bridge Ni and Fe1, two inorganic μ_3 S, and a cystein sulfur (Fig. 3B and 4A) and lies approximately 0.3 Å above the center of the plane spanned by its four ligands (Dobbek *et al.* 2001). A diamagnetic EPR silent in all oxidation states of CODHII_{Ch} indicates that the Ni ion is in the oxidation state of 2+ (Svetlitchnyi *et al.* 2001).

Biochemical, spectroscopic, sequence, and structural data support that all known NiFe-CODHs from anaerobic bacteria and archaea essentially use the same metal clusters for the CO/CO₂ redox chemistry reaction. It has been reported that cluster C exists in four redox states: C_{ox}, C_{red1}, C_{int}, and C_{red2} (Lindahl *et al.* 1990; Anderson *et al.* 1996; Fraser *et al.* 1999). Under oxidizing conditions ($E^\circ \sim 50$ mV vs NHE), cluster C is EPR silent diamagnetic C_{ox} state and appears not to be involved in CO/CO₂ redox catalysis.

The diamagnetic C_{ox} is converted to the paramagnetic $S = \frac{1}{2}$ C_{red1} state by reduction of one electron and this state exhibits an EPR signal with a g_{av} of 1.82 in CODH_{Mt} (Lindahl *et al.* 1990) and with a g_{av} of 1.87 in CODH_{Rf} (Bonam and Ludden 1987). The midpoint potential for the C_{ox}/C_{red1} couple is about -220 mV for CODH_{Mt} (Lindahl *et al.* 1990) and about -110 mV for CODH_{Rf} (Spangler *et al.* 1996). Further reduction with CO leads to the conversion of C_{red1} to C_{red2} in accordance with an E° of -520 mV at pH 7.0. This state can be also reached by reduction with low-potential reductants like dithionite or Ti(III) citrate (Lindahl *et al.* 1990; Russell *et al.* 1998; Hu *et al.* 1996). C_{red2} also exhibits an EPR signal with a g_{av} of 1.86 in CODH_{Mt} and CODH_{Rf} (Hu *et al.* 1996; Russell *et al.* 1998) and a g_{av} of 1.86 and 1.84 in CODHI_{Ch} and CODHII_{Ch}, respectively (Svetlitchnyi *et al.* 2001). Since C_{red1} disappears at the rate that C_{red2} is formed, the C_{red1} appears to be the state that reacts with CO (Kumar *et al.* 1993), but interaction of CO with the cluster C at the C_{red2} state is evident (Seravalli *et al.* 1997).

A dimer-spanning channel grants accessibility of the active site for the two substrates CO and water (Dobbek *et al.* 2001). There are two channels just above the

Ni site (Fig. 3C). One is a hydrophobic channel that ends directly above the open coordination of Ni at the active site and the other is a hydrophilic channel that is connected to a large water filled basin at the dimer interface near clusters B, B', and D (Dobbek *et al.* 2001; Drennan *et al.* 2001).

Networks for Electron and proton transfer

Oxidation of CO is coupled to the reduction of two electrons, in one-electron steps, of the external electron acceptor. The distance of 33 Å between each cluster C in the homodimer indicates that each active center carries out the catalysis independently. Electrons are transferred through two separate branches, since the distance of 28 Å between cluster C (C') and B (B') and 23 Å between cluster C and D are too long to transfer electrons effectively within the same subunit (Dobbek *et al.* 2001; Lindahl 2002; Ragsdale 2004). Thus, electrons produced from the CO oxidation at cluster C travel via cluster B' that acts as an electron mediator to cluster D that can easily transfer electrons to an external redox protein, which is exposed to the solvent (Dobbek *et al.* 2001; Ragsdale 2004).

Several basic amino acid residues, including Lys⁵⁶³ and four semi-conserved His residues (93, 96, 99, and 102; numbering is based on the CODH_{Ch} sequence) near the cluster C were proposed to participate in the acid-base chemistry in CO oxidation, especially deprotonation. These histidine residues are located on sequential turns of a helix, forming a His-tunnel that is proposed to deliver protons liberated during the CO oxidation (Dobbek *et al.* 2001; Drennan *et al.* 2001). This proposal agrees with studies of CODH_{Mt} mutants on the histidine residues that result in nearly abolished catalytic activity of CODH_{Mt}. EPR spectra of the mutants indicate that these proteins are properly folded and contain the complete set of metal centers found in wild type CODH_{Mt} (Fig. 5) (Kim *et al.* 2004).

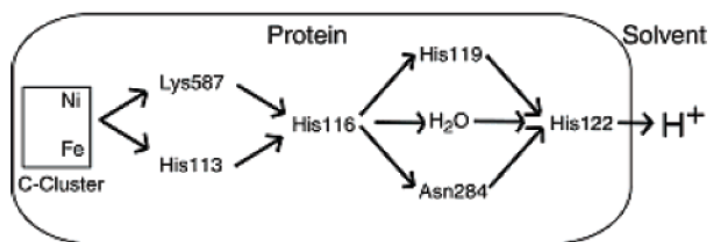


Fig. 5. Proton transfer network. Proposed proton network in CODH_{Mt}. The numbering is based on the *M. thermoacetica* sequence (Kim *et al.* 2004).

Lys⁵⁸⁷, His¹¹³, His¹¹⁶, His¹¹⁹, Asn²⁸⁴, and His¹¹² correspond to Lys⁵⁶³, His⁹³, His⁹⁶, His⁹⁹, Asn²⁶³, and His¹⁰² for *C. hydrogenoformans*, respectively.

2.3.2 Molecular structure of CuMo-CODH from *Oligotropha carboxidovorans*

Oxygen stable CODH that carries Cu and Mo ions in its active site was purified in 1980 from the aerobic carboxidotrophic bacterium *Oligotropha carboxidovorans* (Meyer and Schlegel 1980).

The aerobic CODH_{Oc} from *O. carboxidovorans* is composed of a dimer of heterotrimers ((LMS)₂) (Fig. 6A) (Dobbek *et al.* 1999, 2002; Meyer *et al.* 1986). The L-subunit (88.7 kDa) carries the active site (Fig. 6B) that contains a bimetallic Cu linked to the molybdenum cofactor (Cu-S-Mo(=O)OH), which is a mononuclear complex of Mo and molybdopterin-cytosine dinucleotide (MCD). Initially, it was postulated that Mo is the active site for the binding of CO based on the inhibition of CO oxidation activity by methanol, which traps Mo^V and CO-dependent growth was inhibited by the Mo antagonist, tungstate (Meyer and Schlegel 1983). The crystal structure of CODH_{Oc} in the n-butylicyanide-bound state has shown that Cu is involved in CO binding (Dobbek *et al.* 2002). Furthermore, the Cu ion is always in the oxidation state of +1 (Gnida *et al.* 2003), which enables the Cu ion to bind CO (Pasquali *et al.* 1983). The oxidation states of the bimetallic cluster reveal that an oxidized CODH_{Oc} has a [Cu^ISMo^{VI}(=O)₂] bimetallic cluster that is readily converted to a [Cu^ISMo^{IV}(=O)OH] cluster upon reduction by CO or low-potential reductants like dithionite (Gnida *et al.* 2003). The M-subunit (30.2 kDa) is a flavoprotein, which harbors one FAD cofactor (Bray *et al.* 1983). The S-subunit (17.8 kDa) possesses proximal and distal [2Fe-2S] clusters that are involved in electron transfer from the

molybdenum center to the FAD located in the M subunit (Fig. 6C) (Bray *et al.* 1983; Meyer *et al.* 1986; 1993A; 1993B; Dobbek *et al.* 1999; 2002; Gnida *et al.* 2003).

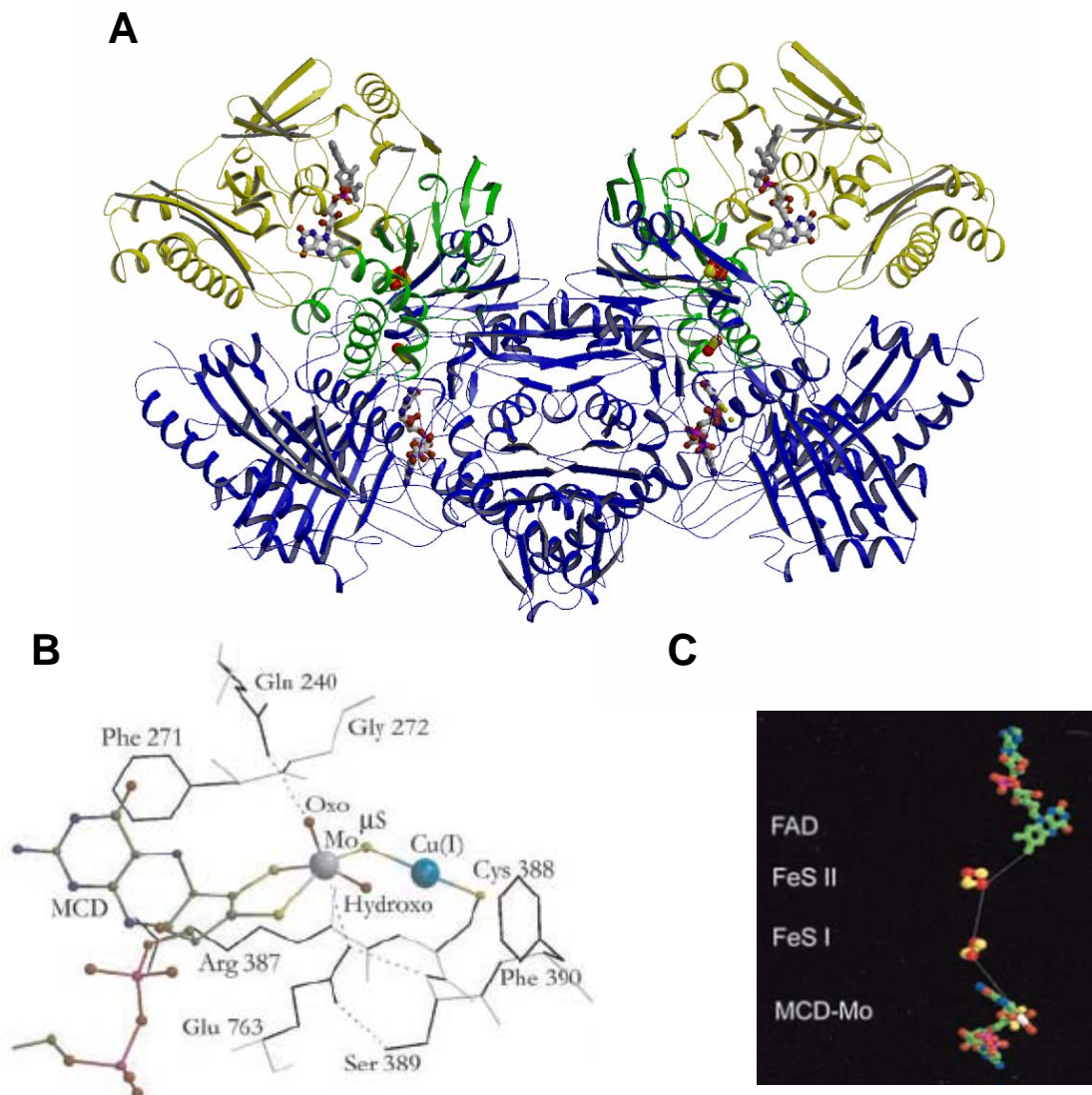


Fig. 6. Crystal structure of aerobic Cu, Mo-containing CODH_{Oc} from *O. carboxidovorans* (Dobbek *et al.* 1999, 2002). (A) Overall structure of CODH_{Oc} represents a dimer of heterotrimers. The L-subunit carrying the active site, the S-subunit carrying two [2Fe-2S] cluster, and the M-subunit containing FAD is represented in blue, green, and yellow, respectively. (B) The structure of the active site in L-subunit reveals a binuclear [Cu-S-Mo(=O)OH] cluster linked to a MCD. O atom colored in red, S atom in yellow, Cu atom in cyan, and Mo atom in gray. (C) The shortest connection between the cofactors, starting from the molybdo-oxo group (MCD-Mo) at the active site via the proximal C-terminal [2Fe-2S] cluster (FeS I) (14.6 Å distance from the Mo atom to the closest iron atom) and the distal N-terminal [2Fe-2S] cluster (FeS II) (12.4 Å distance between the closest iron atoms), ending at the FAD (8.7 Å distance between C7 of FAD and the closest iron atom).

2.4 Modeling of CO oxidation mechanism based on the crystal structure of CODHII_{Ch}

Previously, a mechanism of CO oxidation was proposed based on the crystal structure of CODHII_{Ch} (Dobbek *et al.* 2001). It has been assumed that the enzyme catalyzes the oxidation of CO at the Ni-(μ_2 S)-Fe1 subsite of cluster C (Fig. 7) (Dobbek *et al.* 2001). In accordance with the structures of cluster C and the localization of the hydrophobic CO channel, an open apical coordination site above the Ni ion in cluster C is the potential prime candidate for CO binding (Dobbek *et al.* 2001; Drennan *et al.* 2001). This proposal is consistent with Fourier transform infrared (FT-IR) studies that revealed several IR bands that were attributed to a Ni-CO complex in the cluster C of CODH_{Mt} (Chen *et al.* 2003). Besides, binding of hydroxide to the histidine-coordinated Fe1 (called ferrous component II, FCII) has been proposed by DeRose *et al.* (1998) based on ENDOR spectroscopy of CODH_{Mt} and shown by Jeoung and Dobbek (2007) with the structure of recombinant CODHII_{Ch}. It is likely that the binding of water to the histidine-coordinated Fe1 lowers its pK_a, which would facilitate formation of an active hydroxide.

Enzymatic catalysis of CO oxidation will be equivalent with an industrial process, called water-gas shift reaction (WGSR) which is used to produce H₂ from CO and water under mild conditions (Ragsdale 1996). This reaction involves a nucleophilic attack of a hydroxide-ion on a metal bound CO and release of CO₂. A major difference between CODH and the WGSR is that CODH produces two protons and two electrons, while the WGSR produces H₂.

The oxidation of CO by CODH is a Ping Pong mechanism that exists in two states (Ragsdale 1996). The first step includes binding of substrates, CO and water, and formation of a metal-carboxyl complex as intermediate that results in the reduction of CODH (Fig. 7A-D). The second step includes electron transfer from the reduced active center to an external electron acceptor and regeneration of the enzyme, which can proceed to the next catalytic reaction (Fig. 7E). The reduced acceptor, then, couples to other cellular processes to conserve energy or to generate reducing-power.

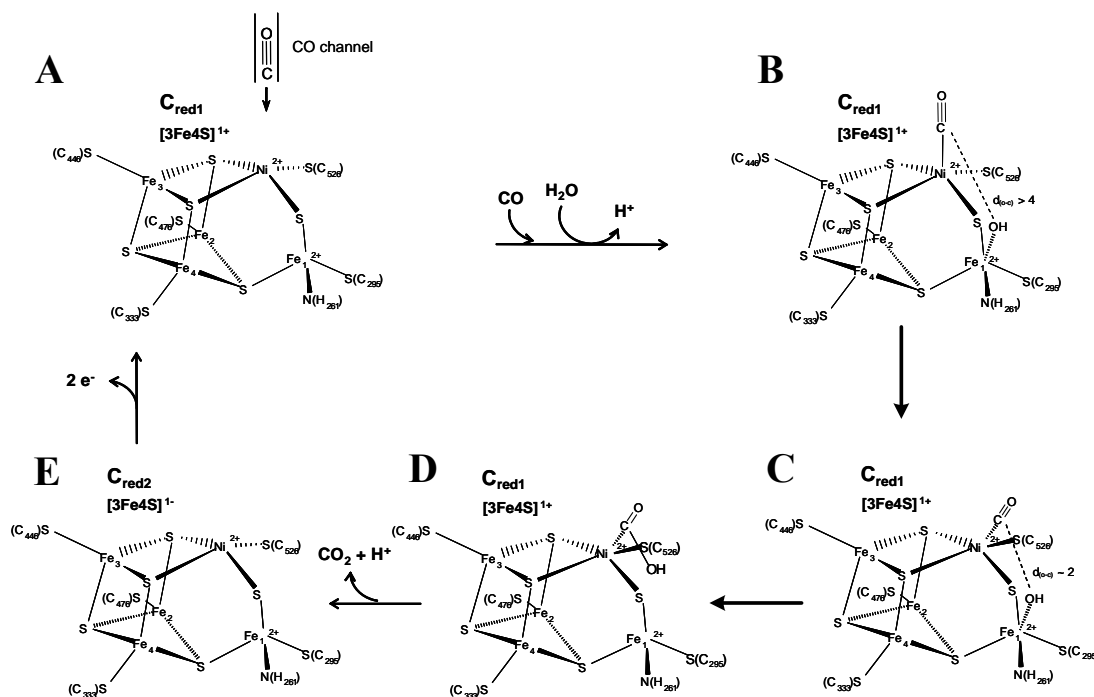


Fig. 7. Proposed mechanism of CO binding and oxidation at cluster C of CODHIII_{Ch} (details in the text; modified from Dobbek *et al.* 2001).

In the first step, CO that comes through the hydrophobic channel binds to a vacant apical coordination site of a Ni ion (Fig. 7A). This leads to a square-pyramidal ligated Ni ion, coordination geometry frequently found for penta-coordinated Ni-complexes (Coyle and Stiefel 1988; Macgregor *et al.* 1994) (Fig. 7B). The binding of hydroxide (or water) leads to a trigonal-bipyramidal geometry of the Fe1 (Fig. 7B). Since the distance of more than 4 Å between Ni bound CO and Fe1 bound OH is too long to allow effective interaction, the initial square-pyramidal Ni coordination will undergo a rearrangement into trigonal-bipyramidal geometry by shifting CO towards the OH. The resulting rearrangement allows a nucleophilic attack of OH⁻ on the carbon atom of Ni-carbonyl (Fig. 7C). A Ni-bound COOH could be a tentative intermediate product (Fig. 7D). Consequently, CO₂ is generated and released from Ni. Protons that are released during this reaction would be shuttled away from the active site through the His-tunnel that consists of conserved basic residues near cluster C (Dobbek *et al.* 2001; Drennan *et al.* 2001; Kim *et al.* 2004; Ragsdale 2004).

Oxidation of Ni-bound CO would leave two electrons at the Ni site, presumably resulting in either a transient Ni⁰ state as proposed by Lindahl (2002) or resulting in a

Ni^{2+} with two electron reduced cluster C. The fact seems to be obscure because the Ni ion has not been observed in a paramagnetic state under all experimental conditions applied so far with the CODH_{Ch} (Svetlitchnyi *et al.* 2001), or CODHs from other anaerobes (Lindahl 2002; Ragsdale 2004). The incorporation of Ni into a polynuclear cluster with $\mu\text{-S}$ ligands might allow significant delocalization of the metal *d* electrons over the ligand orbital and adjacent Fe atoms. This would favor fast electron withdrawal from Ni or Fe1 by using the [3Fe-4S] subsite that is probably used for the uptake of the electrons (Fig. 7E). The electrons, then, would be transferred to cluster B' and further to cluster D. As cluster D is exposed to the solvent, it can allow facile electron transfer to external acceptors.

This mechanism of CO oxidation at the heterobimetallic (Ni- $\mu_2\text{S}$ -Fe1) subcluster is in some respect similar to the mechanism of CO oxidation at the $[\text{CuSMo}(=\text{O})\text{OH}]$ active center of the CODH_{Oc} (Fig. 8) (Dobbek *et al.* 2002; Gnida *et al.* 2003).

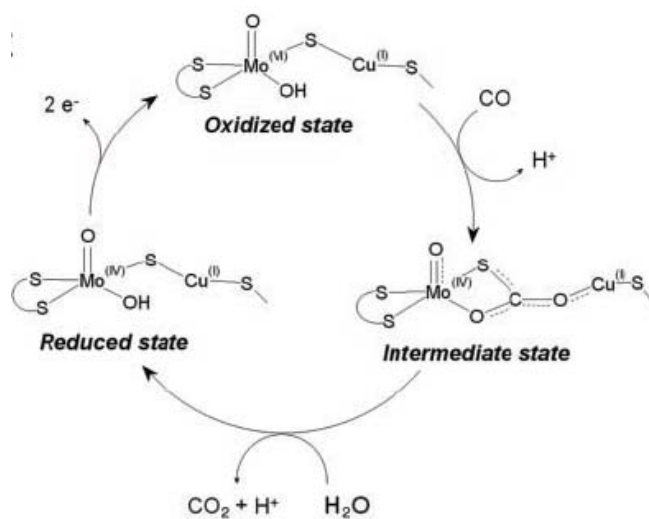


Fig. 8. Hypothetical scheme showing the oxidation of CO to CO_2 at the $[\text{CuSMo}(=\text{O})\text{OH}]$ site of CODH_{Oc} . The catalytic cycle starts at the oxidized cluster with integration of CO between the Cu ion, $\mu_2\text{S}$ and the equatorial O-ligand of the Mo. The intermediate state shown is deduced from the crystal structure of the *n*-butylisocyanide-bound state. Other states shown are based on their individual crystal structures. In the intermediate state CO undergoes a nucleophilic attack by the equatorial O with the formation of a thiocarbonate intermediate and reduction of the Mo ion from the +VI to the +IV state. The thiocarbonate then breaks down to CO_2 , and the equatorial OH-group is regenerated from water, yielding the reduced state of the cluster. Finally, the Mo(+IV) is oxidized to Mo(+VI) through the transfer of the electrons into the intramolecular electron chain, which completes the reaction cycle (Dobbek *et al.* 2002).

The mechanism of the CODH_{Oc} involves the binding of CO at Cu, the binding of OH at Mo and formation of a thiocarbonate species at $\mu_2\text{S}$. Although both NiFe-CODHII_{Ch} and CuMo-CODH_{Oc} have completely different structures and cofactor compositions, the CO oxidation in both enzymes is performed at heterobimetallic clusters of a general structure [M1- $\mu_2\text{S}$ -M2]. M1 and M2 correspond to Cu and Mo in the CODH_{Oc}, respectively, and to Ni and Fe1 in the CODHII_{Ch}, respectively. Accordingly, it suggests that the $\mu_2\text{S}$ is involved in catalytic mechanism of CODHII_{Ch}.

2.5. Objectives of this research work

(1) First aim of the research was to elucidate a CO oxidation mechanism at the [Ni-4Fe-5S] cluster C of CODHII_{Ch} that can be achieved by identification of binding partners for the substrates, CO and H₂O.

Before the start of research, a CO ligand in crystal structures of ACS_{Mt}/CODH_{Mt} and CODHII_{Ch} was modeled at the apical free coordination site of the nickel (Fig. 6B) (Darnault *et al.* 2003; Dobbek *et al.* 2004; Volbeda and Fontecilla-Camps 2005). However, the occupancies of potential CO ligands were too low to support the model and the ligand was identified in a non-functional species of CODHII_{Ch}. Moreover, x-ray absorption spectroscopy could not detect the binding of CO to the nickel ion (Gu *et al.* 2004). These aspects can be ascribed to the extremely high turnover rate of CO oxidation of 4,000 s⁻¹ at 23 °C (Svetlitchnyi *et al.* 2001).

Therefore, this thesis investigates the binding position of CO using a CO analogous inhibitor, cyanide. Since CO and cyanide are isosteric and isoelectronic and display a similar ligand character, the binding partner for CO can be described by interaction of cyanide with the active center of CODHII_{Ch}. To support this assumption, the study encompasses both biochemical and structural examinations:

- **Does cyanide interact with CODHII_{Ch} as a competitive inhibitor?**
- **What are the conditions for the interaction of cyanide with the active center?**

- **Where is the binding position of cyanide and how is the nickel geometry altered by cyanide binding?**

(2) **Second aim** of the research was to describe the functionalities of the bridging $\mu_2\text{S}$ in the active center of native CODHII_{Ch}.

In recent years, two dissimilar structures of the active site have been reported, [Ni-4Fe-5S] and [Ni-4Fe-4S], differing in the presence of the $\mu_2\text{S}$ bridge between Ni and Fe1 in the cluster C (Dobbek *et al.* 2001, 2004; Drennan *et al.* 2001; Doukov *et al.* 2002; Darnault *et al.* 2003; Jeoung and Dobbek 2007). Based on the inhibitory effect of sulfide on CODHs containing the [Ni-4Fe-4S] form of cluster C and the presence of hydroxo ligand at the $\mu_2\text{S}$ position, cluster C containing the bridging $\mu_2\text{S}$ has been proposed as a non-functional active center (Feng and Lindahl 2004; Jeoung and Dobbek 2007). On the other hand, the [Ni-4Fe-5S] cluster C in highly active CODHII_{Ch} was also apparent from x-ray crystallography and x-ray absorption spectroscopy and stabilization of the active center by the bridging $\mu_2\text{S}$ has been proposed (Dobbek *et al.* 2001, 2004; Gu *et al.* 2004).

To clarify the controversy, this study further investigates the relationship between the catalytic activity and the bridging $\mu_2\text{S}$:

- **Is there an inhibitory effect of sulfide on the CO oxidation activity of native CODHII_{Ch}?**
- **What role does the bridging $\mu_2\text{S}$ play in CO oxidation and CO₂ reduction?**
- **What is the physiological necessity of the $\mu_2\text{S}$ ligand in native CODHII_{Ch}?**

3 SYNOPSIS

3.1 The [Ni-4Fe-5S] cluster C containing bimetallic Ni-(μ_2 S)-Fe1 subsite is the functional active site of native CODHII_{Ch}

The crystal structures of native CODHII_{Ch} have revealed the [Ni-4Fe-5S] cluster C as active center, wherein Ni and Fe1 are bridged by inorganic μ_2 S (Dobbek *et al.* 2001, 2004). To confirm the structure of the functional cluster C in solutions, highly active dithionite-reduced native CODHII_{Ch} (15,400 units mg⁻¹; 1 unit corresponds to 1 μ mol CO oxidized per min) was analyzed employing x-ray absorption spectroscopy (XAS).

The x-ray absorption near edge spectroscopy (XANES) spectrum of highly active dithionite-reduced CODHII_{Ch} is assigned to tetragonal geometries lacking one or more axial ligand (Colpas *et al.* 1991) and edge energy indicates that four homogenous ligand spheres on square-planar geometry coordinate the nickel ion in a Ni²⁺ oxidation state. Fourier transformed EXAFS data show four Ni-S interactions at 2.23 Å, which fulfills the Ni-S bond lengths in square-planar complexes of Ni²⁺ containing thiolate ligands and no further interactions with light atoms, e.g. oxygen (chapter 5).

To identify a nickel-carbonyl complex in the cluster C, change of nickel-coordination was analyzed after treatment with CO in the absence of an electron acceptor, but the attempts were not successful (Gu *et al.* 2004; chapter 5). Ni-K edge and EXAFS spectra of reduced CODHII_{Ch} after exposing to CO are almost identical to that of the dithionite-reduced CODHII_{Ch} indicating no alteration of nickel geometry and ligand sphere upon CO treatment (chapter 5). The reason of failure can be interpreted by a high turnover rate of CODHII_{Ch} (4,000 s⁻¹ at 23 °C) (Svetlitchnyi *et al.* 2001), i.e. the samples analyzed by XAS have already undergone the complete catalytic cycle.

The model comprising 4 S atoms at 2.23 Å in a square-planar geometry and 2 Fe atoms at 2.71 and 2.99 Å correlates well with the crystal structure of functional native CODHII_{Ch} (Dobbek *et al.* 2001, 2004). However, the 2.71 Å Ni-Fe distance is shorter than the shortest Ni-Fe distance found by x-ray crystallography (Dobbek *et al.* 2001, 2004). It might reflect a redox-dependent conformational change in cluster C due to

the slightly different redox state of the enzyme in samples studied by XAS and crystallography as it was previously suggested (Gu *et al.* 2004).

3.2 Interaction of potassium cyanide with cluster C of native CODHII_{Ch}

Cyanide ion is a potent inhibitor of all anaerobic NiFe-CODHs investigated so far (Ragsdale *et al.* 1983; Abbanat and Ferry 1990; Drake *et al.* 1981; Grahame and Stadtman 1987; Eikmanns *et al.* 1985). Previously, our group has studied inhibition of CODHII_{Ch} by cyanide as well as isocyanides (C≡N-R; R = n-butyl, benzyl, or tert-butyl) under non-turnover conditions. The results show that the effect of cyanide on inhibition of CODHII_{Ch} is significantly stronger than that of isocyanide (Svetlitchnyi, personal communication). The weaker effect of isocyanide can be described by the difficulty to access the active site, whereas cyanide has a similar size as CO, facilitating its passage through the substrate channel of CODHII_{Ch} (Dobbek *et al.* 2001). Moreover, the CO (C≡O) and cyanide molecules (C≡N) show similar reactivities since they are isosteric and isoelectronic, display a similar σ -donor and π -acceptor ligand character, and share the presence of a non-bonding pair of electrons in the *sp*-hybridized orbital of the terminal carbon atom (Brunori *et al.* 1992; Dobbek *et al.* 1999). These characteristics suggest that cyanide is a suitable molecule to proof the mechanism of CO oxidation proposed before (Fig. 7). Accordingly, investigation of the effect of cyanide as CO analogue in detail seems to be an appropriate strategy for structural studies to identify the binding position for CO at cluster C.

3.2.1 Potassium cyanide is a competitive inhibitor of the reduced CODHII_{Ch}

The addition of cyanide in the presence of CO (100 % in the gas phase) and electron acceptor, methyl viologen, (i.e. turnover condition) diminished CO oxidation activity of CODHII_{Ch} (chapter 5). The results show that the rate of inhibition depends on the cyanide concentrations applied and the assay temperatures. Increasing of assay temperature significantly enhanced the inhibition rate (chapter 5). Based on high growth temperature optimum for *C. hydrogenoformans* as well as of high temperature

optimum of the CO oxidation activity of CODHII_{Ch} (Svetlitchnyi *et al.* 2001), the tendency of the inhibition suggests that CO and cyanide act in a similar mode.

The results of the double reciprocal plot of initial activity versus CO concentration as a function of cyanide concentration supported the suggestion (Fig. 9A). The resulting plot corresponds to a characteristic of competitive inhibition and similar K_M and K_I values indicate similar affinity of CO and cyanide to the active center. Potassium cyanide also inhibited CODHII_{Ch} when CO was replaced by N₂ and the electron acceptor was eliminated (i.e. non-turnover conditions). Under this condition, the inhibition by cyanide strongly depended on the redox potentials of the enzyme solution (Fig. 9B). Cyanide in micromolar concentrations efficiently interacted with the reduced cluster C, which had been incubated with low-potential reductants like dithionite and Ti(III) citrate (redox potential ~ -500 mV). This state is defined as C_{red2} state (Lindahl *et al.* 1990; Anderson *et al.* 1996; Fraser *et al.* 1999).

On the contrary, CODHII_{Ch} was insensitive to cyanide under more oxidizing conditions with a weak reductant dithiothreitol (DTT) (~ -320 mV), defined as C_{red1} state, or in the absence of reductants (Fig. 9B).

The redox potential required for cyanide binding to cluster C of CODHII_{Ch} with respect to CO is inconsistent with other Ni containing CODHs from *R. rubrum* (CODH_{Rr}) and *M. thermoacetica* (CODH_{Mt}). In the model proposed, CO oxidation in CODH_{Rr} and CODH_{Mt}, CO is oxidized to CO₂ at C_{red1} state, which is the reduced form of the C_{ox} state by one electron and can be established at a redox potential around -200 mV (Lindahl *et al.* 1990; Spangler *et al.* 1996; Feng and Lindahl 2004). However, interaction of CO with cluster C of CODH_{Mt} at C_{red2} state has been also demonstrated by EPR (Seravalli *et al.* 1997). It is certain that CO interacts with cluster C of CODHII_{Ch} at redox potentials below -500 mV because the oxidation of CO in *C. hydrogenoformans* (-520 mV) is coupled to the reduction of protons to H₂ (-410 mV) (Svetlitchnyi *et al.* 2001). Furthermore, reduced CODHII_{Ch} was secured from inhibition by potassium cyanide when CO replaced atmosphere of N₂. This protection by CO is an additional evidence to support the competitive inhibition by cyanide.

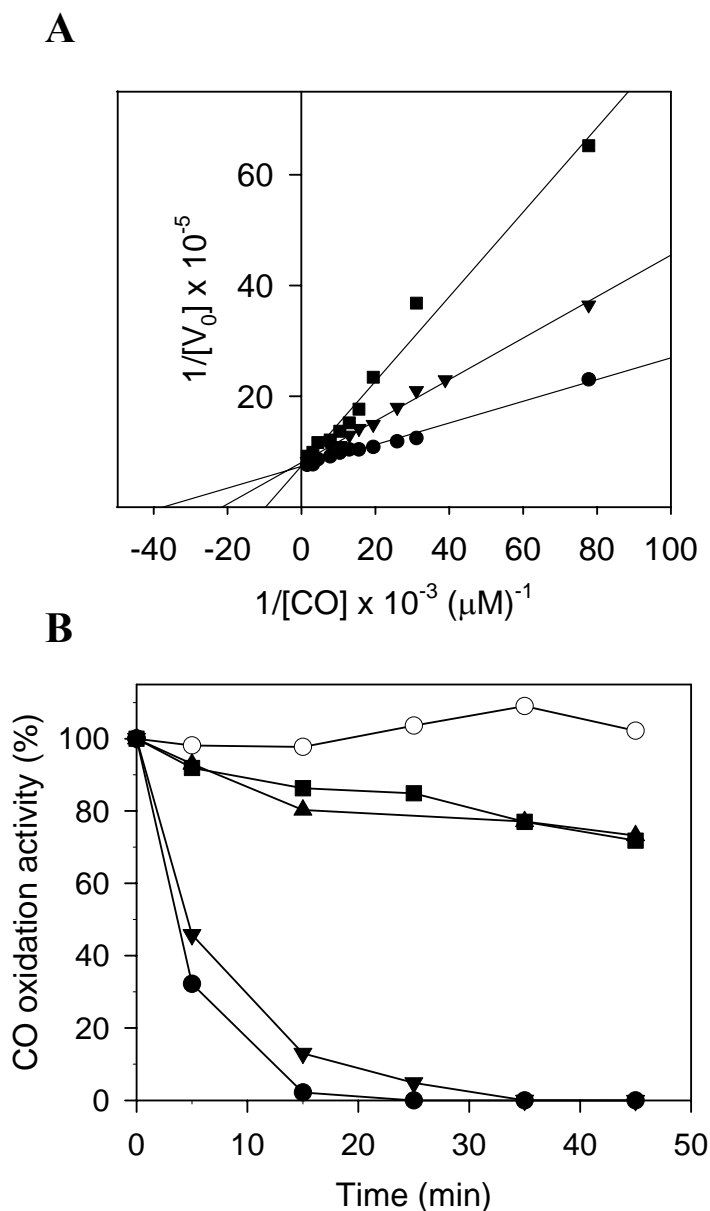


Fig. 9. Inhibition of $\text{CODHII}_{\text{Ch}}$ by potassium cyanide under turnover (A) and under non-turnover conditions (B). (A) The double reciprocal plot of initial activity (V_0 in units mg^{-1}) versus CO concentration as a function of cyanide concentration. Potassium cyanide concentrations in the cuvettes were 0 (\bullet), 24.6 (\blacktriangledown), and 49.0 (\blacksquare) μM . Assays in (B) contained $0.19 \mu\text{g ml}^{-1}$ $\text{CODHII}_{\text{Ch}}$ under N_2 (filled symbols) or CO (open symbols), 15 μM KCN, and 4 mM dithionite plus 2 mM DTT (\bullet , \circ), 4 mM Ti(III) citrate (\blacktriangledown), 2 mM DTT (\blacksquare) or no reductants (\blacktriangle) at 23 °C. 100 % activity corresponds to $14,800 \text{ units mg}^{-1}$ at 70°C. For further details, see chapter 5.

3.2.2 Cyanide provokes a chemical decomposition of cluster C under oxidizing conditions

Oxidized CODHII_{Ch} in the absence of reductants was not inhibited applying micromolar concentrations of cyanide. An increasing amount of cyanide to millimolar concentrations inhibited CO oxidation activity of the oxidized enzyme suggesting different modes of cyanide reaction with the reduced and the oxidized active centers (chapter 7).

Obviously, CO could not protect the oxidized enzyme against inhibition by potassium cyanide (chapter 5). The decrease of activity coincided with the yield of thiocyanate, which is the reaction product of sulfane sulfur and cyanide (Fig. 10) (Westley 1981; Wood 1987; Iciek and Wlodek 2001; Ubuka 2002). Apparently, no thiocyanate was produced from the reduced enzyme by treatment with cyanide (Fig. 10). These results indicate that the oxidized CODHII_{Ch} contains cyanolyzable sulfane sulfur (S⁰), which is the labile bridging μ_2 S in the bimetallic Ni-(μ_2 S)-Fe1 subsite of cluster C based on the ratio of the values of liberated cyanolyzable sulfur and the content of μ_2 S in the CODHII_{Ch} and the cyanolyzability of μ_2 S in oxidized [CuSMo(=O)O] active site of CO-dehydrogenase from the aerobic bacterium *Oligotropha carboxidovorans* (CODH_{Oc}) (Meyer *et al.* 2000; Dobbek *et al.* 2002; Gnida *et al.* 2003; Resch *et al.* 2005).

Under oxidizing conditions, the removal of μ_2 S induced irreversible chemical decomposition of cluster C, which was caused by release of nickel and iron ions. Decrease of the absorption peak at 419 nm, which corresponds to the content of FeS cluster in the enzyme, described the decompositions of cluster C as well as cluster B and D upon prolonged incubation with cyanide (chapter 7).

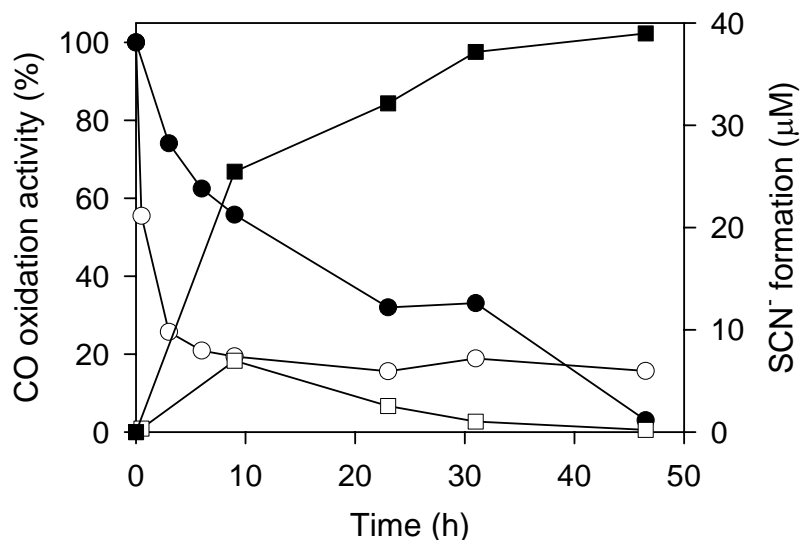


Fig. 10. Inhibition of CO oxidation activity (circles) and thiocyanate formation (squares) of oxidized- (closed symbols) and reduced CODHII_{Ch} (open symbols) by cyanide treatment. Both different redox states of CODHII_{Ch} (2.2 mg ml⁻¹: approx. 17 μM CODHII_{Ch}) were incubated at 23 °C with 5 mM cyanide for the oxidized enzyme and with 1 mM cyanide for the reduced enzyme under N₂ atmosphere. 100 % of activity corresponds to 14,200 U mg⁻¹. For further details, see chapter 7.

3.2.3 The inhibition of reduced CODHII_{Ch} by cyanide is fully reversible

The inhibition of reduced CODHII_{Ch} was not caused by irreversible decomposition of the active site because the cyanide-inhibited enzyme completely recovers catalytic activity without any chemical reconstitution (chapter 7). Like CO-dependent reactivation of CODH_{Rr} (Ensign *et al.* 1989), cyanide-inhibited reduced CODHII_{Ch} slowly recovered activity by incubation at low temperature (23 °C) under CO in the presence of low potential reductants, whereas no reactivation could be observed under N₂ gas phase. The rate of reactivation was apparently increased by ascent of incubation temperatures, which diminished the dependency. After incubation at 70 °C, full level of reversibility was also achieved under N₂ gas phase in the presence of dithionite or Ti(III) citrate, but the rate of reactivation was obviously accelerated by CO (chapter 5). Until now, it is unclear how the inhibited enzyme can recover the catalytic function

under N₂, but it might be explained by the fact that high temperature encourages better flexibility of the enzyme that promotes release of bound-cyanide. Moreover, the reactivations of the enzyme is likely to be a redox-state related process, i.e. completely reduced metal clusters, by chemical reductants or by CO oxidation, induce release of bound-cyanide and prevent the enzyme from rebinding of cyanide because fully reduced clusters do not allow CO as well as cyanide to interact with the active site.

The same levels of remained activity and reversibility indicate that prolonged incubation with cyanide does not provoke irreversible decomposition of active center under reducing condition whereas irreversible decomposition of active center by cyanide is evident under oxidizing condition (chapter 7). Accordingly, these properties on reactivation further substantiate that the inhibition of reduced CODHII_{Ch} originates from the occupation of the CO binding position by cyanide and this inhibited state should represent the intermediate state of metal-carbonyl complex in the enzyme.

3.2.4 Potassium cyanide interacts with the Ni of cluster C

The inhibition of CODH_{Rt} from *R. rubrum* by cyanide is evident for direct interaction of cyanide with nickel ion from ¹⁴CN⁻ based comparison between holo- and apo-enzyme, which lacks Ni atom only (Ensign *et al.* 1989). So far, studies about cyanide-binding brought inconclusive results since Ni and Fe, serving as CO and H₂O binding partners in the active center, are highly reactive with cyanide and form tight metal-cyanide complexes. Indeed, infrared spectroscopy indicated the binding of the C atom of cyanide to the Fe ion, suggesting a bent Fe-CN-Ni bridging geometry (Qiu *et al.* 1996). To solve this question, the change of nickel geometry and ligands composition in cluster C of native CODHII_{Ch} after inhibition by cyanide was analyzed by XAS. The results show that the inhibition by cyanide induced a significant XANES spectrum altered to that of reduced and CO treated CODHII_{Ch} (chapter 5). Edge energy shift of the spectrum indicates that binding of cyanide does not affect a change in the Ni geometry, i.e. square planar, but changes the ligands composition of nickel.

Ni-K edge x-ray absorption spectrum reveals one CN ligand bound to nickel in square-planar geometry, wherein the carbon atom of cyanide binds to nickel

suggesting the cleavage of one of the Ni-S bonds (chapter 5). In agreement with the assumption that the bridging $\mu_2\text{S}$ is the most labile bond in the cluster C of CODHII_{Ch} (Dobbek *et al.* 2001), cyanide breaks the bond between nickel and $\mu_2\text{S}$ and then binds to nickel at the coordination site previously occupied by $\mu_2\text{S}$.

3.2.5 Crystal structure of reversibly inhibited CODHII_{Ch} confirms the Ni-CN complex in the equatorial plane

XAS did not allow the localization of the bridging $\mu_2\text{S}$ after ligand-replacement by cyanide. To identify the localization of the bridging $\mu_2\text{S}$ and to confirm XAS data on cyanide binding, the structure of reversibly inhibited CODHII_{Ch} was solved by crystallography. Cyanide-inhibited CODHII_{Ch} contained a cyanide ligand at the Ni ion (Fig. 11) (chapter 6). In agreement with XAS on the cyanide-inhibited enzyme, the C atom of cyanide replaced the $\mu_2\text{S}$ and recovered the slightly distorted square-planar coordination. This distortion can be described by doming over the S5-Ni-C-N plane, whereas in the structure before inhibition the doming is shown over the S3-Ni-S^γ(Cys⁵²⁶) plane.

The N atom of cyanide is in hydrogen bonding distance (2.8 Å) to Nε2 of well ordered His⁹³ and Lys⁵⁶³ (chapter 6). The His⁹³ residue was well ordered by cyanide binding. Cyanide binding induced significant structural rearrangement of cluster C as well as protein environment (chapter 6). Remarkably, binding of cyanide converts the initial “iron-out” conformation to “iron-in” conformation and results in a small displacement of Ni and Cys⁵²⁶. Coordination of Fe1 by His²⁶¹ is recovered via large conformational changes extending over two consecutive turns of the α -helix in the His²⁵⁹ to Val²⁷⁰. This involves displacements of side-chain atoms by more than 3.5 Å. The conformational change extends, via hydrophobic interactions as well as via the rearrangement of the bound solvent water, over further segments of the structure, notably involving large displacements of Phe³⁶⁶ phenyl and His⁹⁹ pyrrol rings, which are involved in the proton transfer network (see section 2.3.1 Fig. 5) (Dobbek *et al.* 2001; Drennan *et al.* 2001; Kim *et al.* 2004).

The occupancy of the bound cyanide is estimated to 80 % and is consistent with the occupancies of resolved major conformations of S1, Fe1, Fe2, and their protein

ligands as well as protein residues that are involved in an extended conformational change (chapter 6). Based on the evidence that cyanide is a competitive inhibitor of reduced CODHII_{Ch} with respect to CO and that cyanide mimics the substrate CO, the cyanide-bound conformation represents a model for the NiS₃-coordinated state with bound CO, which appears during the catalytic cycle of CO-oxidation after displacement of μ_2 S. However, bound μ_2 S could not be identified in the structure.

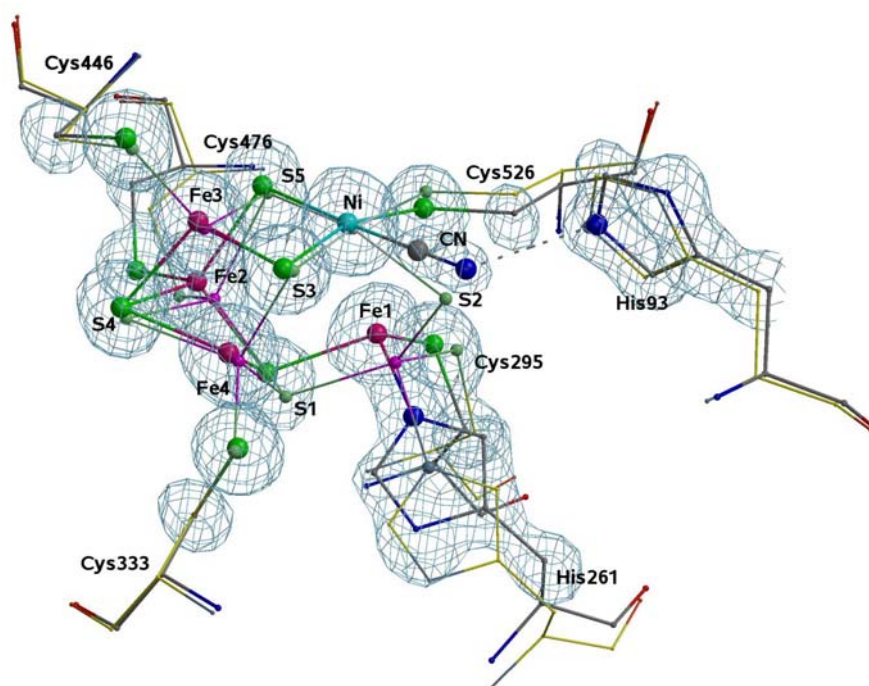


Fig. 11. Structure of cluster C in cyanide-inhibited state. A $F_{\text{obs}} - F_{\text{calc}}$ omit electron density map is contoured at 5σ level. The model presents a complex with 80 % occupancy of cyanide (large balls). Superimposed is the structure in activated state of CODHII_{Ch} (small balls). Fe atom colored in red, S atom in green, Ni atom in cyan, N atom in blue, and C atom in gray. For further details, see chapter 6.

3.3 Sulfide-dependent reformation of the bimetallic Ni-(μ_2 S)-Fe1 subcluster

As mentioned before, the binding pattern of cyanide to reduced CODHII_{Ch} agrees with competitive inhibition. However, the fact that no bound μ_2 S in the structure of cyanide-inhibited CODHII_{Ch} was detected gives rise to the question whether μ_2 S in cyanide-inhibited CODHII_{Ch} remains bound as flexible ligand or is completely released.

Inhibition of reduced CODHII_{Ch} by cyanide was readily recovered by simple incubation at high temperatures (70°C) in the presence of Ti(III) citrate (chapter 5 and 6). Nevertheless, addition of sodium sulfide endowed higher level of reversibility of cyanide-inhibited CODHII_{Ch} (Fig. 12) (chapter 6). The level of reactivation of the enzyme incubated with Ti(III) citrate alone was approximately 35 % lower than the level of reactivation in the presence of either Ti(III) citrate plus sodium sulfide or dithionite, which are substances that serve as reductants as well as sulfide source (Das and Kanatzidis 1995; Wahl and Rajagopalan 1982). This indicates that there are two distinct conformations of a functional active site and the differences may be correlated to the presence of the bridging μ_2 S because cluster C in the cyanide-inhibited CODHII_{Ch} does not contain bound- μ_2 S ligand.

Consequently, the structures of cluster C after reactivation with sulfide and without sulfide were analyzed by XAS and x-ray crystallography to distinct the conformations (chapter 6). The results show that the structure of cluster C in reactivated CODHII_{Ch} treated with dithionite was almost identical to the structure of cluster C before cyanide treatment indicating sulfide-dependent reformation of the NiS₄-conformation in cluster C ([Ni-4Fe-5S]). In contrast, the NiS₃-conformation of cluster C ([Ni-4Fe-4S]) lacking the μ_2 S and cyanide ligands was established by reactivation in the presence of Ti(III) citrate alone indicating complete release of μ_2 S ligand upon inhibition by cyanide (chapter 6). Therefore, reactivation in the presence of a source of sulfide results in reincorporation of μ_2 S in the bridging position between Ni and Fe1. This conformation of the active center displays higher CO oxidation activity than the NiS₃-conformation of cluster C devoid of μ_2 S.

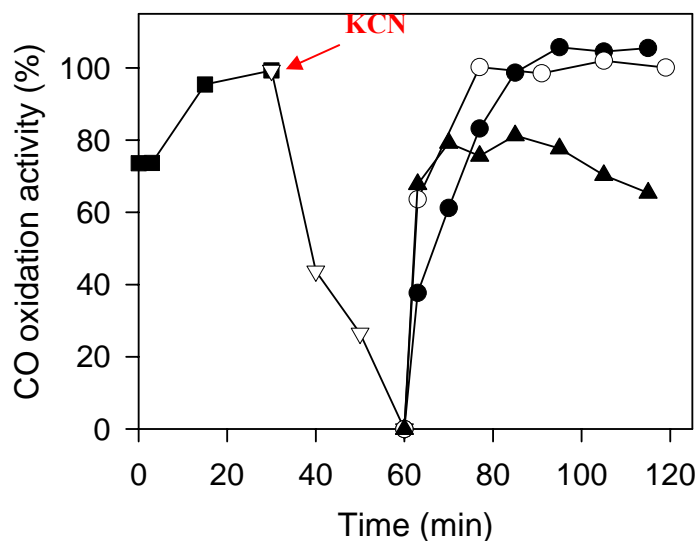


Fig. 12. Effect of sulfide on reactivation and stability of cyanide-inhibited CODHII_{Ch}. As-isolated state of CODHII_{Ch} (0.5 mg ml⁻¹) was activated at 70°C under N₂ in the presence of 4 mM dithionite as reductant and source of sulfide (■) and then activated state of CODHII_{Ch} was inhibited by 250 μM KCN at 23°C under N₂ yielding reversibly inhibited state of CODHII_{Ch} (CODH_CN) (▽). CODH_CN was reactivated at 70°C under N₂ in the presence of 4 mM dithionite (●), 4 mM Ti(III) citrate + 1 mM Na₂S (○), or 4 mM Ti(III) citrate (▲). 100 % of CO oxidation activity corresponds to 15,900 units mg⁻¹. For further details, see chapter 6.

Similarly, the removal of μ₂S as thiocyanate from the oxidized CODHII_{Ch} by cyanide treatment was directly connected to the decrease of CO oxidation activity (see section 3.2.2 Fig. 10). Since cyanide could not interact with oxidized cluster C as a CO analogue (chapter 5), the loss of activity is apparently caused by the absence of the bridging μ₂S.

This outcome incipiently shows that both forms, NiS₄ and NiS₃, of cluster C in CODHII_{Ch} are able to oxidize CO to CO₂ (chapter 6). However, the NiS₄-conformation CODHII_{Ch} has a higher CO oxidation activity. Conversions of the NiS₃-conformation to NiS₄-conformation under conditions, which are comparable to the habitats of *C. hydrogeniformans* (volcanic highly reduced sulfide-rich hot environments) suggest that the native CODHII_{Ch} contains the [Ni-4Fe-5S] cluster C as the catalytic active site.

3.4 The fate of $\mu_2\text{S}$ in cyanide-induced inhibition and CO oxidation

Absence of bound $\mu_2\text{S}$ in cluster C of cyanide-inhibited $\text{CODHII}_{\text{Ch}}$ and subsequent partial reactivation in the presence of Ti(III) citrate and the absence of sulfide indicates that inhibition of reduced enzyme by cyanide causes the release of this ligand. The binding of cyanide to the Ni ion apparently labilizes the ligand from Fe1. Reversible inhibition of Ti(III) citrate-reduced enzyme with cyanide released $\mu_2\text{S}$ as H_2S indicating its oxidation state of S^{2-} , since approximately 2 mol of H_2S per mol of homodimeric $\text{CODHII}_{\text{Ch}}$ was formed (chapter 6). This result agrees with the fact that no thiocyanate was found after cyanide treatment of the Ti(III) citrate-reduced enzyme. In contrast to cyanide inhibition, no H_2S was liberated upon exposure of $\text{CODHII}_{\text{Ch}}$ to catalytic turnover conditions with CO and methyl viologen as electron acceptor suggesting reformation of the Ni-($\mu_2\text{S}$)-Fe1 bridge after the catalytic cycle (chapter 6). This assumption was proved by XAS analysis of the Ni coordination after CO oxidation. The results of Ni-K edge XAS came out with the same coordination numbers of S ligands to Ni before (3.7 S) and after exposure to CO (3.7 S). Since CO oxidation did not change the number of the S ligands, $\mu_2\text{S}$ is displaced from the bridging position when the enzyme oxidizes CO and reestablishes the bridge after completion of the catalytic cycle. This hypothesis can be interpreted by the high rate of CO oxidation (K_{cat}/K_m of $1.7 \cdot 10^9 \text{ M}^{-1} \text{ s}^{-1}$ at 70 °C, Svetlitchnyi *et al.* 2001) and subsequent $\mu_2\text{S}$ rebinding which would prevent the release of this ion from the protein by a diffusion-controlled process (10^8 to $10^9 \text{ M}^{-1} \text{ s}^{-1}$), as it is the case in cyanide-inhibited state.

3.5. Why does native CODHII_{Ch} contain the bridging $\mu_2\text{S}$ in [Ni-4Fe-5S] cluster C?

Native NiFe-CODHs isolated from the mesophilic phototrophic bacterium *R. rubrum* (CODH_{Rr}) (Drennan *et al.* 2001) and from CO₂-reducing moderately thermophilic acetogenic bacterium *M. thermoacetica* (CODH_{Mt}) (Doukov *et al.* 2002; Darnault *et al.* 2003) as well as a recombinant CODHII_{Ch} expressed in *E. coli* (Jeoung and Dobbek 2007) reveal NiS₃-coordinated cluster C as a catalytic competent active site. Based on attenuation of steady-state CO oxidation activity of CODH_{Rr} and CODH_{Mt} by external sulfide and observation of bound CO₂ between Ni and Fe1, an inhibitory role of the bridging $\mu_2\text{S}$ has been proposed (Feng and Lindahl 2004; Jeoung and Dobbek 2007). At the same time, however, crystalline and aqueous native CODHII_{Ch} isolated from CO grown bacteria contain a planar NiS₄-coordinated cluster C and the enzyme is highly active in CO oxidation, indicating catalytically competent enzyme species (Svetlitchnyi *et al.* 2001; Dobbek *et al.* 2001; Gu *et al.* 2004; Ha *et al.* 2007). The ability of CODHs on CO oxidation with both forms of cluster C suggests that the bridging $\mu_2\text{S}$ has to be flexible, promoting the question, what is the biologically relevant species in *C. hydrogenoformans* and what function does this $\mu_2\text{S}$ fulfill in the native CODHII_{Ch}.

3.5.1 The $\mu_2\text{S}$ enhances the rate of CO oxidation

Preparations of native CODHII_{Ch} purified so far in our lab from CO-grown bacteria displayed CO oxidation activities from 7,000 to 16,000 units mg⁻¹ at 70 °C. Preparations that display activities below 12,000 units mg⁻¹ could be further activated up to 40 % by incubation at 70 °C in the presence of external sulfide and low potential reductants under turnover (Fig. 13) as well as non-turnover conditions (Fig. 14A). No activation in the absence of sulfide indicates the activation to be related to incorporation of sulfide (chapter 6). The results from crystallography and XAS studies show that various activities generally correlated with the occupancy of the bridging $\mu_2\text{S}$ ligand in cluster C (chapter 5 and 6). In other words, a homogenous [Ni-4Fe-5S] cluster C fully occupied with $\mu_2\text{S}$ displays the highest CO oxidation activity and no

further activation by incubation with sulfide implies that the activation is coupled to the incorporation of sulfide as bridging $\mu_2\text{S}$ into the active center.

Structure of cluster C in as-isolated native CODHII_{Ch} with a CO oxidation activity of 11,600 units mg^{-1} is highly heterogeneous and displays at least two conformations, which rely on the existence of the $\mu_2\text{S}$ bridge (Fig. 14B) (chapter 6). Incubation of the as-isolated enzyme with reductants plus sodium sulfide increases CO oxidation activity to 16,300 units mg^{-1} and the $\mu_2\text{S}$ content increased from 60 to 85 % (chapter 6). That significantly reduces the heterogeneity of cluster C (Fig. 14C).

Additional evidence of $\mu_2\text{S}$ -dependent activation was shown by the highest reversibility level of cyanide-inhibited CODHII_{Ch} in the presence of sulfide (see section 3.3 Fig. 12). As expected, XAS reveals that cluster C of as-isolated CODHII_{Ch}, which can not be activated by sulfide, is already fully occupied with bridging $\mu_2\text{S}$ (chapter 5). Therefore, this sulfide-dependent activation of CODHII_{Ch} disproves the proposed inhibitory role of the bridging $\mu_2\text{S}$ (Feng and Lindahl 2004; Jeoung and Dobbek 2007).

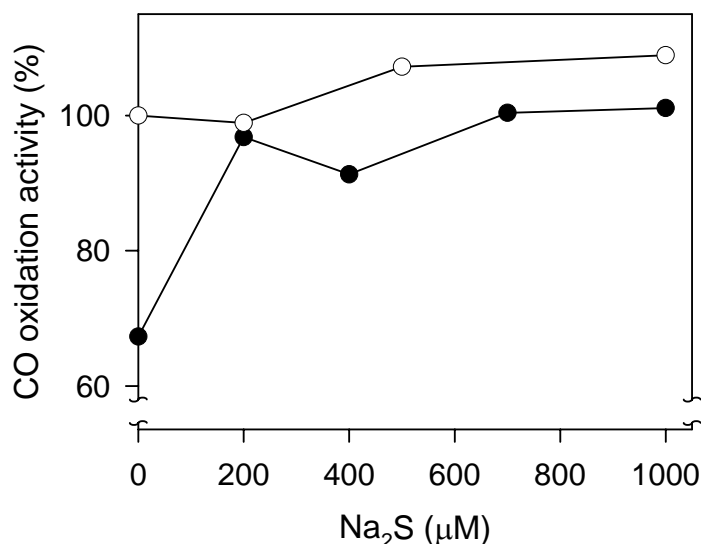


Fig. 13. Effect of sulfide on catalytic activities of CODHII_{Ch} under turnover conditions in the presence of CO and methyl viologen at 70 °C. For the assay, sodium sulfide was added to serum-stoppered cuvettes containing 1.0 ng ml^{-1} CODHII_{Ch} in activated state with NiS₄-coordination (○) and in reactivated NiS₃-coordinated (●) cluster C. 100 % activity corresponds to 15,900 units mg^{-1} . For further details, see chapter 6.

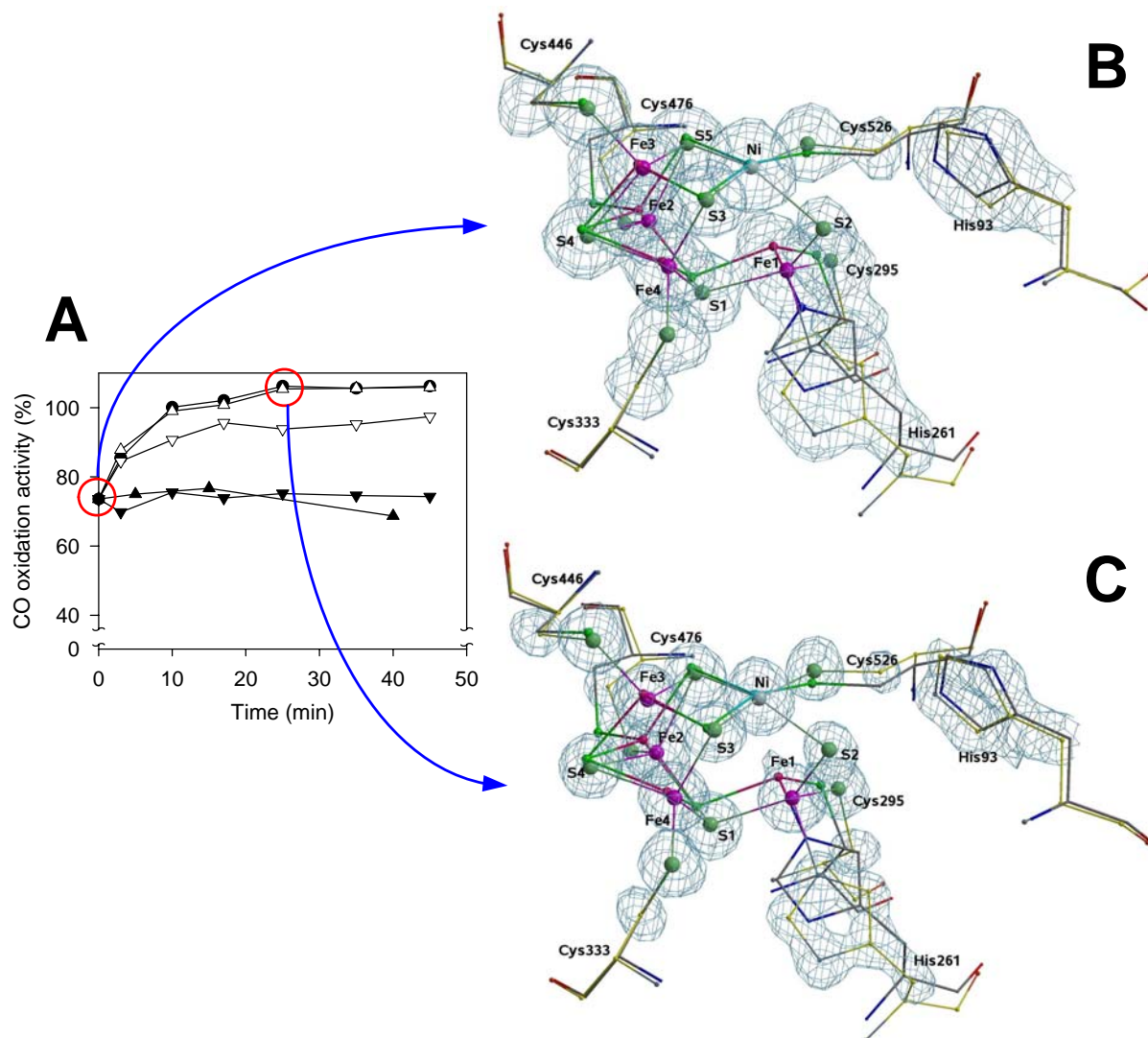


Fig. 14. Sulfide-dependent activation of CO oxidation activity (A) and $\mu_2\text{S}$ induced structural rearrangement of cluster C (B and C). (A) CODHIII_{Ch} in as-isolated state was incubated under N_2 with 4 mM dithionite + 2 mM dithiothreitol (DTT) + 1 mM Na_2S (●), 4 mM dithionite + 2 mM DTT (△), 2 mM Ti(III) citrate + 1 mM Na_2S (▽), 2 mM Ti(III) citrate (▲), or 1 mM Na_2S (▼). 100 % of CO oxidation activity corresponds to 15,900 units mg^{-1} . (B) Structure of cluster C in as-isolated state. The model presents the [Ni-4Fe-5S]-conformation with 60% occupancy (large balls) and the [Ni-4Fe-4S]-conformation with 40% occupancy (small balls). (C) Structure of cluster C in activated state. The model presents the [Ni-4Fe-5S]-conformation with 85% occupancy (large balls) and the traces of [Ni-4Fe-4S]-conformation with 40% occupancy (small balls). A $F_{\text{obs}}-F_{\text{calc}}$ omit electron density map is depicted in blue. Fe atom colored in red, S atom in green, Ni atom in gray, N atom in blue, and C atom in yellow. For further details, see chapter 6.

3.5.2 The $\mu_2\text{S}$ stabilizes cluster C at high temperature

Although the NiS_4 -coordinated cluster C displays higher CO oxidation activity than NiS_3 -conformation (Figs. 12, 13 and 14), it is not sufficient to interpret the reason of existence of bridging $\mu_2\text{S}$ in the active site because both forms of cluster C are able to oxidize CO.

Accordingly, thermostabilities of both enzyme species were compared at 70 °C, which is the optimum growth temperature of *C. hydrogenoformans* (Svetlitchnyi *et al.* 1991A, B). The results show that both forms of $\text{CODHII}_{\text{Ch}}$ are stable at 70°C under N_2 gas phase only in the presence of external sulfide and the $\text{CODHII}_{\text{Ch}}$ containing NiS_3 -coordinated cluster C again displays activation (Fig. 15) (chapter 6). The enzymes are generally less stable under CO atmosphere, which is in agreement with CO-induced decomposition of cluster C of $\text{CODHII}_{\text{Ch}}$ (Dobbek *et al.* 2004).

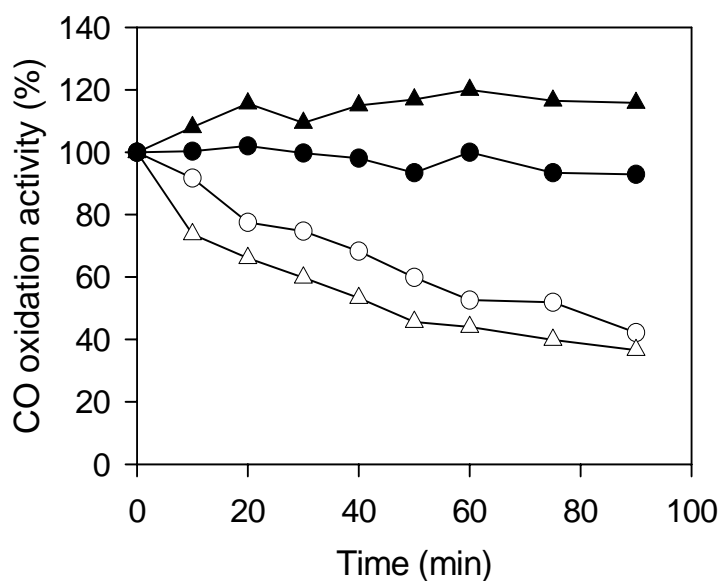


Fig. 15. Sulfide-dependent thermostability of native $\text{CODHII}_{\text{Ch}}$. Stability at 70 °C of the NiS_4 -conformation (●, ○) and of the NiS_3 -conformation (▲, △) of the enzyme ($0.11 \mu\text{g ml}^{-1}$) incubated under N_2 with 4 mM Ti(III) citrate in the presence of 1.5 mM Na_2S (closed symbols) and in the absence of Na_2S (open symbols). 100 % of CO oxidation activity corresponds to 16,400 and 10,700 units mg^{-1} for NiS_4 - and NiS_3 -conformations, respectively. For further details, see chapter 6.

In the absence of external sulfide, the enzymes lose their thermostability even under N_2 , but the half-life of CODH_{Ch} with the NiS₄-conformation is two times higher than the half-life of the enzyme with the NiS₃-conformation (chapter 6).

This indicates that the μ_2S ligand can also dissociate when the external sulfide concentration is lowered significantly, which leads to destabilization of the active center. At 25 °C, both forms are stable regardless of the addition of external sulfide as well as the type of the gas phase (CO or N_2). These results suggest that at high growth temperatures of *C. hydrogenoformans* in sulfide-rich (normally in millimolar concentrations) volcanic habitats the NiS₄-conformation of cluster C is the biologically relevant species.

3.5.3 The bridging μ_2S diminishes the CO₂ reduction activity

Ecologically, the extremely thermophilic anaerobe *C. hydrogenoformans* lives in CO-limited and CO₂-rich highly reducing hot volcanic environments (Svetlitchnyi *et al.* 1991A, B). As introduced before, all anaerobic NiFe-CODHs are able to perform both forward (oxidation of CO) and reverse (reduction of CO₂) reactions. Both reactions proceed at the same active site. Since CO is the sole source of energy and carbon for the growth of *C. hydrogenoformans* (Svetlitchnyi *et al.* 1991A, B), the active center should prevent binding of CO₂ to ensure the survival of the bacteria under the CO-limited harsh conditions. This aspect brought the hypothesis that the bridging μ_2S may prevent binding of CO₂ because the position of μ_2S may reduce the accessibility of CO₂ to the Ni ion. To prove this assumption the affinities of CO to the NiS₄- and the NiS₃-conformation of cluster C were compared and the effect of bridging μ_2S on CO₂ reduction was examined. The results of the analysis of initial activity versus CO concentrations show that the NiS₄-conformation has an approximately two times lower K_M value for CO, has obviously higher initial activity at low CO concentrations and displays 4.2-fold higher K_{cat}/K_m values compared to the NiS₃-conformation (Fig. 16) (chapter 6). These data indicate that the NiS₄-coordinated cluster C has better catalytic efficiency of CO oxidation than the NiS₃-form at CO concentrations of natural habitats.

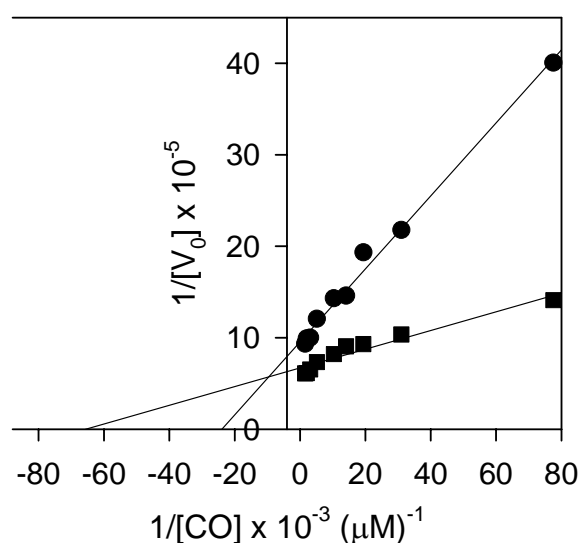


Fig. 16. Catalytic efficiencies of CODHII_{Ch} with NiS₄- (■) and NiS₃-conformation (●). The double reciprocal plot of initial activity (V_0 in units mg^{-1}) versus CO concentration. The different CO concentrations were established by adding the appropriate amounts of CO-saturated reaction mixture to assays containing the same reaction mixture saturated with N₂. K_{cat}/K_m of $2.3 \cdot 10^9$ and $5.5 \cdot 10^8 \text{ M}^{-1} \text{ s}^{-1}$ correspond to NiS₄- and NiS₃-conformation, respectively. For further details, see chapter 6.

Unlike sulfide-dependent activation of CO oxidation, sulfide strongly inhibits the CO₂ reduction activity of CODHII_{Ch} under turnover conditions in the presence of hemoglobin (Fig. 17A). Although the level of inhibition depends on the sulfide concentration, the CO₂ reduction activity cannot be inhibited completely at millimolar concentrations of sulfide (chapter 6). Inhibition in hemoglobin-dependent assay is not due to any interaction of sulfide with hemoglobin because sulfide did not alter CO trapping ability of hemoglobin and had no effect on absorption spectra of carboxyhemoglobin upon binding of CO. Moreover, hemoglobin-independent CO evolution assay also shows sulfide-dependence inhibition of CODHII_{Ch} on CO₂ reduction (Fig. 17B) (chapter 6).

This negative effect of sulfide on the reverse reaction implies that the NiS₃-form of cluster C is the more appropriate structure for CO₂ reduction rather than NiS₄-form. Indeed, the NiS₃-coordinated cluster C displays 56 % higher CO₂ reduction activity than NiS₄-conformation when the enzyme is assayed in the absence of sulfide with Ti(III) citrate as electron donor (chapter 6). Furthermore, the activity is lowered with dithionite as electron donor instead of Ti(III) citrate (chapter 6) indicating inhibition by dithionite-derived sulfide (Robert and Rajagopalan 1982; Das and Kanatzidis 1995).

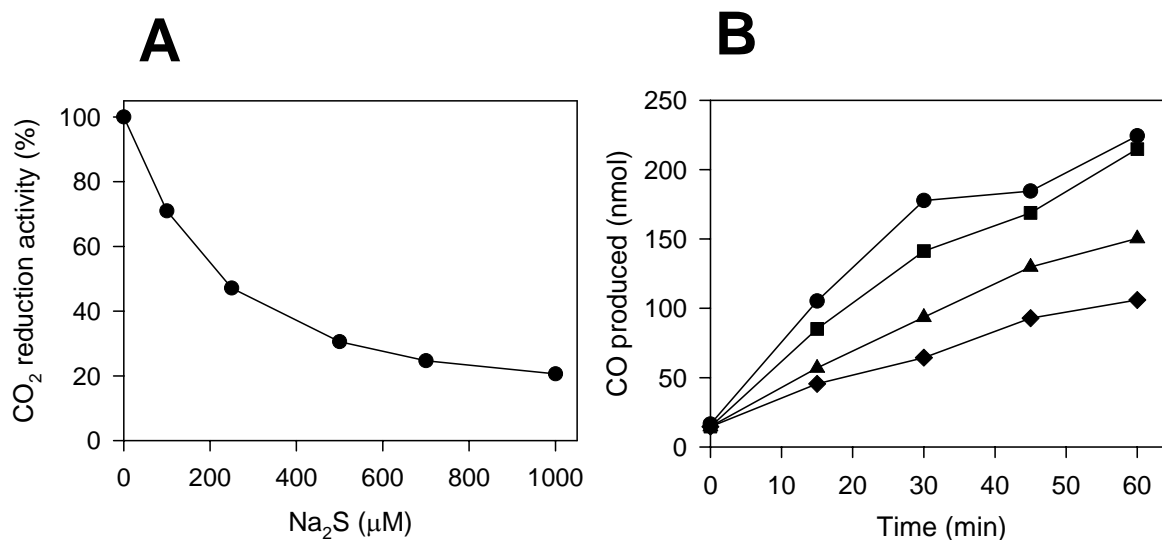


Fig. 17. Effect of sulfide on reduction of CO₂ in CODHII_{Ch}. (A) Sulfide-dependent inhibition of CO₂ reduction activity of CODHII_{Ch} in hemoglobin-based assay. Assays contained 0.1 μg ml⁻¹ of CODHII_{Ch} containing NiS₃-coordinated cluster C. (B) Head space analysis of CO₂ reduction to CO. As-isolated CODHII_{Ch} (8 μg) was incubated in the presence of 0 (●), 0.5 (■), 1 (▲), or 2 (◆) mM Na₂S at 25 °C. CO in headspace was quantified by gas chromatography. For further details, see chapter 6.

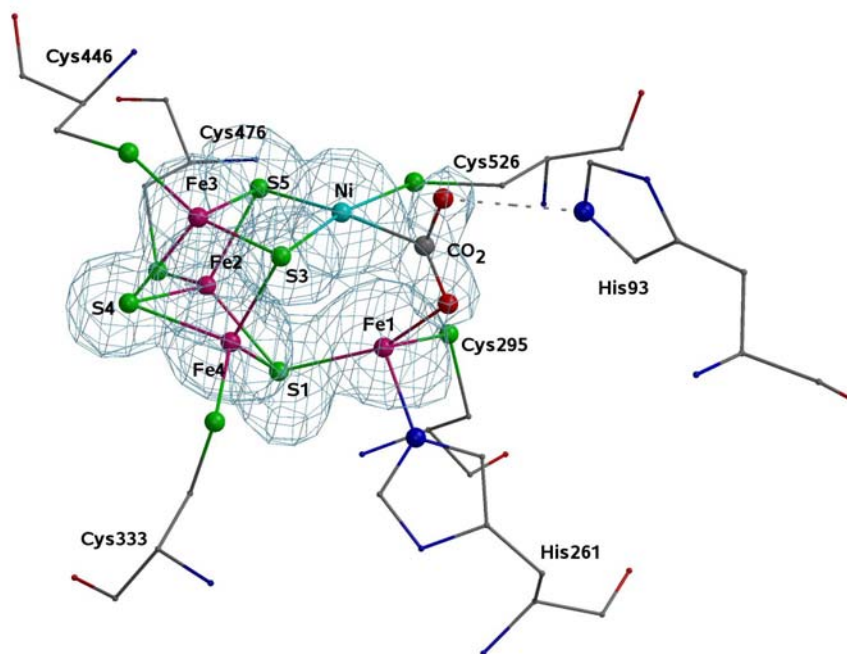


Fig. 18. Crystal structure of cluster C in native CODHII_{Ch} with bound CO₂. A $F_{\text{obs}} - F_{\text{calc}}$ omit electron density map is depicted in blue. The model presents a complex with 50% occupancy of CO₂. Fe atom colored in purple, S atom in green, Ni atom in cyan, O atom in red, N atom in blue, and C atom in gray. For further details, see chapter 6.

The crystal structure of the CO₂ loaded NiS₃-conformation of cluster C in a recombinant CODHII_{Ch} further supports this assumption (Jeoung and Dobbek 2007). CO₂ binding to the NiS₄-form is only possible after removal of free sulfide by extensive washing (chapter 6). Approximately 50% of μ₂S was replaced by the carboxylic acid group bridging Ni and Fe1 in NaHCO₃ soaked crystals of CODHII_{Ch} after removal of free sulfide (Fig. 18). On the contrary, no bound-CO₂ could be identified in NaHCO₃ soaked crystals of CODHII_{Ch} before removal of free sulfide. From the results, it can be suggested that the μ₂S ligand governs the activity towards CO oxidation and restrains the unwanted reaction of CO₂ reduction.

3.6 Mechanism of CO oxidation in cluster C of native CODHII_{Ch}

As the results of sulfide-dependent activation of CO oxidation, sulfide-dependent inhibition of CO₂ reduction, and reversible inhibition by cyanide, the improved mechanism of CO oxidation at the active site of CODHII_{Ch} is proposed here as follows:

The reaction starts from the highly stable resting state of cluster C in the [Ni-4Fe-5S]-conformation which preserves the functional enzyme in the absence of CO. An incoming CO molecule through the substrate channel reaches the active site (Fig. 19A). One scenario assumes its binding to the unoccupied apical position of the Ni coordinated by 4 S ligands. The μ₂S ligand is labilized by the binding of CO and dissociates from the Ni as S²⁻ ion; then it stays in a cavity or in the vicinity of Ni. A simultaneous rearrangement leads to a transient [Ni-4Fe-4S]-conformation of square-planar Ni with 3 S and one CO ligands (Fig. 19B). The proposed rearrangement agrees with the models describing the conversion of CO by a nickel to sulfur rebound mechanism studied with model compounds containing four-coordinated nickel (Sellmann *et al.* 2000; Fan and Hall 2004). The second scenario assumes direct displacement of μ₂S by CO resulting in planar Ni-carbonyl (Fig. 19B). A water molecule binds as OH⁻ to Fe1 as proposed previously (DeRose *et al.* 1998) and identified in recombinant CODHII_{Ch} (Jeoung and Dobbek 2007). This reestablishes the [Ni-4Fe-5S]-conformation with covalently bound CO and transiently bound OH⁻ in

place of the bridging $\mu_2\text{S}$ (Fig. 19C). The Ni-bound CO undergoes a nucleophilic attack by the Fe1-bound OH leading to the formation of a Ni- and Fe1-bridging carboxylic acid group (Fig. 19D), which is subsequently deprotonated by the neighboring basic residues (His⁹³ and Lys⁵⁶³) forming a proton transfer network (Kim et al. 2004). Finally, the S^{2-} ion displaces the preformed CO_2 and reconstitutes the Ni- ($\mu_2\text{S}$)-Fe1 bridge (Fig. 19A), converting the unstable NiS_3 -conformation to a stable NiS_4 -conformation, and a new reaction cycle can proceed.

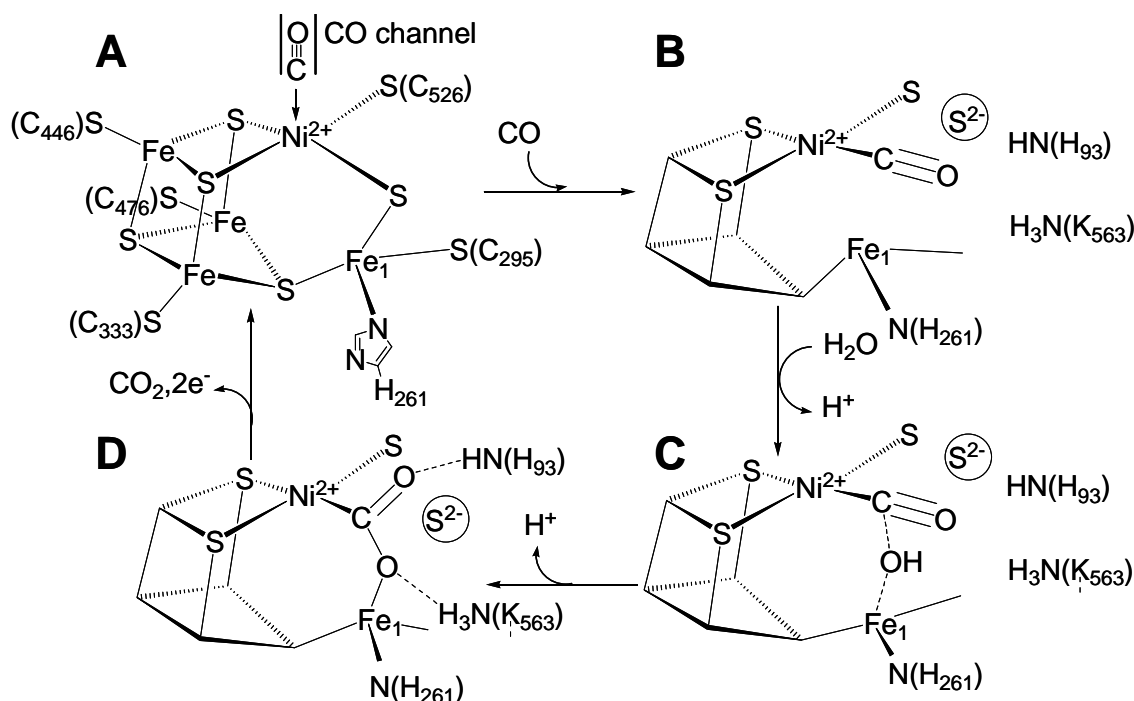


Fig. 19. Proposed mechanism of CO oxidation of CODHII_{Ch}. Scheme showing the oxidation of CO to CO₂ and the function of the bridging $\mu_2\text{S}$ in the [Ni-4Fe-5S] cluster of CODHII_{Ch} from CO grown *C. hydrogeniformans*. For further details, see chapter 6.

3.7 Conclusions

The binding position of CO at the active site cluster C of native CODHII_{Ch} was investigated using a CO analogous inhibitor potassium cyanide. In addition, the important functions of the bridging μ_2 S for CO-dependent growth of *C. hydrogenoformans* were demonstrated.

Potassium cyanide displays two different modes of interaction with cluster C of native CODHII_{Ch} depending on the redox states of the enzyme. Cyanide inhibits native CODHII_{Ch} and competes with CO for the same binding position in cluster C when the enzyme is in highly reduced state. In contrast, cyanide does not behave as CO analogue with oxidized cluster C. X-ray absorption spectroscopy (XAS) shows that the inhibition of reduced CODHII_{Ch} is caused by cyanide binding to the nickel ion in cluster C that apparently represents the position for CO binding. XAS on cyanide-inhibited CODHII_{Ch} incipiently reveals that one of the four square-planar sulfur ligands is replaced by the carbon atom of cyanide with no change of the Ni geometry. Crystal structure of reversibly inhibited CODHII_{Ch} supports the results of the XAS studies, shows the displacement of μ_2 S by cyanide, and provides further insight into the conformational changes during CO oxidation. The cyanide-bound conformation likely represents an appropriate structural model for the unstable NiS₃-coordinated cluster C, which can be easily converted to a NiS₄-conformation by incorporation of sulfide as the bridging μ_2 S. The square-planar coordination of Ni by 4 S ligands is reestablished when bound cyanide is dissociated from the enzyme by reactivation with external sulfide, whereas reactivation in the absence of sulfide yields the NiS₃-coordinated cluster C lacking the μ_2 S.

Both conformations of cluster C, the NiS₄- and NiS₃-coordination, oxidize CO to CO₂, which reflects that the bridging μ_2 S is not obligately required for catalytic CO oxidation. Nevertheless, the NiS₄-conformation of cluster C containing the bridging μ_2 S displays better catalytic efficiency than the NiS₃-conformation. It is obvious that sulfide enhances CO oxidation activity of CODHII_{Ch} containing the NiS₃-form under turnover conditions. In contrast, sulfide strongly inhibits catalytic activity of CODHII_{Ch} in the physiologically unwanted reverse reaction; i.e. the bridging μ_2 S prevents the binding of CO₂ to the Ni ion. Sulfide-dependent activation of the forward

reaction and inhibition of the reverse reaction indicate that $\mu_2\text{S}$ controls the catalytic activity of CODHIII_{Ch}. Thus, it accelerates the physiologically relevant CO oxidation, prevents the inhibition by the product CO_2 , and inhibits the non-physiological CO_2 reduction. This function is especially important under highly reducing, CO-limited and CO_2 -rich conditions in volcanic environments (Svetlitchnyi *et al.* 1991A, B; Stetter 1999; Kelley *et al.* 2002), which would favor the CO_2 reduction activity of the enzyme.

Besides catalytic functions, the bridging $\mu_2\text{S}$ stabilizes the active site cluster C at high growth temperature of the bacteria. Stabilization prevents inactivation via removal of Ni and decomposition of the cluster as observed in several crystal structures (Dobbek *et al.* 2004; Jeoung and Dobbek 2007) and is essential at 70 °C. Sulfide significantly improves stability by maintenance of the Ni-($\mu_2\text{S}$)-Fe1 subsite. Since the hydrogenogenic bacterium *C. hydrogenoformans* produces H_2S (Svetlitchnyi *et al.* 2001; Henstra and Stams 2004) and lives in volcanic vents with millimolar concentrations of sulfide (Stetter 1999; Kelley *et al.* 2002), the stabilization of the enzyme by $\mu_2\text{S}$ is physiologically relevant.

4 REFERENCES

- Abbanat, D. R. and Ferry, J. G.** (1990) Synthesis of acetyl coenzyme A by carbon monoxide dehydrogenase complex from acetate-grown *Methanosarcina thermophila*. *J. Bacteriol.* **172**: 7145-7150.
- Alonso, J. R., Cardellach, F., Lopez, S., Casademont, J., and Miro, O.** (2003) Carbon monoxide specifically inhibits cytochrome c oxidase of human mitochondrial respiratory chain. *Pharmacol. Toxicol.* **93**: 142-146.
- Anderson, M. E. and Lindahl, P. A.** (1994) Organization of Clusters and internal electron pathways in CO dehydrogenase from *Clostridium thermoaceticum*: Relevance to the mechanism of catalysis and cyanide inhibition. *Biochemistry* **33**: 8702-8711.
- Anderson, M. E. and Lindahl, P. A.** (1996) Spectroscopic states of the CO oxidation/CO₂ reduction active site of carbon monoxide dehydrogenase and mechanistic implications. *Biochemistry* **35**: 8371-8380.
- Arnold, S.** (2006) Synthese von Acetyl-CoA durch die monomere Acetyl-CoA-synthase aus *Carboxydotherrnus hydrogenoformans*. Diplomarbeit, Lehrstuhl für Mikrobiologie, Universität Bayreuth, Germany.
- Bassham, J. A., Benson, A. A., and Calvin, M.** (1950) The path of carbon in photosynthesis. VIII. The role of malic acid. *J. Biol. Chem.* **185**: 781-787.
- Bonam, D. and Ludden, P. W.** (1987) Purification and characterization of carbon monoxide dehydrogenase, a nickel, zink, iron-sulfur protein, from *Rhodospirillum rubrum*. *J. Biol. Chem.* **262**: 2980-2987.
- Bonam, D., Murrell, S. A., and Ludden, P. W.** (1984) Carbon monoxide dehydrogenase from *Rhodospirillum rubrum*. *J. Bacteriol.* **159**: 693-699.
- Brunori, M., Anonini, G., Castagnola, M., and Bellelli, A.** (1992) Cooperative cyanide dissociation from ferrous hemoglobin. *J. Biol. Chem.* **267**: 2258-2263.

- Chen, J., Huang, S., Seravalli, J., Gutzman, H. Jr., Swartz, D. J., Ragsdale, S. W., and Bagley, K. A.** (2003) Infrared studies of carbon monoxide binding to carbon monoxide dehydrogenase/acetyl-CoA synthase from *Moorella thermoacetica*. *Biochemistry* **42**: 14822-14830.
- Colpas, G. J., Maroney, M. J., Bagyinka, C., Kumar, M., Willis, W. S., Suib, S. L., Baidya, N., and Mascharak, P. K.** (1991) X-ray spectroscopic studies of nickel complexes, with application to the structure of nickel sites in hydrogenases. *Inorg. Chem.* **30**: 920-928.
- Coyle, C. L. and Stiefel, E. I.** (1988) The coordination chemistry of nickel: an introductory survey, p. 1-28. In *J. R. J. Lancaster* (ed.), *The bioinorganic chemistry of nickel*. VCH Publishers, New York.
- Crabtree, R. H.** (1988) *The organometallic chem of the transition metals*. John Wiley, New York.
- Darnault, C., Volbeda, A., Kim, E. J., Legrand, P., Vernede, X., Lindahl, P. A., and Fontecilla-Camps, J. C.** (2003) Ni-Zn-[Fe(4)-S(4)] and Ni-Ni-[Fe(4)-S(4)] clusters in closed and open alpha subunits of acetyl-CoA synthase/carbon monoxide dehydrogenase. *Nat. Struct. Biol.* **10**: 271-279.
- Das, B. K. and Kanatzidis, M. G.** (1995) Formation of thioarsenide from the reductive coupling of dithionite and arsenite under hydrothermal conditions. Synthesis of (Ph₄P)[Fe₂(AsS)(CO)₆]. *Inorg. Chem.* **34**: 6505-6508.
- DeRose, V. J., Telser, J., Anderson, M. E., Lindahl, P. A., and Hoffman, B. M.** (1998) A multinuclear ENDOR study of the C-cluster in CO dehydrogenase from *Clostridium thermoaceticum*: evidence for H_xO and histidine coordination to the [Fe₄S₄] center. *J. Am. Chem. Soc.* **120**: 8767-8776.
- Dobbek, H., Svetlitchnyi, V., Liss, J., and Meyer, O.** (2004) Carbon monoxide induced decomposition of the active site [Ni-4Fe-5S] cluster of CO dehydrogenase. *J. Am. Chem. Soc.* **126**: 5382-5387.

- Dobbek, H., Gremer, L., Kiefersauer, R., Huber, R., and Meyer, O.** (2002) Catalysis at a dinuclear [CuSMo(=O)OH] cluster in a CO dehydrogenase resolved at 1.1-Å resolution. *Proc. Natl. Acad. Sci. USA* **99**: 15971-15976.
- Dobbek, H., Svetlitchnyi, V., Gremer, L., Huber, R., and Meyer, O.** (2001) Crystal structure of a carbon monoxide dehydrogenase reveals a [Ni-4Fe-5S] cluster. *Science* **293**: 1281-1285
- Dobbek, H., Gremer, L., Meyer, O., and Huber, R.** (1999) Crystal structure and mechanism of CO dehydrogenase, a molybdo iron-sulfur flavoprotein containing S-selanylcytein. *Proc. Natl. Acad. Sci. USA* **96**: 8884-8889.
- Doukov, T. I., Iverson, T., Seravalli, J., Ragsdale, S. W., and Drennan, C. L.** (2002) A Ni-Fe-Cu center in a bifunctional carbon monoxide dehydrogenase/acetyl-CoA synthase. *Science* **298**: 567-572.
- Drake, H. L.** (1994) Acetogenesis, acetogenic bacteria, and the acetyl-Co A “Wood/Ljungdahl” pathway: past and current perspectives., p. 3-60. In H. L. Drake (ed.), *Acetogenesis*. Chapman & Hall, Inc., New York.
- Drake, H. L., and Hu, S. I., and Wood, H. G.** (1981) Purification of five components from *Clostridium thermoaceticum* which catalyze synthesis of acetate from pyruvate and methyltetrahydrofolate. Properties of phosphotransacetylase. *J. Biol. Chem.* **256**: 11137-11144.
- Drake, H. L., Hu, S. I., and Wood, H. G.** (1980) Purification of carbon monoxide dehydrogenase, a nickel enzyme from *Clostridium thermoaceticum*. *J. Biol. Chem.* **255**: 7174-7180.
- Drennan, C. L., Heo, J., Sintchank, M. D., Schreiter, E., and Ludden, P. W.** (2001) Life on carbon monoxide: X-ray structure of *Rhodospirillum rubrum* Ni-Fe-S carbon monoxide dehydrogenase. *Proc. Natl. Acad. Sci. USA* **98**: 11973-11978.
- Eikmanns, B., Fuchs, G., and Thauer, R. K.** (1985) Formation of carbon monoxide from CO₂ and H₂ by *Methanobacterium thermoautotrophicum*. *Eur. J. Biochem.* **146**: 149-154.

- Ensign, S. A., Hyman, M. R., and Ludden, P. W.** (1989) Nickel-specific, slow-binding inhibition of carbon monoxide dehydrogenase from *Rhodospirillum rubrum* by cyanide. *Biochemistry* **28**: 4973-4979.
- Evans, M. C., Buchanan, B. B., and Arnon, D. I.** (1966) A new ferredoxin-dependent carbon reduction cycle in a photosynthetic bacterium. *Proc. Natl. Acad. Sci. USA* **55**: 928-934.
- Fan, Y. and Hall, M. B.** (2004) Density functional calculations on the conversion of azide and carbon monoxide to isocyanate and dinitrogen by a nickel to sulfur rebound mechanism. *Chem. Eur. J.* **10**: 1805-1814.
- Feng, J. and Lindahl, P. A.** (2004) Effect of sodium sulfide on Ni-containing carbon monoxide dehydrogenases. *J. Am. Chem. Soc.* **126**: 9094-9100.
- Ferry, J. G.** (1999) Enzymology of one-carbon metabolism in methanogenic pathways. *FEMS Microbiol. Rev.* **23**: 13-38.
- Fraser, D. M. and Lindahl, P. A.** (1999) Evidence for a proposed intermediate redox state in the CO/CO₂ active site of acetyl-CoA synthase (Carbon monoxide dehydrogenase) from *Clostridium thermoaceticum*. *Biochemistry* **38**: 15706-15711
- Gerhardt, M., Svetlichny, V., Sokolova, T. G., Zavarzin, G. A., and Ringpfeil, M.** (1991) Bacterial CO utilization with H₂ production by the strictly anaerobic lithoautotrophic thermophilic bacterium *Carboxydotherrmus hydrogenus* DSM 6008 isolated from a hot swamp. *FEMS Microbiol. Lett.* **83**: 267-272.
- Gnida, M., Ferner, R., Gremer, L., Meyer, O., and Meyer-Klaucke, W.** (2003) A novel binuclear [CuSMo] cluster at the active site of carbon monoxide dehydrogenase: characterization by X-ray absorption spectroscopy. *Biochemistry* **42**: 222-230.
- Grahame, D. A. and Stadtman, T. C.** (1987) Carbon monoxide dehydrogenase from *Methanosarcina barkeri*. Disaggregation, purification, and physicochemical properties of the enzyme. *J Biol Chem.* **262**: 3706-3712.

- Gu, W., Seravalli, J., Ragsdale, S. W., and Cramer, S. P.** (2004) CO-induced structural rearrangement of the C cluster in *Carboxydothemus hydrogenoformans* CO dehydrogenase – evidence from Ni K-edge X-ray absorption spectroscopy. *Biochemistry* **43**: 9029-9035.
- Ha, S.-W., Korbas, M., Klepsch, M., Meyer-Klaucke, W., Meyer, O., and Svetlitchnyi, V.** (2007) Interaction of potassium cyanide with the [Ni-4Fe-5S] active site cluster of CO dehydrogenase from *Carboxydothemus hydrogenoformans*. *J. Biol. Chem.* **282**: 10639-10646.
- Haldane, J.** (1895) The action of carbonic oxide on man. *J. Physiol.* **18**: 430-462.
- Henstra, A. M. and Stams, A. J.** (2004) Novel physiological features of *Carboxydothemus hydrogenoformans* and *Thermoterrabacterium ferrireducens*. *Appl. Environ. Microbiol.* **70**: 7236-40.
- Holo, H.** (1989) *Chloroflexus aurantiacus* secretes 3-hydroxypropionate, a possible intermediate in the assimilation of CO₂ and acetate. *Arch. Microbiol.* **151**: 252-256.
- Hu, Z. G., Spangler, N. J., Anderson, M. E., Xia, J. Q., Ludden, P. W., Lindahl, P. A., and Münck, E.** (1996) Nature of the C-cluster in Ni-containing carbon monoxide dehydrogenases. *J. Am. Chem. Soc.* **118**: 830-845.
- Hugenholtz, J. and Ljungdahl, L. G.** (1989) Electron transport and electrochemical proton gradient in membrane vesicles of *Clostridium thermoautotrophicum*. *J. Bacteriol.* **171**: 2873-2875.
- Iciek, M. and Wlodek, L.** (2001) Biosynthesis and biological properties of compounds containing highly reactive, reduced sulfane sulfur. *Pol. J. Pharmacol.* **53**: 215-225.
- Jeong, J. H. and Dobbek, H.** (2007) Carbon Dioxide activation at the Ni,Fe-cluster of anaerobic carbon monoxide dehydrogenase. *Science* **318**: 1461-1464.
- Khalil, M. A. K. and Rasmussen, R. A.** (1984) Carbon monoxide in the earth's atmosphere: increasing trend. *Science* **224**: 54-56.

- Kelley, D. S., Baross, J. A., and Delaney, J. R.** (2002) Volcanoes, fluids, and life at mid-ocean ridge spreading centers. *Annu. Rev. Earth. Planet. Sci.* **30**: 385-491.
- Kim, E. J., Feng, J., Bramlett, M. R., Lindahl, P. A.** (2004) Evidence for a proton transfer network and a required persulfide-bond-forming cystein residue in Ni-containing carbon monoxide dehydrogenases. *Biochemistry* **43**: 5728-5734.
- Klatt, C. G., Bryant, D. A., and Ward, D. M.** (2007) Comparative genomics provides evidence for the 3-hydroxypropionate autotrophic pathway in filamentous anoxygenic phototrophic bacteria and in hot spring microbial mats. *Environ. Microbiol.* **9**: 2067-2078.
- Kumar, M., Lu, W.-P., and Ragsdale, S. W.** (1994) Binding of carbon disulfide to the site of acetyl-CoA synthesis by the nickel-iron-sulfur protein, CO dehydrogenase, from *Clostridium thermoaceticum*. *Biochemistry* **33**: 9769-9777.
- Kumar, M., Lu, W.-P., Liu, L., and Ragsdale, S. W.** (1993) Kinetic evidence that CO dehydrogenase catalyzes the oxidation of CO and the synthesis of acetyl-CoA at separate metal centers. *J. Am. Chem. Soc.* **115**: 11646-11647.
- Ljungdahl, L. G.** (1986) The autotrophic pathway of acetate synthesis in acetogenic bacteria. *Annu. Rev. Microbiol.* **40**: 415-450.
- Lindahl, P. A.** (2002) The Ni-containing carbon monoxide dehydrogenase family: light at the end of the tunnel? *Biochemistry* **41**: 2097-2105.
- Lindahl, P. A., Münck, E., and Ragsdale, S. W.** (1990A) CO-dehydrogenase from *Clostridium thermoaceticum*: EPR and electrochemical studies in CO₂ and argon atmospheres. *J. Biol. Chem.* **265**: 3873-3879.
- Lindahl, P. A., Ragsdale, S. W., and Münck, E.** (1990B) Mössbauer studies of CO dehydrogenase from *Clostridium thermoaceticum*. *J. Biol. Chem.* **265**: 3880-3888.
- Macgregor, S. A., Lu, Z., Eisenstein, O., and Crabtree, R. H.** (1994) Why nickel (II) binds CO best in trigonal bipyramidal and square pyramidal geometries and possible consequences for CO dehydrogenase. *Inorg. Chem.* **33**: 3616-3618.

- Meyer, O., Gremer, L., Ferner, R., Ferner, M., Dobbek, H., Gnida, M., Meyer-Klaucke, W., and Huber, R.** (2000) The role of Se, Mo, and Fe in the structure and function of carbon monoxide dehydrogenase. *Biol. Chem.* **381**: 865-876.
- Meyer, O., Frunzke, K., and Mörsdorf, G.** (1993) Biochemistry of the aerobic utilization of carbon monoxide. In *Microbial growth on C1 compounds*, p.433-459. J. C. Murrell, and D. P. Kelly, Eds., Intercept, Ltd., Andover, MA.
- Meyer, O., Jacobitz, S., and Kruger, B.** (1986) Biochemistry and physiology of aerobic carbon monoxide-utilizing bacteria. *FEMS Microbiol. Rev.* **39**: 161-179.
- Meyer, O. and Schlegel, H. G.** (1983) Biology of aerobic carbon monoxide-oxidizing bacteria. *Annu Rev Microbiol.* **37**: 277-310.
- Mörsdorf, G., Frunzke, K., Gadkari, D., and Meyer, O.** (1992) Microbial growth on carbon monoxide. *Biodegradation* **3**: 61-82.
- Omaye S. T.** (2002) Metabolic modulation of carbon monoxide toxicity. *Toxicology* **180**: 139-150.
- Pasquali, M., and Floriani, C.** (1983) Copper(I)-carbon monoxide Chemistry: Recent Advances and perspectives in Copper Coordination Chemistry: *Biochemical and Inorganic Perspectives* (Karlin, K. D., and Zubieta, J., Eds.) pp 311-330, Adenine Press, Guilderland, NY.
- Poston, J. M., Kuratomi, K., and Stadtman, E. R.** (1964) Methyl-bitamin B₁₂ as a source of methyl groups fro the synthesis of acetate by cell-free extracts of *Clostridium thermoaceticum*. *Ann. Y.N. Acad. Sci.* **112**: 804-806.
- Qiu, D., Kumar, M., Ragsdale, S. W., and Spiro, T. G.** (1996) Raman and infrared spectroscopy of cyanide-inhibited CO dehydrogenase/acetyl-CoA synthase from *Clostridium thermoaceticum*: Evidence for bimetallic enzymatic CO oxidation. *J. Am. Chem. Soc.* **118**: 10429-10435.
- Ragsdale, S. W. and Pierce, E.** (2008) Acetogenesis and the Wood-Ljungdahl pathway of CO₂ fixation. *Biochim. Biophys. Acta* (Article in press).

Ragsdale, S. W. (2004) Life with carbon monoxide. *Crit. Rev. Biochem. Mol. Biol.* **39**: 165-195.

Ragsdale, S. W. (1997) The Eastern and Western branches of the Wood/Ljungdahl pathway: how the East and West were born. *BioFactors* **9**: 1-9.

Ragsdale, S. W. and Kumar, M. (1996) Nickel-containing carbon monoxide dehydrogenase/acetyl-CoA synthase. *Chem. Rev.* **96**: 2515-2539.

Ragsdale, S. W., Clark, J. E., Ljungdahl, L. G., Lundie, L. L., and Drake, H. L. (1983) Properties of purified carbon monoxide dehydrogenase from *Clostridium thermoaceticum*, a nickel, iron-sulfur protein. *J. Biol. Chem.* **258**: 2364-2369.

Resch, M., Dobbek, H., and Meyer, O. (2005) Structural and functional reconstruction *in situ* of the [CuSMoO₂] active site of carbon monoxide dehydrogenase from the carbon monoxide oxidizing eubacterium *Oligotropha carboxidovorans*. *J. Biol. Inorg. Chem.* **10**: 518-528.

Robert, C. W. and Rajagopalan, K. V. (1982) Evidence for the inorganic nature of the cyanolyzable sulfur of molybdenum hydroxylase. *J. Biol. Chem.* **257**: 1354-1359.

Russell, W. K., Stalhandske, C. M. V., Xia, J. Q., Scott, R. A., and Lindahl, P. A. (1998) Spectroscopic, redox, and structural characterization of the Ni-labile and nonlabile forms of the acetyl-CoA synthase active site of carbon monoxide dehydrogenase. *J. Am. Chem. Soc.* **120**: 7502-7510.

Sellmann, D., Geipel, F., and Heinemann, F. W. (2000) Activation and desoxygenation of CO, CO₂, and SO₂ with sulfur-rich azide and amide [Ni(L)(S₃')] complexes (S₃'²⁻ = Bis (2-mercaptophenyl) sulfide (2-)). *Chem. Eur. J. Transition metal complexes with sulfur ligands part 146.* **6**: 4279-4284.

Seravalli, J., Kumar, M., Lu, W.-P., and Ragsdale, S. W. (1997) Mechanism of carbon monoxide oxidation by the carbon monoxide dehydrogenase/acetyl-CoA synthase from *Clostridium thermoaceticum*: kinetic characterization of the intermediates. *Biochemistry* **36**: 11241-11251.

- Shiba, H., Kawasumi, T., Igarashi, Y., Kodama, T., and Minoda, Y.** (1985) The CO₂ assimilation via the reductive tricarboxylic acid cycle in an obligately autotrophic, aerobic hydrogen-oxidizing bacterium, *Hydrogenobacter thermophilus*. *Arch. Microbiol.* **141**: 198-203.
- Soboh, B., Linder, D., and Hedderich, R.** (2002) Purification and catalytic properties of a CO-oxidizing:H₂-evolving enzyme complex from *Carboxydotherrmus hydrogenoformans*. *Eur. J. Biochem.* **269**: 5712-5721.
- Spangler, N. J., Lindahl, P. A., Bandarian, V., and Ludden, P. W.** (1996) Spectroelectrochemical characterization of the metal centers in carbon monoxide dehydrogenase (CODH) and nickel-deficient CODH from *Rhodospirillum rubrum*. *J. Biol. Chem.* **271**: 7973-7977.
- Stetter, K. O.** (1999) Extremophiles and their adaptation to hot environments. *FEBS Letters Review* **452**: 22-25.
- Strauss, G. and Fuchs, G.** (1993) Enzymes of a novel autotrophic CO₂ fixation pathway in the phototrophic bacterium *Chloroflexus aurantiacus*, the 3-hydroxypropionate cycle. *Eur. J. Biochem.* **215**: 633-643.
- Svetlitchnyi, V., Dobbek, H., Meyer-Klaucke, W., Meins, T., Thiele, B., Römer, P., Huber, R., and Meyer, O.** (2004) A functional Ni-Ni-[4Fe-4S] cluster in the monomeric acetyl-CoA synthase from *Carboxydotherrmus hydrogenoformans*. *Proc. Natl. Acad. Sci. USA* **101**: 446-451.
- Svetlitchnyi, V., Peschel, C., Acker, G., and Meyer, O.** (2001) Two membrane-associated NiFeS-carbon monoxide dehydrogenases from the anaerobic carbon monoxide utilizing eubacterium *Carboxydotherrmus hydrogenoformans*. *J. Bacteriol.* **183**: 5134-5144.
- Svetlichny, V. A., Sokolova, T. G., Kostrikina, N. A., and Zavarzin, G. A.** (1991A) Anaerobic extremely thermophilic carboxydotrophic bacteria in hydrotherms of Kuril Islands. *Microb. Ecol.* **21**: 1-10.

- Svetlichny, V. A., Sokolova, T. G., Gerhardt, M., Ringpfeil, M., Kostrikina, N. A., and Zavarzin, G. A.** (1991B) *Carboxydotherrnus hydrogenoformans* gen. nov., sp. Nov., a CO-utilizing thermophilic anaerobic bacterium from hydrothermal environments of Kunashir island. *Syst. Appl. Microbiol.* **14**: 254-260.
- Tan, G. O., Ensign, S. A., Ciurli, S., Scott, M. J., Hedman, B. Holm, R. H., Ludden, P. W., Korszun, Z. R., Stephens, P. J., and Hodgson, K. O.** (1992) On the structure of the nickel/iron/sulfur center of the carbon monoxide dehydrogenase from *Rhodospirillum rubrum*: An x-ray absorption spectroscopy study. *Proc. Natl. Acad. Sci. USA* **89**: 4427-4431.
- Ubuka, T.** (2002) Assay methods and biological roles of labile sulfur in animal tissues. *J. Chromatogr. B* **781**: 227-249.
- Voet, D. and Voet, J. G.** (1995) *Biochemistry*, 2nd ed. John Wiley, New York.
- Wahl, R. C. and Rajagopalan, K. V.** (1982) Evidence for the inorganic nature of the cyanolyzable sulfur of molybdenum hydroxylases. *J. Biol. Chem.* **257**: 1354-1359.
- Westley, J.** (1981) Thiosulfate: cyanide sulfurtransferase (rhodanese). *Methods in Enzymology* **77**: 285-291.
- Wood, J.** (1987) Sulfane sulfur. *Methods in Enzymology* **143**: 25-29.
- Wu, M., Ren, Q., Durkin, A. S., Daugherty, S. C., Brinkac, L. M., Dodson, R. J., Madupu, R., Sullivan, S. A., Kolonay, J. F., Nelson, W. C., Tallon, L. J., Jones, K. M., Ulrich, L. E., Gonzalez, J. M., Zhulin, I. B., Robb, F. T., and Eisen, J. A.** (2005) Life in hot carbon monoxide: the complete genome sequence of *Carboxydotherrnus hydrogenoformans* Z-2901. *PLoS Genet.* **1**: e65.
- Yagi, T. and Tamiya, N.** (1962) Enzymic oxidation of carbon monoxide. III. Reversibility. *Biochim. Biophys. Acta* **17**: 508-509.

II Publications

5 Interaction of potassium cyanide with the [Ni-4Fe-5S] active site cluster of CO dehydrogenase from *Carboxydotherrmus hydrogenoformans*

Seung-Wook Ha^{1, ‡}, Malgorzata Korbas^{2, ‡}, Mirjam Klepsch¹,
Wolfram Meyer-Klaucke², Ortwin Meyer^{1, 3}, and Vitali Svetlitchnyi^{1, §}

¹Lehrstuhl für Mikrobiologie and ³Bayreuther Zentrum für Molekulare Biowissenschaften (BZMB), Universität Bayreuth, Universitätsstrasse 30, D-95440 Bayreuth, Germany

²European Molecular Biology Laboratory (EMBL), Outstation Hamburg at Deutsches Elektronen-Synchrotron (DESY), Notkestrasse 85, D-22603 Hamburg, Germany

[‡] Both authors contributed equally to this work

[§] Corresponding author

Tel.: 49-921-552790, Fax: 49-921-552727

E-mail: vitali.svetlitchnyi@uni-bayreuth.de

Published in Journal of Biological Chemistry (2007) **282**: 10639-10646

ABSTRACT

The Ni-Fe carbon monoxide (CO) dehydrogenase II (CODHII_{Ch}) from the anaerobic CO-utilizing hydrogenogenic bacterium *Carboxydotherrmus hydrogenoformans* catalyzes the oxidation of CO, presumably at the Ni-(μ_2 S)-Fe1 subsite of the [Ni-4S-5S] cluster in the active site. The CO oxidation mechanism proposed on the basis of several CODHII_{Ch} crystal structures involved the apical binding of CO at the nickel ion and the activation of water at the Fe1 ion of the cluster. To understand how CO interacts with the active site, we have studied the reactivity of the cluster with potassium cyanide and analyzed the resulting type of nickel coordination by x-ray absorption spectroscopy. Cyanide acts as a competitive inhibitor of reduced CODHII_{Ch} with respect to the substrate CO and is therefore expected to mimic the substrate. It inhibits the enzyme reversibly, forming a nickel cyanide. In this reaction, one of the four square-planar sulfur ligands of nickel is replaced by the carbon atom of cyanide, suggesting removal of the μ_2 S from the Ni-(μ_2 S)-Fe1 subsite. Upon reactivation of the inhibited enzyme, cyanide is released, and the square-planar coordination of nickel by 4S ligands is recovered, which includes the reformation of the Ni-(μ_2 S)-Fe1 bridge. The results are summarized in a model of the CO oxidation mechanism at the [Ni-4Fe-5S] active site cluster of CODHII_{Ch} from *C. hydrogenoformans*.

Abbreviations footnote: CO, carbon monoxide; CODH, CO dehydrogenase; CODH-DT, dithionite-reduced CODHII_{Ch}; CODHII_{Ch}, CODH from *C. hydrogenoformans*; CODH_{Oc}, CODH from *O. carboxidovorans*; CODH_{Rr}, CODH from *R. rubrum*; CODH_{Mt}, CODH from *M. thermoacetica*; XAS, x-ray absorption spectroscopy; EXAFS, extended x-ray absorption fine structure; XANES, x-ray absorption near edge structure; DTT, dithiothreitol.

INTRODUCTION

The hydrogenogenic thermophilic bacterium *Carboxydotherrmus hydrogenoformans* utilizes CO as a sole source of energy and carbon under anaerobic chemolithoautotrophic conditions (1, 2). The oxidation of CO is catalyzed by two Ni-Fe CO dehydrogenases, designated CODHI_{Ch} and CODHII_{Ch}, according to the equation $\text{CO} + \text{H}_2\text{O} \rightarrow \text{CO}_2 + 2\text{H}^+ + 2\text{e}^-$. Crystal structures of CODHII_{Ch} in different functional states have been solved to 1.1 Å resolution (3, 4). The homodimeric enzyme contains five metal clusters, of which clusters B, B', and a subunit-bridging cluster D are conventional cubane-type [4Fe-4S] clusters (3). The active site clusters C and C' in dithionite-reduced active CODHII_{Ch} (CO oxidation activity $\approx 14,000 \mu\text{mol}$ of CO oxidized $\text{min}^{-1} \text{mg}^{-1}$ at 70 °C) have been modeled as [Ni-4Fe-5S] centers containing a Ni-($\mu_2\text{S}$)-Fe1 subsite. Their integral nickel ion is coordinated by 4S ligands with square-planar geometry (3, 4). The nickel coordination by 4S ligands in CODHII_{Ch} was also apparent from x-ray absorption spectroscopy (XAS) (5). A defined non-functional [Ni-4Fe-4S] form of cluster C can be produced by treatment of CODHII_{Ch} with CO in the absence of low potential reductants, resulting in inactivation and the loss of the bridging $\mu_2\text{S}$ (4).

It has been assumed that CODHII_{Ch} catalyzes the oxidation of CO at the Ni-($\mu_2\text{S}$)-Fe1 subsite of cluster C (3). The prime candidate for CO binding is the nickel ion because of its facile accessibility through the substrate channel and its empty apical coordination site (3). Fe1 is the presumed OH⁻ donor ligand in CO₂ formation (3, 6). The CODH_{Oc} from the aerobic bacterium *Oligotropha carboxidovorans* oxidizes CO at the Mo-($\mu_2\text{S}$)-Cu subsite of the [Cu-S-MoO₂] active site, in which copper and molybdenum are bridged by a cyanolyzable sulfane $\mu_2\text{S}$ (7, 8). The enzyme is inactivated when $\mu_2\text{S}$ is removed and reactivated when $\mu_2\text{S}$ is reinserted (9). The Mo-($\mu_2\text{S}$)-Cu subsite resembles the Ni-($\mu_2\text{S}$)-Fe1 bridge in cluster C of CODHII_{Ch}. The mechanism of CO oxidation based on the x-ray structure of [Cu-S-MoO₂] CODH_{Oc} with bound inhibitor *n*-butyl isocyanide involves a thiocarbonate-like intermediate state and proposes the binding of CO between the $\mu_2\text{S}$ and copper (equivalent to nickel

in CODHII_{Ch}) and the binding of an OH⁻ group at molybdenum (equivalent to Fe1 in CODHII_{Ch}) (7).

Structures of cluster C of Ni-Fe CODHs from *Rhodospirillum rubrum* (CODH_{Rr}) (10) and *Moorella thermoacetica* (CODH_{Mt}) (11, 12) also showed the positions of the five metal ions in cluster C of CODHII_{Ch} but did not reveal the bridging μ_2 S. Since sodium sulfide was found to inhibit CODH_{Rr} and CODH_{Mt}, it has been concluded that cluster C with the bridging μ_2 S, as has been observed in CODHII_{Ch} from *C. hydrogeniformans* (3, 4), might represent an inhibited form (13). On the other hand, it has been shown that the [Ni-4Fe-4S] cluster missing the bridging μ_2 S is an inactivated decomposition product originating from the [Ni-4Fe-5S] cluster (4). A catalytic mechanism suggesting the apical binding of CO at nickel and the coordination of OH⁻ in the bridging position between the nickel and Fe1 ions was proposed for CODH_{Rr} and CODH_{Mt} (13-15).

To clarify some of these aspects and get further insights into the mechanism of CO oxidation, we were interested to study how CO interacts with cluster C of CODHII_{Ch} and how the bridging μ_2 S might be involved in catalysis. Although some crystal structures have modeled apical CO at the nickel ion, the occupancies of CO were very low in CODH_{Mt} (12), or the potential CO was observed in the non-functional [Ni-4Fe-4S] cluster C of CODHII_{Ch} (4). We could not identify a CO ligand in the functional cluster C of CODHII_{Ch}, which can be ascribed to the high turnover rate of CO oxidation (4,000 s⁻¹ at 23 °C) (2, 4). Therefore, we have focused on the reactivity of CODHII_{Ch} with potassium cyanide. CO and the cyanide ion show similar reactivities because they are isosteric and isoelectronic, display a similar σ -donor and π -acceptor ligand character, and share the presence of a non-bonding pair of electrons in the *sp*-hybridized orbital of the terminal carbon atom. Cyanide has a similar size as CO, allowing its passage through the substrate channel of CODHII_{Ch} (3), and inhibits the oxidation of CO by Ni-Fe CODHs and [Cu-S-MoO₂] CODH_{Oc} (9, 16-19). The inhibition of Ni-Fe CODHs has been attributed to the binding of cyanide to the nickel ion of cluster C in CODH_{Rr} (17) or to the Fe1 ion (ferrous component II) of cluster C in CODH_{Rr} and CODH_{Mt} (20). It has been established that the inhibition of [Cu-S-MoO₂] CODH_{Oc} is due to the removal of the copper ion as copper cyanide and the sulfane μ_2 S

as thiocyanate, resulting in the formation of a [MoO₃] center, which is catalytically inactive (7, 9).

We have studied the reactivity of CODHII_{Ch} with potassium cyanide and the nickel coordination derived from XAS. We show that cyanide behaves as a competitive inhibitor of CODHII_{Ch} with respect to the substrate CO and apparently interacts with cluster C in a similar fashion. It inhibits reduced CODHII_{Ch} reversibly and forms a nickel cyanide in the equatorial plane. Thereby one of the four square-planar sulfur ligands of nickel, apparently the labile μ₂S, is replaced but remains bound to Fe1. Reactivation cleaves the nickel cyanide and results in square-planar 4S-coordination of nickel and reformation of the Ni-(μ₂S)-Fe1 bridge. The results are summarized in a model of CO oxidation at cluster C of CODHII_{Ch} from *C. hydrogeniformans*.

EXPERIMENTAL PROCEDURES

All experiments were done under strictly anoxic conditions because of the oxygen sensitivity of CODHII_{Ch} (2).

Purification and Assay of CODHII_{Ch}—Growth of *C. hydrogeniformans* Z-2901 (DSM 6008) on CO and purification of CODHII_{Ch} were carried out as detailed (2, 21). CO oxidation activity of CODHII_{Ch} was assayed at 70 °C by following the CO-dependent reduction of oxidized methyl viologen employing an ϵ_{578} of 9.7 mM⁻¹ cm⁻¹ as described (2). For the assays, 1-ml volumes of reaction mixture composed of anoxic 50 mM HEPES/NaOH (pH 8.0) (buffer A) with 20 mM methyl viologen and 2 mM dithiothreitol (DTT) were flushed with CO in screw-capped cuvettes sealed with a rubber septum. Reactions were initiated by injecting 10 μl of diluted enzyme solution. One unit of CO oxidation activity is defined as 1 μmol of CO oxidized/min. Protein estimation employed conventional methods with bovine serum albumin as a standard (22). Purified as isolated CODHII_{Ch} displayed a CO oxidation activity of 14,800 units mg⁻¹ of protein and had a protein concentration of 8.8 mg ml⁻¹.

Inhibition of CODHII_{Ch} by Potassium Cyanide under Turnover Conditions—Potassium cyanide (KCN) stock solutions were prepared in anoxic 10 mM aqueous NaOH under N₂. KCN was added to the cuvettes for the assay of CO oxidation activity prior to the addition of CODHII_{Ch}. The different CO concentrations for kinetic

measurements were established by adding the appropriate amounts of CO-saturated reaction mixture to N₂-saturated reaction mixture. At 70 °C and 1 atm pressure, the CO concentration in CO-saturated reaction mixtures was taken to be 645 μM (23).

Inhibition of CODHII_{Ch} by Potassium Cyanide under Non-turnover Conditions—Assays (1 ml) were performed at 23 °C and contained CODHII_{Ch} in buffer A with 4 mM sodium dithionite plus 2 mM DTT, 4 mM Ti(III) citrate, 2 mM DTT or without reductants under an atmosphere of CO or N₂. Inhibition was initiated by the addition of KCN. Aliquots were removed with time and analyzed for CO oxidation activity.

Reactivation of Cyanide-inhibited Reduced CODHII_{Ch}—Cyanide-inhibited reduced CODHII_{Ch} was prepared by treatment of the enzyme with KCN under non-turnover conditions. CODHII_{Ch} (109 μg) was incubated for 20 min at 23 °C under N₂ in 1 ml of buffer A containing 75 μM KCN, 4 mM dithionite, and 4mM DTT. Such treatment resulted in complete loss of CO oxidation activity. To lower the concentration of KCN in reactivation assays to non-inhibitory 0.07 μM, samples of inhibited CODHII_{Ch} were diluted 11 times in buffer A containing 2 mM DTT under N₂. For reactivation, 10 μl of diluted samples were added to 1 ml of buffer A without reductants or with 4 mM dithionite plus 2 mM DTT, 4 mM Ti(III) citrate, or 2 mM DTT under CO or N₂. Reactivations were performed at 23, 50, and 70 °C.

Effect of Sodium Sulfide on CODHII_{Ch}—Sodium sulfide (Na₂S) was added to CODHII_{Ch} activity assays under turnover conditions, to the reactivation assays of cyanide-inhibited reduced CODHII_{Ch}, and to the as isolated CODHII_{Ch} under non-turnover conditions.

Preparation of Samples for XAS—Dithionite-reduced CODHII_{Ch} (CODH-DT, 15,400 units mg⁻¹) was produced by treatment of as isolated enzyme under N₂ with 4 mM dithionite for 5 min at 23 °C followed by concentration under N₂ to 99 mg ml⁻¹. CO-treated dithionite-reduced CODHII_{Ch} (CODH-CO, 14,600 units mg⁻¹) was produced by incubation of as isolated enzyme under CO in the presence of 4 mM dithionite for 1 h at 50 °C followed by concentration under CO to 85 mg ml⁻¹. For dithionite-reduced CODHII_{Ch} reversibly inhibited by cyanide (CODH-CN^a and CODH-CN^b), the as isolated enzyme was diluted under N₂ with buffer A containing 4 mM dithionite and 2mM DTT to 0.25 (CODH-CN^a) or 0.46 mg ml⁻¹ (CODH-CN^b). KCN was added to the final concentrations of 1 mM (CODH-CN^a) and 200 μM (CODH-CN^b). After a 40-min

incubation at 23 °C with gentle stirring, the activity was completely inhibited. The samples were concentrated under N₂ to 64 (CODH-CN^a) and 132 mg ml⁻¹ (CODH-CN^b) and displayed activities of 700 and 44 units mg⁻¹, respectively. CODH-CN^a and CODH-CN^b were reversibly inhibited since they could be reactivated to 5,400 and 13,100 units mg⁻¹, respectively, upon incubation at 70 °C under CO or N₂ in buffer A containing 4 mM Ti(III) citrate or 4 mM dithionite plus 2 mM DTT.

CODH_{Ch} reactivated after the inhibition by cyanide (CODH-react., 13,100 units mg⁻¹) was prepared from the concentrated CODH-CN^b. To remove the unbound cyanide, CODH-CN^b (70 μl) was dissolved in 0.5 ml of buffer A under N₂ containing 4 mM dithionite and 2 mM DTT and concentrated to 50 μl by ultrafiltration under N₂. The procedure was repeated two times. For the reactivation, the concentrated enzyme (50 μl) was dissolved in 30 ml of buffer A with 4 mM dithionite and 2 mM DTT to a protein concentration of 0.3 mg ml⁻¹ and incubated at 70 °C under N₂ for 40 min. Reactivated CODH_{Ch} was concentrated under N₂ to 157 mg ml⁻¹, yielding sample CODH-react.

Ni-K Edge XAS Measurements—For XAS measurements, 25 μl of each sample were filled into plastic cells covered with Kapton foil. Cells were sealed and kept in liquid N₂. The Ni-K edge XAS data, 8.2-9.2 keV, were collected in fluorescence mode with a silicon (111) monochromator at the EMBL beam-line D2 (DESY, Hamburg, Germany). Harmonic rejection was achieved by a focusing mirror (cut-off energy 20.5 KeV) and a monochromator detuning to 70% of its peak intensity. The sample cells were kept at ~20 K in a two-stage Displex cryostat. Automated data reduction, such as normalization and extraction of the fine structure, was performed with KEMP (24) assuming an energy threshold E_{0,Ni} = 8,333 eV. Sample integrity during exposure to synchrotron radiation was checked by monitoring the position and shape of the absorption edge on sequential scans. No change in redox state or metal environment was detectable.

X-ray Absorption near Edge Structure (XANES) Analysis—The Ni-K edge position was defined at the energy corresponding to a normalized absorbance of 0.5 (25). The extracted 1s →3d pre-edge feature, isolated by subtracting an arctangent function and a first order polynomial to the rising edge (25), was fitted to a single Gaussian function centered at ~8,332 eV. Its intensity corresponds to the integrated area of the Gaussian function.

Extended X-ray Absorption Fine Structure (EXAFS) Analysis—The extracted Ni-K edge (20-700 eV) EXAFS were converted to photoelectron wave vector k -space and weighted by k^3 . The spectra were analyzed with EXCURV98 (26), refining the theoretical EXAFS for defined structural models based on the curved-wave theory. In addition to single scattering contributions, multiple scattering units were defined for linear Ni-C-N and square-planar Ni-4S. Parameters of each structural model, namely the atomic distances (R), the Debye-Waller factors ($2\sigma^2$), and a residual shift of the energy origin (EF), were optimized, minimizing the fit index (χ) while keeping the number of free parameters below those of the independent points (26, 27). Throughout the data analysis, the amplitude reduction factor was kept at 1.0. The reduced χ^2 test verified the significance of an additional ligand in the models (26).

RESULTS AND DISCUSSION

Inhibition of CODHII_{Ch} by Potassium Cyanide—Potassium cyanide inhibits CO oxidation activity of CODHII_{Ch} under catalytic (turnover) conditions in the presence of CO and electron acceptor methyl viologen (Figs. 1, A and B, and 2A) as well as under non-turnover conditions in the absence of CO and acceptor (Fig. 1, C and D). The rate of inhibition depends on time (Fig. 1, A-D), the cyanide concentration (Fig. 1, A-C), and the incubation temperature (Fig. 1, A and B). Since CODHII_{Ch} displays a high temperature optimum for activity (2), the temperature dependence of inhibition indicates a similar mode of interaction of cyanide and CO with the active site. This is supported by the double reciprocal plot of initial activity *versus* CO concentration as a function of cyanide concentration, revealing a pattern characteristic of competitive inhibition and a K_i of 21.7 μ M cyanide (Fig. 2A).

The inhibition by cyanide under non-turnover conditions greatly depends on the redox state of CODHII_{Ch} (Fig. 1, C and D). Reduced CODHII_{Ch} incubated with low potential reductants dithionite or Ti(III) citrate (redox potential \sim -500 mV) is inhibited more

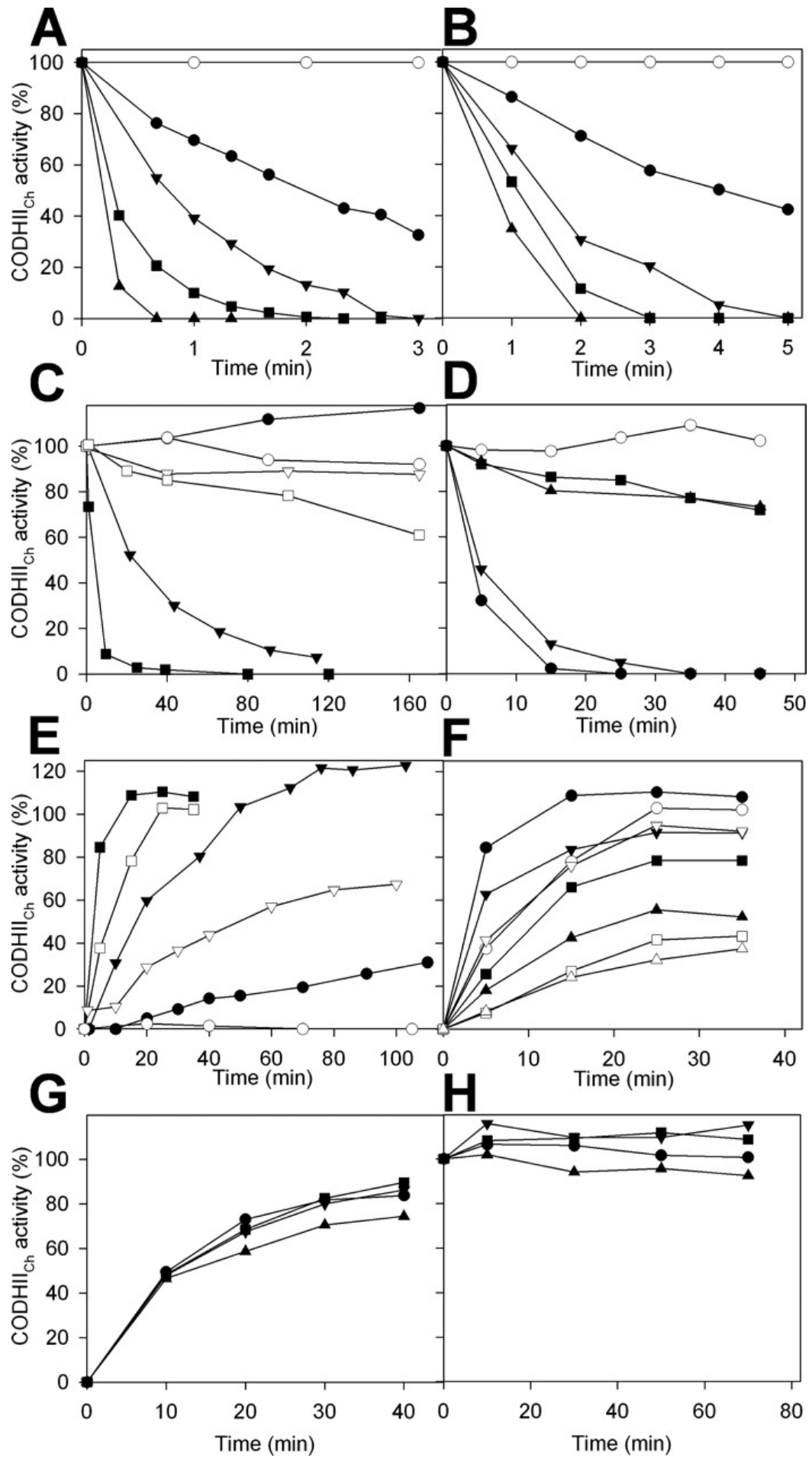
strongly than the more oxidized enzyme incubated with the weak reductant DTT (\sim -330 mV) or without reductants. This indicates an efficient interaction of cyanide with the highly reduced cluster C of CODHII_{Ch} at redox potentials of \sim -500 mV. Obviously,

CO also interacts with cluster C of CODHII_{Ch} at very low potentials since the oxidation of CO in *C. hydrogenoformans* (-520 mV) is coupled to the reduction of protons to H₂ (-410 mV) (2). Therefore, cyanide interacts with the reduced cluster C of CODHII_{Ch} in a similar fashion as the substrate CO.

CO protects reduced CODHII_{Ch} against inhibition by potassium cyanide since there is no decrease of activity under CO in contrast to complete inhibition under N₂ (Fig. 1D), whereas the oxidized enzyme is not protected by CO (Fig. 2B). The protection by CO suggests that cyanide and CO share a common binding site at the reduced cluster C. The effects of temperature (Fig. 1, A and B), redox dependence (Fig. 1, C and D), protection by CO (Fig. 1D), and competitive character of inhibition with respect to CO (Fig. 2A) suggest that the inhibition of reduced CODHII_{Ch} by cyanide is due to the occupation of the CO binding site.

FIGURE 1. A and B, inhibition of CODHII_{Ch} by potassium cyanide under turnover conditions. Assays in A contained 0.87 ng ml⁻¹ CODHII_{Ch} and 0 (○), 50 (●), 100 (▼), 250 (■), or 1,000 (▲) μM KCN at 70 °C. 100% activity in A and C-H corresponds to 14,800 units mg⁻¹. Assays in B contained 5.35 ng ml⁻¹ CODHII_{Ch} and 0 (○), 1 (●), 5 (▼), 10 (■), or 20 (▲) mM KCN at 23 °C. 100% corresponds to 1,400 units mg⁻¹. C and D, inhibition of CODHII_{Ch} by potassium cyanide under non-turnover conditions. Assays in C contained 1.4 μg ml⁻¹ CODHII_{Ch} under N₂, 4 mM dithionite (filled symbols), or no reductants (open symbols) and 0 (●, ○), 10 (▼, ▽), or 100 (■, □) μM KCN at 23 °C. Assays in D contained 0.19 μg ml⁻¹ CODHII_{Ch} under N₂ (filled symbols) or CO (open symbols), 15 μM KCN, and 4 mM dithionite plus 2 mM DTT (●, ○), 4 mM Ti(III) citrate (▼, ▽), 2 mM DTT (■, □), or no reductants (▲, △) at 23 °C. E and F, reactivation of cyanide-inhibited CODHII_{Ch}. Assays contained 0.1 μg ml⁻¹ of inhibited CODHII_{Ch} under CO (filled symbols) or N₂ (open symbols). Reactivation in E was performed in the presence of 4 mM dithionite plus 2 mM DTT at 23 (●, ○), 50 (▼, ▽), or 70 °C (■, □). Reactivation in F was performed in the presence of 4 mM dithionite plus 2 mM DTT (●, ○), 4 mM Ti(III) citrate (▼, ▽), 2 mM DTT (■, □), or without reductants (▲, △) at 70 °C. G and H, effect of sodium sulfide on CODHII_{Ch}. Reactivation assays in G contained 0.1 μg ml⁻¹ of cyanide-inhibited CODHII_{Ch}. Assays in H were under non-turnover conditions and contained 0.12 μg ml⁻¹ of as isolated CODHII_{Ch}. Assays were performed in the presence of 4 mM dithionite and 2 mM DTT (●), 4 mM dithionite, 2 mM DTT, and 0.2 mM Na₂S (▼), 4 mM dithionite, 2 mM DTT, and 1.0 mM Na₂S (■) or 1 mM Na₂S (▲) at 70 °C.





Reactivation of Cyanide-inhibited Reduced CODHII_{Ch}—Inhibition of dithionite- or Ti(III) citrate-reduced CODHII_{Ch} by potassium cyanide is fully reversible since the enzyme can be completely reactivated (Fig. 1, *E* and *F*). CO, high temperature (70 °C), and the presence of dithionite or Ti(III) citrate accelerate the reactivation and increase the maximum level of regained activity as compared with reactivation under N₂ at lower incubation temperatures (23 or 50 °C) and in the absence of low potential reductants (Fig. 1, *E* and *F*).

The significant acceleration of reactivation under CO (Fig. 1, *E* and *F*), which apparently displaces cyanide at the CO binding site, indicates again that the interaction of reduced CODHII_{Ch} with cyanide mimics its interaction with CO. The effect of CO is evident at 23 and 50 °C (Fig. 1*E*). At 70 °C, the effect of CO is negligible, and CODHII_{Ch} can be completely reactivated after 25 min in the absence of CO (Fig. 1, *E* and *F*). Apparently, the dissociation of cyanide from the active site is accelerated by high temperatures, whereas at low temperatures, CO is required to displace the bound cyanide.

Low potential reductants are required for fast and complete reactivation (Fig. 1*F*). Inhibited CODHII_{Ch} regains initial activity after a 15-25-min incubation at 70 °C with dithionite or Ti(III) citrate under CO or N₂. In contrast, slower and partial reactivation to 30-50% of the initial activity occurs with DTT or without reductants (Fig. 1*F*).

The reactivation patterns discussed above further substantiate that the inhibition of reduced CODHII_{Ch} originates from the occupation of the CO binding site by cyanide. This inhibition is not due to any decomposition of cluster C since the activity can be completely recovered (Fig. 1, *E* and *F*).

Effect of Sodium Sulfide on CODHII_{Ch}—Sodium sulfide has no effect on the reactivation of cyanide-inhibited CODHII_{Ch} in the presence of dithionite (Fig. 1*G*). Partial reactivation with sulfide alone (Fig. 1*G*) is brought about by its function as a strong reductant and not as a sulfur source since the enzyme can be completely reactivated in the presence of Ti(III) citrate alone (Fig. 1*F*). Sulfide does not inhibit CODHII_{Ch} under non-turnover conditions in the presence or absence of dithionite (Fig. 1*H*) as well as under turnover conditions (Fig. 2*C*). Apparently, sulfide does not affect CO oxidation by CODHII_{Ch}, which is in contrast to the reported inhibition of CODH_{Rr} and CODH_{Mt} by sulfide and to the suggested inhibitory role of the bridging μ₂S (13).

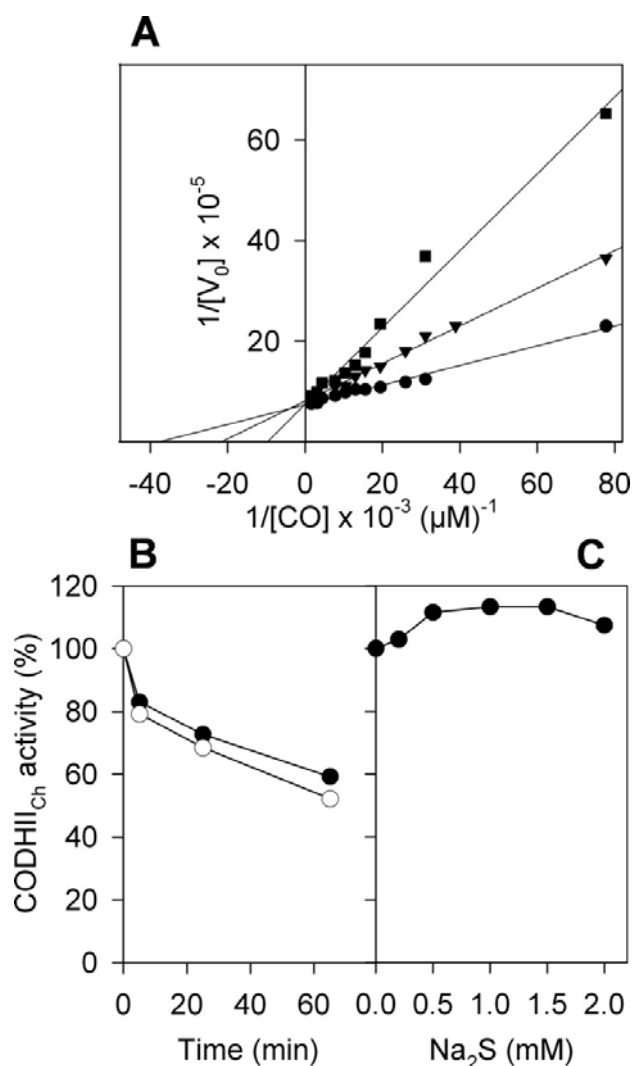


FIGURE 2. A, competitive inhibition of CO oxidation by CODHII_{Ch} under turnover conditions in the presence of CO, methyl viologen, and cyanide. KCN was added to serum-stoppered cuvettes for the assay of CO oxidation activity prior to the addition of CODHII_{Ch}. Reactions were initiated by the addition of 10 μl of stock enzyme solution ($0.144 \mu\text{g ml}^{-1}$). The different CO concentrations were established by adding the appropriate amounts of CO-saturated reaction mixture to assays containing the same reaction mixture saturated with N₂. V_0 indicates the initial activity in units mg^{-1} . KCN concentrations in the cuvettes were 0 (●), 24.6 (▼), and 49.0 (■) μM . B, effect of CO on the inhibition of oxidized CODHII_{Ch} by cyanide under non-turnover conditions. CODHII_{Ch} ($0.19 \mu\text{g ml}^{-1}$) was incubated with 2 mM KCN in the absence of reductants under an atmosphere of CO (●) or N₂ (○) at 23 °C. C, effect of sodium sulfide on the activity of CODHII_{Ch} under turnover conditions in the presence of CO and methyl viologen. Na₂S was added to serum-stoppered cuvettes for the assay of CO oxidation activity containing 1.05 ng ml^{-1} CODHII_{Ch}. 100% activity corresponds to $14,800 \text{ units mg}^{-1}$.

XAS of Dithionite-reduced CODHII_{Ch}—Ni-K edge XAS on highly active dithionite-reduced CODHII_{Ch} (CODH-DT, 15,400 units mg⁻¹) reveals the nickel coordination in functional CODHII_{Ch} in solution. The XANES spectrum (Fig. 3A) resembles that of the four-coordinate square-planar complexes of nickel (25). It shows a small shoulder near 8,337 eV, which has been observed in tetragonal geometries lacking one or more axial ligands and has been assigned to a 1s →4p_z transition (with shakedown contributions). The spectrum exhibits a very weak 1s →3d pre-edge peak centered at ~8,332 eV. The normalized integrated area of this peak is 0.030 eV. The 1s →3d transition is dipole-forbidden; however, it can gain intensity due to p-d mixing in non-centrosymmetric geometries. Thus, planar complexes will feature weak transitions with areas of ~0.0-0.029 eV, whereas the tetrahedral ones will display stronger transitions with areas of ~0.08-0.114 eV (25). In CODH-DT, the combination of weak 1s →3d transition and a shoulder on the rising edge indicates that the nickel ion is four-coordinate with a square-planar geometry. The edge energy of 8338.5 eV is consistent with a Ni²⁺ oxidation state of the nickel ion (25).

The EXAFS spectrum provides further insight into the metal coordination (Fig. 3B, trace a). The amplitude envelope of the oscillations, e.g. its maximum at ~6.5 Å⁻¹, is indicative of the presence of elements heavier than oxygen and nitrogen in the vicinity of the absorber atom. The lack of the beat node-like change in the EXAFS amplitude marks a homogenous ligand sphere. This is further substantiated by the Fourier transform of the EXAFS data showing one dominant peak at ~2.2 Å and small contributions at ~2.8 and ~4.4 Å (Fig. 3C, trace a). Both 2.2 and 4.4 Å peaks could be best fitted with four Ni-S interactions at 2.23 Å in the square-planar geometry (Table 1). No further interactions with light atoms, e.g. Ni-O, at shorter bond lengths were required for a good fit.

The Ni-S bond lengths depend on the nickel geometry. In four-coordinate Ni²⁺ complexes containing thiolate ligands, the Ni-S bond lengths range from 2.14 to 2.24 Å for approximately square-planar geometries and from 2.26 to 2.33 Å for tetrahedral geometries (28). The Ni-S distances in CODHII_{Ch} (Table 1) are in the range for square-planar complexes. Independent evidence for this coordination arises from the multiple scattering via the central nickel atom within the Ni-4S system, visible at about 4.4 Å in

the Fourier transforms. Such features only occur when the scattering vector is close to 180° .

To identify the potential contributors to the ~ 2.8 Å peak in the Fourier transform spectrum, two different scenarios have been considered. Based on the crystal structure of functional CODHII_{Ch}, the most probable ligands to nickel at this distance are 2Fe ions at ~ 2.8 and ~ 2.9 Å (3). To test their presence, a single 2Fe shell was modeled first, but its refinement resulted in a relatively high Debye-Waller factor, and thus, had to be discarded. Followed by that, a single 1Fe shell at ~ 2.7 Å was fitted (supplemental Table 1). The inclusion of a second iron contribution at ~ 2.9 Å significantly improved the fit, as shown by the 5% drop of the fit index (Table 1). The data published previously on the as isolated CODHII_{Ch} did not show any evidence for Ni-Fe contribution(s), whereas for the CO-treated and Ti(III) citrate-reduced samples, only one Ni-Fe interaction at ~ 2.74 Å was detected (5). The lack of the Ni-Fe contributions or their weak signal was then attributed to the destructive interference between 2.7 and 2.9 Å Ni-Fe components within the ~ 5 - 10 Å⁻¹ range (5). In the present studies, a partial cancellation of both Ni-Fe signals takes place as well (especially between 5 and 8 Å⁻¹). However, a longer photoelectron wave number (k) range as compared with the previous XAS data on CODHII_{Ch} (5) ensures that both of the components can be detected. The lack of any substantial numerical correlation during the EXAFS data refinement between the structural parameters of both iron shells further supports this statement.

The model comprising 4S atoms at 2.23 Å in a square-planar geometry and 2Fe atoms at 2.71 and 2.99 Å (Table 1) correlates well with the crystal structure of functional CODHII_{Ch} (3, 4). However, the 2.71 Å Ni-Fe distance is shorter than the shortest Ni-Fe bond (2.82 Å) found by x-ray crystallography (3, 4). It may reflect a redox-dependent conformational change in cluster C due to the slightly different redox state of the protein in samples studied by XAS and crystallography as it was previously suggested (5).

XAS of CO-treated Dithionite-reduced CODHII_{Ch}—XAS on highly active CO-treated dithionite-reduced CODHII_{Ch} (CODH-CO, 14,600 units mg⁻¹) was performed to determine the effect of CO on the nickel coordination and to identify the binding position of CO. XAS revealed no change in nickel geometry and ligand sphere

composition upon CO treatment. The Ni-K edge spectrum is almost identical to that of the CODH-DT with a small shoulder at $\sim 8,337$ eV and a pre-edge peak at $\sim 8,332$ eV (Fig. 3A). The edge energy has not changed and is consistent with the Ni^{2+} state. EXAFS demonstrated that the nickel coordination has not been altered by CO treatment (Fig. 3, B and C, traces b). The final structural model is consistent with the model for CODH-DT and comprises 4S atoms at 2.23 Å in a square-planar geometry and 2Fe atoms at 2.71 and 2.96 Å (Table 1). A single 1Fe shell at ~ 2.7 Å was tested as well, but the fit was significantly worse, as demonstrated by the 8% increase of the fit index value, as compared with 2Fe model (supplemental Table 1). The obtained results are similar to the data on CO-treated CODHII_{Ch} published previously (5). However, the average Ni-S bond length found in this study is slightly shorter (2.231 (2) *versus* 2.252 (3) Å) and has a lower Debye-Waller factor (0.0080 (3) *versus* 0.0155 Å²), which indicates the lower structural disorder of the 4S shell in the present CO-treated CODHII_{Ch} sample. As the crystal structure of functional CODHII_{Ch}, briefly treated with CO (4), the model for CODH-CO indicates the presence of $\mu_2\text{S}$ and the absence of bound CO. Therefore, after turnover of CO, cluster C remains in the functional state with 4S ligands at nickel. Since a carbon atom was not apparent in the vicinity of the nickel ion, the reaction product CO_2 obviously leaves the active site very quickly without the formation of a stable carboxyl intermediate.

XAS of Dithionite-reduced CODHII_{Ch} Reversibly Inhibited by Cyanide—XAS on dithionite-reduced CODHII_{Ch} reversibly inhibited by cyanide (CODH-CN^a with 700 units mg^{-1} and CODH-CN^b with 44 units mg^{-1}) elucidates cyanide binding to cluster C. The XANES patterns of both samples almost line up with each other (Fig. 3A) but differ significantly from those of CODH-DT and CODH-CO, indicating significant changes of structure and/or ligand composition of the nickel site. Both XANES spectra also exhibit features of CODH-DT and CODH-CO, *i.e.* weak 1s \rightarrow 3d pre-edge peak and a small shoulder due to the 1s \rightarrow 4p_z transition. However, the position of the shoulder is shifted slightly toward lower energies, and the edge energy increases by ~ 1.2 eV. This edge shift could indicate an increase in the nickel oxidation state. However, the preserved low intensities of the 1s \rightarrow 3d transition (0.031 and 0.036 eV for CODH-CN^a and CODH-CN^b, respectively) exclude such a possibility and are consistent with the Ni^{2+} oxidation state of the nickel ion (25). Instead, the change in the

hardness of some of the donor atoms is more likely. A general shift to lower edge energies has been observed for complexes with increasing numbers of sulfur-donor ligands (25). Thus, the observed changes indicate that cyanide substitutes for one of the sulfur ligands without affecting the square-planar geometry of the nickel site.

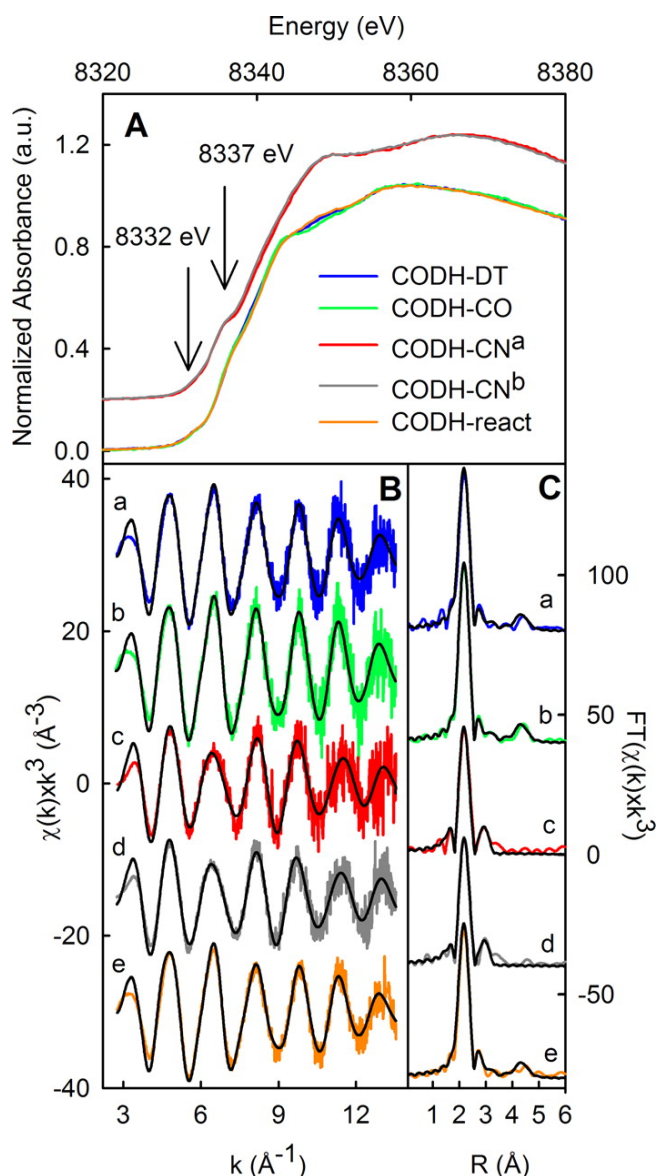


FIGURE 3. A, normalized Ni-K edge x-ray absorption spectra, B, Ni-K edge k^3 -weighted EXAFS spectra, and C, Fourier transforms of EXAFS spectra of different CODHII_{Ch} samples. Samples are as follows: CODH-DT (trace a), CODH-CO (trace b), CODH-CN^a (trace c), CODH-CN^b (trace d), and CODH-react. (trace e). Calculated spectra in B and C are shown by black lines; experimental spectra based on the models given in Table 1 are represented by colored curves. The abbreviations are: χ , EXAFS signal; k , photoelectron wave number; R , interatomic distance; FT , Fourier transform (modulus). The Fourier transform is phase-corrected for the shortest metal ligand contribution, and therefore, the peaks do not appear at the refined metal neighbor distances. For sample labels, see "Experimental Procedures."

In the EXAFS spectra of CODH-CN^a and CODH-CN^b, the sharp oscillations at $\sim 6.5 \text{ \AA}^{-1}$, present in CODH-DT and CODH-CO, are diminished (Fig. 3B, traces c and d), and a beat node-like change in the regular sinusoidal pattern emerges. This indicates heterogeneous ligand sphere, most probably caused by cyanide binding, and is visualized in both Fourier transform spectra (Fig. 3C, traces c and d). As compared with CODH-DT and CODH-CO, a small peak at $\sim 1.8 \text{ \AA}$ emerges, whereas the $\sim 2.8 \text{ \AA}$ contribution is replaced by a broad peak centered at $\sim 3.0 \text{ \AA}$. The 4.4 \AA peak marking a 4S square-planar geometry in CODH-DT and CODH-CO decreases to the noise level. The 2.2 \AA peak intensity decreases by $\sim 30\%$. These features are likely caused by a cyanide ligand replacing one of the sulfur ligands. Based on the reduced χ^2 test (26), the best fit among all considered models was obtained for a nickel ion coordinated by three sulfur atoms at ~ 2.20 or $\sim 2.23 \text{ \AA}$ and one CN group with a Ni-C distance of 1.81 or 1.84 \AA for CODH-CN^a and CODH-CN^b, respectively (Table 1). The refined Ni-C and C-N bond lengths are consistent with Ni²⁺ complexes with cyanide ligands (29). Assuming Ni-C distances of 1.81 or 1.84 \AA , Ni-N distances of 3.00 \AA , and C-N distance in cyanide of 1.15 - 1.18 \AA (29, 30), cyanide binds to the nickel ion of cluster C by its carbon atom in a linear fashion.

Therefore, in CODH_{Ch} reversibly inhibited by cyanide, one of the Ni-S bonds is cleaved and one CN ligand is bound to nickel in square-planar geometry. This suggests that cyanide cleaves the labile bond between nickel and the bridging $\mu_2\text{S}$ (4) and binds to nickel at the coordination site previously occupied by the $\mu_2\text{S}$.

XAS of CODH_{Ch} Reversibly Inhibited by Cyanide and Then Reactivated—XAS on CODH-react. ($13,100 \text{ units mg}^{-1}$) determines the nickel coordination in highly active CODH_{Ch} formed after reactivation of enzyme reversibly inhibited by cyanide. The Ni-K edge shape is almost identical to that of CODH-DT and CODH-CO, indicating the same square-planar geometry and oxidation state of nickel in CODH-react. (Fig. 3A). However, the normalized integrated area of the $1s \rightarrow 3d$ increases (0.040 eV), suggesting a slightly disordered geometry of the nickel site. EXAFS confirms this observation (Fig. 3B, trace e). As compared with CODH-DT, the intensity of the Ni-S backscattering contribution is lowered by $\sim 15\%$ (Fig. 3C, trace e), but multiple scattering contributions within the square-planar Ni-4S unit significantly improve the fit. Thus, a slightly disordered square-planar geometry of the nickel site is likely,

especially because the average Ni-S bond length has not changed as compared with CODH-DT and CODH-CO (Table 1).

TABLE 1. EXAFS refinement parameters for different CODH_{Ch} samples

The numbers (N) of ligand atoms (L), their distance to the nickel ion (R), the respective Debye-Waller factor ($2\sigma^2$), the C-N bond length (R_{CN}), the Fermi energy for all shells (EF), and the Fit Index (Φ), indicating the quality of the fit, are shown. For the Ni-4S square-planar (*) and Ni-C-N linear (***) units, multiple scattering up to the fifth or third order has been included, respectively. The presence of the first shell Ni-4S multiple scattering is visualized by the peak at 4.4 Å in the Fourier transforms of the respective samples. Values in parentheses represent statistical errors (2·SD, SD - standard deviation) of the least square refinement. For sample labels, see "Experimental Procedures."

N	Ni ... L	R (Å)	$2\sigma^2$ (Å ²)	R_{CN} (Å)	EF (eV)	$\Phi \cdot 10^3$
CODH-DT						
4	Ni ... S*	2.230 (2)	0.0095 (3)		-9.9 (4)	0.1416
1	Ni ... Fe	2.71 (2)	0.020 (4)			
1	Ni ... Fe	2.99 (2)	0.020 (5)			
CODH-CO						
4	Ni ... S*	2.231 (2)	0.0080 (3)		-10.6 (4)	0.1414
1	Ni ... Fe	2.71 (1)	0.015 (3)			
1	Ni ... Fe	2.96 (2)	0.015 (3)			
CODH-CN^a						
1	Ni ... C***	1.81 (1)	0.005 (2)	1.19 (2)	-9.5 (5)	0.2857
3	Ni ... S	2.220 (3)	0.0094 (6)			
1	Ni ... N***	3.00 (1)	0.009 (2)			
CODH-CN^b						
1	Ni ... C***	1.84 (1)	0.010 (2)	1.16 (2)	-9.8 (4)	0.1625
3	Ni ... S	2.229 (3)	0.0090 (4)			
1	Ni ... N***	3.00 (1)	0.011 (2)			
CODH-react.						
4	Ni ... S*	2.231 (2)	0.0103 (3)		-9.7 (3)	0.0774
1	Ni ... Fe	2.686 (7)	0.016 (2)			
1	Ni ... Fe	2.969 (9)	0.020 (2)			

This is consistent with the CODHII_{Ch} crystal structure where the partial occupancy of the $\mu_2\text{S}$ has been observed (4) and refers to a minor component lacking the fourth sulfur ligand. Activities (15,400 units mg^{-1} in CODH-DT *versus* 13,100 units mg^{-1} in CODH-react.) indicate the presence of roughly 15% catalytically non-competent enzyme in CODH-react., which presumably contains a Ni-CN. Then, the reactivated component must be formed entirely as a NiS₄ site. Thus, the model for reactivated CODHII_{Ch} is similar to that of CODH-DT, comprising four square-planar sulfur at 2.23 Å and 2Fe at 2.69 and 2.97 Å (Table 1).

CO Oxidation at the [Ni-4Fe-5S] Cluster of CODHII_{Ch}—This study shows that cyanide is an inhibitor of CODHII_{Ch} because it competes with CO at the reduced [Ni-4Fe-5S] cluster. XAS indicates that the reversible inhibition of CODHII_{Ch} with 4S coordinated nickel (CODH-DT) results in a 3S and 1CN coordinated nickel (CODH-CN^a and CODH-CN^b). The binding of cyanide to nickel cleaves the bond between the nickel ion and the bridging $\mu_2\text{S}$, which stays bound to Fe1 since after reactivation, the 4S coordination of nickel is reestablished (CODH-react.), and external sulfide is not required for reactivation (Fig. 1, *F* and *G*). The requirement of reduced conditions for reactivation (Fig. 1*F*) indicates that the Fe1-bound $\mu_2\text{S}$ should be in its S²⁻ state to produce the bridge.

We feel that our data do not support a mechanism of CO oxidation at the [Ni-4Fe-5S] cluster of CODHII_{Ch} from *C. hydrogenoformans* involving binding of oxygen in a bridging position between nickel and iron (13-15) since this position will be occupied by sulfur in as isolated state or by CO after the binding of the substrate, and XAS did not identify an oxygen ligand to nickel in any of the examined states of the enzyme. On the other hand, since we have not captured any of the intermediates described in Fig. 4, the possibility of an oxygen atom, which transiently bridges the two metals during catalysis, cannot finally be ruled out. Our results also argue against an inhibitory role of the bridging $\mu_2\text{S}$ in cluster C of CODHII_{Ch} (13). We did not observe an inhibition of CODHII_{Ch} by sulfide. As we cultivate *C. hydrogenoformans* in the presence of 3.3 mM Na₂S₂O₄ reductant of the growth medium, the compound is apparently not toxic to the bacteria.

In analogy to the dithionite-reduced, cyanide-inhibited, and reactivated states of CODHII_{Ch} analyzed by XAS, as well as in accordance with the structure-based

mechanism of CODH_{ICh} (3), we propose a mechanism of CO oxidation at the [Ni-4Fe-5S] cluster (Fig. 4). An incoming CO molecule reaches the cluster through the substrate channel ending at the nickel ion (Fig. 4A) where it binds, resulting in a square-pyramidal five-coordinate intermediate (Fig. 4B). A water molecule binds as OH⁻ to the histidine-coordinated Fe1 as proposed previously (6). The resulting CO to OH⁻ distance exceeds 4 Å, which does not allow interaction (3). The μ₂S ligand dissociates from the nickel and remains bound to pentacoordinated Fe1 as S²⁻. A simultaneous rearrangement leads to a square-planar nickel intermediate with three sulfur and one CO ligand. This moves CO toward the OH⁻, making a nucleophilic attack possible (Fig. 4C). The proposed rearrangement agrees with the models describing the conversion of CO by a nickel to sulfur rebound mechanism studied with model compounds containing four-coordinate nickel (31, 32). The nickel-bound CO undergoes a nucleophilic attack by the Fe1-bound OH⁻, forming a nickel-bound carboxylic acid group. The carboxylic acid group is deprotonated by the Fe1-bound S²⁻, which is ideally situated to act as a catalytic base, resulting in a thiol group and a preformed CO₂ (Fig. 4D). The proton of the thiol group is subsequently transmitted via His-261 to His-93 and Lys-563 of the assumed proton transfer chain (33), whereas the sulfide stays bound to Fe1 (Fig. 4E). Dissociation of the nickel carboxyl generates two electrons that are delocalized on the [3Fe-4S] subcluster and transferred further through clusters B, B', and D to the external electron acceptor. Simultaneously, the Ni-(μ₂S)-Fe1 bridge is being reformed (Fig. 4A), and a new reaction cycle can proceed. This mechanism resembles that of CODH_{Oc} from *O. carboxidovorans*, containing a Cu-(μ₂S)-Mo bridge in the active site. In that enzyme, the insertion of CO between the copper, the sulfido-ligand, and the hydroxo-group at molybdenum, thereby forming a thiocarbonate intermediate, has been proposed (7, 8).

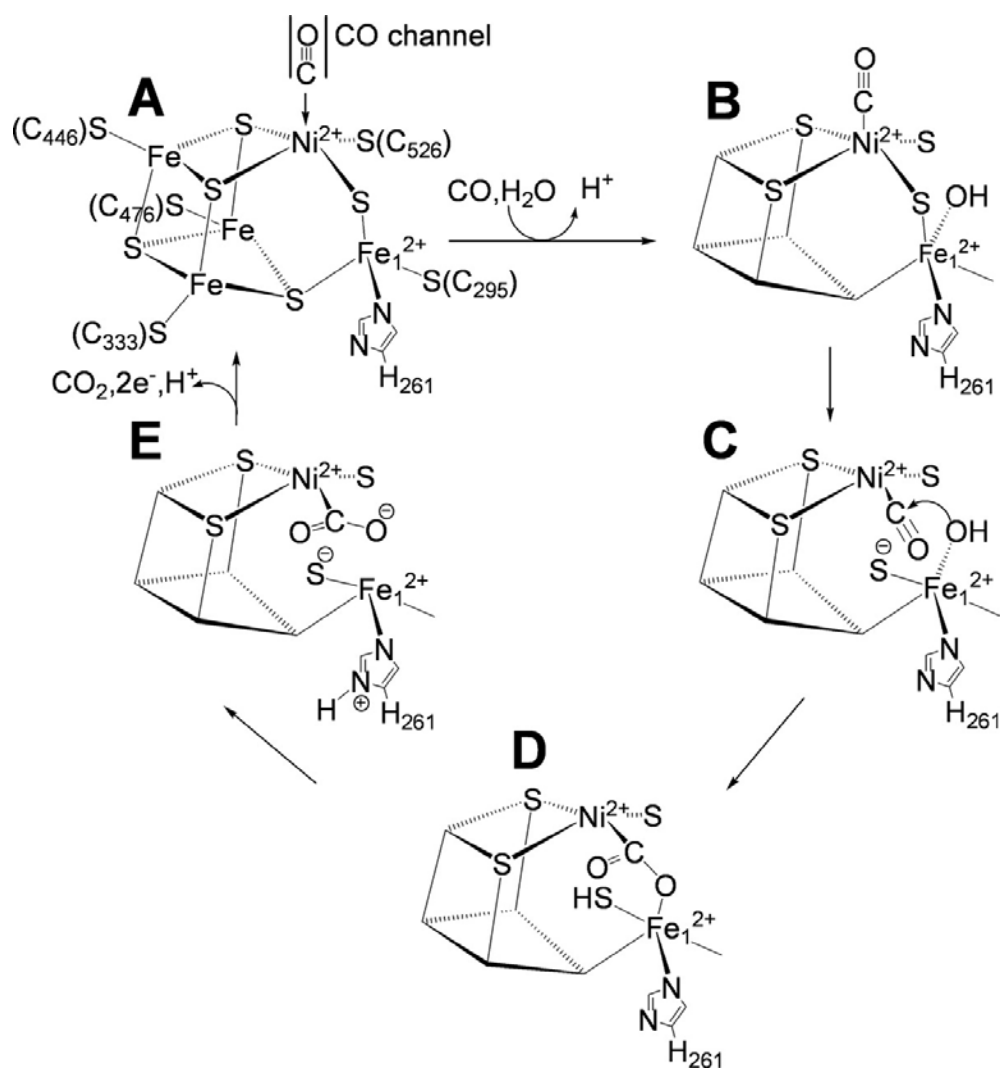


FIGURE 4. Hypothetical scheme showing the oxidation of CO to CO₂ at the [Ni-4Fe-5S] cluster in the active site of CODHIII_{Ch}. A-E, the reaction cycle of CODHIII_{Ch}. See "Results and Discussion" for details.

ACKNOWLEDGMENTS

This work was supported by the Deutsche Forschungsgemeinschaft (Grants SV10/1-1 and SV10/1-2). This research has employed equipment financed by the Freistaat Bayern and the Fonds der Chemischen Industrie.

REFERENCES

1. Svetlichny, V. A., Sokolova, T. G., Gerhardt, M., Ringpfeil, M., Kostrikina, N. A., and Zavarzin, G. A. (1991) *Syst. Appl. Microbiol.* **14**, 254-260
2. Svetlitchnyi, V., Peschel, C., Acker, G., and Meyer, O. (2001) *J. Bacteriol.* **183**, 5134-5144
3. Dobbek, H., Svetlitchnyi, V., Gremer, L., Huber, R., and Meyer, O. (2001) *Science* **293**, 1281-1285
4. Dobbek, H., Svetlitchnyi, V., Liss, J., and Meyer, O. (2004) *J. Am. Chem. Soc.* **126**, 5382-5387
5. Gu, W., Seravalli, J., Ragsdale, S. W., and Cramer, S. P. (2004) *Biochemistry* **43**, 9029-9035
6. DeRose, V. J., Telser, J., Anderson, M. E., Lindahl, P. A., and Hoffman, B. M. (1998) *J. Am. Chem. Soc.* **120**, 8767-8776
7. Dobbek, H., Gremer, L., Kiefersauer, R., Huber, R., and Meyer, O. (2002) *Proc. Natl. Acad. Sci. U. S. A.* **99**, 15971-15976
8. Gnida, M., Ferner, R., Gremer, L., Meyer, O., and Meyer-Klaucke, W. (2003) *Biochemistry* **42**, 222-230
9. Resch, M., Dobbek, H., and Meyer, O. (2005) *J. Biol. Inorg. Chem.* **10**, 518-528
10. Drennan, C. L., Heo, J., Sintchak, M. D., Schreiter, E., and Ludden, P. W. (2001) *Proc. Natl. Acad. Sci. U. S. A.* **98**, 11973-11978
11. Doukov, T. I., Iverson, T. M., Seravalli, J., Ragsdale, S. W., and Drennan, C. L. (2002) *Science* **298**, 567-672
12. Darnault, C., Volbeda, A., Kim, E. J., Legrand, P., Vernede, X., Lindahl, P. A., and Fontecilla-Camps, J. C. (2003) *Nat. Struct. Biol.* **10**, 271-279
13. Feng, J., and Lindahl, P. A. (2004) *J. Am. Chem. Soc.* **126**, 9094-9100
14. Ragsdale, S. W. (2004) *CRC Crit. Rev. Biochem. Mol. Biol.* **39**, 165-195
15. Volbeda, A., and Fontecilla-Camps, J. C. (2005) *Dalton Trans.* **21**, 3443-3450
16. Anderson, M. E., DeRose, V. J., Hoffman, B. M., and Lindahl, P. A. (1993) *J. Am. Chem. Soc.* **115**, 12204-12205
17. Ensign, S. A., Hyman, M. R., and Ludden, P. W. (1989) *Biochemistry* **28**, 4973-4979

18. Meyer, O. (1982) *J. Biol. Chem.* **257**, 1333-1341
19. Ragsdale, S. W., and Kumar, M. (1996) *Chem. Rev.* **96**, 2515-2540
20. Hu, Z., Spangler, N. J., Anderson, M. E., Xia, J., Ludden, P. W., Lindahl, P. A., and Münck, E. (1996) *J. Am. Chem. Soc.* **118**, 830-845
21. Svetlitchnyi, V., Dobbek, H., Meyer-Klaucke, W., Meins, T., Thiele, B., Römer, P., Huber, R., and Meyer, O. (2004) *Proc. Natl. Acad. Sci. U. S. A.* **101**, 446-451
22. Bradford, M. M. (1976) *Anal. Biochem.* **72**, 248-254
Lax, E. (1967) *D'Ans-Lax: Taschenbuch für Chemiker und Physiker*, Vol. 1, pp. I-1025, Springer, Berlin, Germany
24. Korbas, M., Fulla Marsa, D., and Meyer-Klaucke, W. (2006) *Rev. Sci. Instrum.* **77**, 063105
25. Colpas, G. J., Maroney, M. J., Bagyinka, C., Kumar, M., Willis, W. S., Suib, S. L., Baidya, N., and Mascharak, P. K. (1991) *Inorg. Chem.* **30**, 920-928
26. Binsted, N., Strange, R. W., and Hasnain, S. S. (1992) *Biochemistry* **31**, 12117-12125
27. Stern, E. A. (1993) *Physiol. Rev. B* **48**, 9825-9827
28. Halcrow, M. A., and Christou, G. (1994) *Chem. Rev.* **94**, 2421-2481
29. Chastain, B. B., Rick, E. A., Pruett, R. L., and Gray, H. B. (1968) *J. Am. Chem. Soc.* **90**, 3994-4000
30. Shores, M. P., Sokol, J. J., and Long, J. R. (2002) *J. Am. Chem. Soc.* **124**, 2279-2292
31. Sellmann, D., Geipel, F., and Heinemann, F. W. (2000) *Chemistry* **6**, 4279-4284
32. Fan, Y., and Hall, M. B. (2004) *Chemistry* **10**, 1805-1814
33. Kim, E. J., Feng, J., Bramlett, M. R., and Lindahl, P. A. (2004) *Biochemistry* **43**, 5728-5734

6 The [Ni-4Fe-5S] cluster of *Carboxydotherrnus hydrogenoformans* CO dehydrogenase is biologically relevant

Seung-Wook Ha¹, Gleb Bourenkov², Wolfram Meyer-Klaucke², Ortwin Meyer¹,
and Vitali Svetlitchnyi^{1, §}

¹Lehrstuhl für Mikrobiologie, Universität Bayreuth, Universitätsstrasse 30, D-95440
Bayreuth, Germany

²European Molecular Biology Laboratory (EMBL), Outstation Hamburg at Deutsches
Elektronen-Synchrotron (DESY), Notkestrasse 85, D-22603 Hamburg, Germany

§ Corresponding author

Tel.: 49-921-552790, Fax: 49-921-552727

E-mail: vitali.svetlitchnyi@googlemail.com

Present address: Centre “Bioengineering”, The Russian Academy of Sciences, Prosp.
60 let Oktiabria, bld. 7-1, Moscow, 117312 Russian Federation

Manuscript for the submission to Science

ABSTRACT

CO dehydrogenase II (CODHII_{Ch}) from the CO-utilizing extremely thermophilic bacterium *Carboxydotherrnus hydrogenoformans* oxidizes CO at a [Ni-4Fe-5S] center (cluster C) which contains a 4S-coordinated Ni ion and a μ_2 S ligand bridging the Ni and Fe1 ions. We have studied the function of μ_2 S in CODHII_{Ch}, since μ_2 S-depleted CO dehydrogenases with a [Ni-4Fe-4S]-form of cluster C found in other bacteria are active. Here we show that the [Ni-4Fe-5S]-form of the cluster is the biologically relevant species in CODHII_{Ch} which enables the bacteria to live on CO at high temperatures in CO-limited, sulfide-rich volcanic vents. The μ_2 S ligand originates from external sulfide and has two functions: (i) it stabilizes the cluster and protects CODHII_{Ch} against thermal inactivation, (ii) it accelerates CO oxidation by prevention of inhibition by the product CO₂, and represses the non-physiological reaction of CO₂ reduction. CO oxidation in CODHII_{Ch} is activated by sulfide and reversibly inhibited by cyanide. We have determined the structures and Ni-coordinations in as-isolated, sulfide-activated, cyanide-inhibited, and reactivated states of CODHII_{Ch} as well as of the enzyme exposed to CO oxidation and CO₂ reduction. The resulting model of CO oxidation at the [Ni-4Fe-5S] center in CODHII_{Ch} discloses the functions of μ_2 S and shows how CO and CO₂ interact with the cluster.

The extremely thermophilic anaerobic bacterium *Carboxydotherrmus hydrogenoformans* lives in CO-limited highly reducing hot volcanic environments containing large amounts of H₂S and CO₂ (Svetlitchnyi et al. 1991 a,b; Stetter 1999; Kelley et al. 2002). It grows at temperatures up to 78°C and utilizes CO from volcanic gases as the source of energy and carbon (Svetlitchnyi et al. 1991). The energy metabolism is hydrogenogenic since the energy-generating CO oxidation is coupled to the reducton of protons to hydrogen (Svetlitchnyi et al. 2001; Soboh et al. 2002). CO is oxidized by two NiFe CO dehydrogenases, designated CODHI_{Ch} and CODHII_{Ch} (Svetlitchnyi et al. 2001).

The native CODHII_{Ch} isolated from CO grown bacteria contains a [Ni-4Fe-5S] center (cluster C) in the active site (Dobbek et al. 2001). It displays a planar NiS₄-coordination in which the Ni ion is bound to an asymmetrically coordinated Fe ion (Fe1) by an inorganic bridging μ₂S ligand. The enzyme is highly active in CO oxidation and is not inhibited by sulfide (Svetlitchnyi et al. 2001; Ha et al. 2007). Involvement in catalysis and a role in stabilization of cluster C were proposed for μ₂S in the native CODHII_{Ch} (Dobbek et al. 2004).

Native NiFe CODHs isolated from CO-oxidizing mesophilic phototrophic bacterium *Rhodospirillum rubrum* (Drennan et al. 2001) and from CO₂-reducing moderately thermophilic acetogenic bacterium *Moorella thermoacetica* (Doukov et al. 2002; Darnault et al. 2003) as well as a recombinant CODHII_{Ch} expressed in *Escherichia coli* (Jeoung and Dobbek 2007) reveal a [Ni-4Fe-4S] form of cluster C with a NiS₃-coordination and without the bridging μ₂S. These enzymes are active and an inhibitory role of μ₂S has been proposed (Feng and Lindahl 2004; Jeoung 2007).

Since CODHs with both forms of cluster C can oxidize CO, the question arose what is the biologically relevant species. Here we show, that under the extreme life conditions of *C. hydrogenoformans* the [Ni-4Fe-5S] cluster is the biologically relevant form in CODHII_{Ch}. We provide evidences that the bridging μ₂S protects the enzyme against thermal inactivation, accelerates CO oxidation, and prevents inhibition by the product CO₂. On the basis of kinetic and structural data we present a model of CO oxidation at the [Ni-4Fe-5S] center which shows how μ₂S is involved in stabilization of the metal center and catalysis, and how CO and CO₂ interact with the cluster.

To prove that the bridging $\mu_2\text{S}$ stabilizes $\text{CODHII}_{\text{Ch}}$ at high temperatures and originates from external sulfide, we have compared the effect of temperature on CO oxidation activity of the enzyme with NiS_4 -coordination containing $\mu_2\text{S}$ (CODH_{act} state) and NiS_3 -coordination devoid of $\mu_2\text{S}$ ($\text{CODH}_{\text{react.Ti}}$ state). The assays were done at 70°C (optimum growth temperature of *C. hydrogenoformans*; Svetlitchnyi et al. 1991) and at 25°C under N_2 or CO atmospheres in the presence and in the absence of sodium sulfide. The added reductant Ti(III) citrate (~ -500 mV) excluded oxidative inactivation (Dobbek et al. 2004).

At 70°C under N_2 both forms are completely stable only in the presence of sulfide (Fig. 1A). Moreover, the NiS_3 -form displays an activation. In the absence of sulfide, the enzyme is generally less stable. However, without sulfide the NiS_4 -form (half-life 75 min) is two times more stable than the NiS_3 -form (half-life 40 min). Stability under CO is lower than under N_2 (fig. S1A). But the NiS_4 -form is again more stable and sulfide stabilizes the enzyme. At 25°C under N_2 or CO both forms are stable regardless of sulfide (Fig. 1B and fig. S1B). These data suggest that under high growth temperatures of *C. hydrogenoformans* in sulfide-rich habitats the NiS_4 -form of cluster C is the biologically relevant species.

The conversion of unstable NiS_3 -form to the stable NiS_4 -form is achieved by incorporation of $\mu_2\text{S}$ from sulfide. To demonstrate this, we have generated suitable states of $\text{CODHII}_{\text{Ch}}$ (Fig. 1C) and solved their structures (Fig. 2 and fig. S2). The as-isolated enzyme ($\text{CODH}_{\text{as-isol.}}$) was incubated at 70°C in the presence of sulfide which resulted in its activation ($\text{CODH}_{\text{act.}}$), reversibly inhibited by potassium cyanide at 25°C (CODH_{CN} ; Ha et al. 2007), and then reactivated at 70°C in the presence of sulfide ($\text{CODH}_{\text{react.DT}}$) as well as in the absence of sulfide ($\text{CODH}_{\text{react.Ti}}$).

Crystals of $\text{CODH}_{\text{as-isol.}}$, $\text{CODH}_{\text{act.}}$, CODH_{CN} , and $\text{CODH}_{\text{react.DT}}$ diffracted to 1.1 \AA (table S1). Depending on the state, cluster C reveals interconversion of the NiS_3 -form ($[\text{Ni-4Fe-4S}]$ -conformation) and the NiS_4 -form ($[\text{Ni-4Fe-5S}]$ -conformation) (Fig. 2). The switch from $[\text{Ni-4Fe-4S}]$ to $[\text{Ni-4Fe-5S}]$ results from the incorporation of $\mu_2\text{S}$ and involves displacements of Fe1, Fe2, and their coordinating residues His²⁶¹, Cys²⁹⁵, and Cys⁴⁷⁶. Fe1 is displaced by 1.1 \AA from “iron in” conformation to “iron out” conformation, which changes the Fe1 to Ni distance by 0.1

Å from 2.7 Å to 2.8 Å. Fe2 is displaced by 0.6 Å. Coordination of Fe1 and Fe2 by Cys²⁹⁵ and Cys⁴⁷⁶ is restored via local changes and coordination of Fe1 by His²⁶¹ is recovered via extended conformational change over His²⁵⁹-Val²⁷⁰ segment (fig. S2, A).

In CODH_{as-isol.} (CO oxidation activity 11,700 μmol CO oxidized min⁻¹ mg⁻¹ [units mg⁻¹]) the occupancies of [Ni-4Fe-5S]- and [Ni-4Fe-4S]- conformations are 60% and 40%, respectively, with overall 60% occupancy of μ₂S (Fig. 2 A). In CODH_{act.} state (16,400 units mg⁻¹) the occupancy of [Ni-4Fe-5S]-conformation is ~ 85% indicating that the conversion of cluster conformation and activation are induced by incorporation of μ₂S from external sulfide (Fig. 2 B).

KCN-inhibited CODH_{CN} state (1,300 units mg⁻¹) contains a cyanide ligand at the Ni ion (Fig. 2 C, table S1). Cyanide C atom replaces the μ₂S and recovers the slightly distorted square-planar coordination of Ni, which agrees with XAS on KCN-inhibited CODH_{Ch} (Ha et al. 2007). This distortion can be described by doming about the S5-Ni-C-N plane, whereas in μ₂S-bound structure (CODH_{act.}) the doming is about the S3-Ni-S^γ(Cys⁵²⁶) plane. Cyanide N atom is in hydrogen-bonding distance to His⁹³ and Lys⁵⁶³. Binding of cyanide converts the initial “iron out” [Ni-4Fe-5S]-conformation to the “iron in” [Ni-4Fe-4S]-conformation and results in a small displacement of Ni and Cys⁵²⁶. Coordination of Fe1 by His²⁶¹ is recovered via large conformational changes extending over two consecutive turns of the α-helix in the His²⁵⁹-Val²⁷⁰ segment (fig. S2, A). The occupancy of the bound cyanide is ~ 80% and is consistent with the occupancies of resolved major conformations of S1, Fe1, Fe2, and their protein ligands. Cyanide is a competitive inhibitor of reduced CODH_{Ch} with respect to CO and mimics the substrate CO (Ha et al. 2007). Thus, the cyanide-bound conformation represents a model for NiS₃-coordinated state with bound CO, which appears during the turnover cycle of CO-oxidation after displacement of μ₂S.

In reactivated CODH_{react.DT} state (16,000 units mg⁻¹) the initial [Ni-4Fe-5S]-conformation of CODH_{act.} is recovered (fig. S2,B). Cyanide ligand is displaced by μ₂S, which originates from external sulfide, and the NiS₄-coordination is re-established.

To prove whether μ₂S in CODH_{CN} remains bound as flexible ligand or is released, we have determined the Ni-coordination in CODH_{react.Ti} (10,700 units mg⁻¹) reactivated in the absence of sulfide. XAS revealed NiS₃-coordination (fig. S3 and table S2). Therefore, there was no bound μ₂S in CODH_{react.Ti} and in

CODH_CN. Reversible inhibition by KCN released $\mu_2\text{S}$ as H_2S indicating its S^{2-} -state, since ~ 2 mol of H_2S per mol of homodimeric CODH_{Ch} was formed when Ti(III) citrate-reduced CODH_act. was inhibited by KCN. No H_2S was released in the absence of KCN testifying the stability of the Ni-($\mu_2\text{S}$)-Fe1 bridge.

In contrast to KCN-inhibition, no H_2S was liberated upon exposure of CODH_act. to CO oxidation with CO and electron acceptor methyl viologen. This suggested the reformation of the Ni-($\mu_2\text{S}$)-Fe1 bridge after the catalytic cycle which has been proved by the XAS-analysis of the Ni-coordination after CO oxidation (fig. S3 and table S2). All samples (activated CODH_act.1, CODH_turnov.DT and CODH_turnov.Ti generated by exposure of CODH_act.1 to CO oxidation, and CODH_CO generated by incubation of CODH_act.1 with CO without acceptor) contained 3.7 to 3.8 S ligands at Ni. Since CO oxidation did not change the number of S ligands, $\mu_2\text{S}$ is displaced from the bridging position when the enzyme is oxidizing CO and re-establishes the bridge after completion of the catalytic cycle.

The $\mu_2\text{S}$ ligand is not required for CO oxidation since the $\mu_2\text{S}$ -depleted NiS₃-form in CODH_react.Ti state displayed 65% of NiS₄-activity (Fig. 1C). However, the conversion of the NiS₃-form to the NiS₄-form is accompanied by an increase of activity (Fig. 1, A and C) indicating that $\mu_2\text{S}$ is involved in catalysis. Kinetic (Fig. 3A and fig. S4, A and B) and structural (Fig. 2, A and B, and fig. S2B) data document that the acceleration of CO oxidation is caused by the incorporation of sulfide as $\mu_2\text{S}$. Activation requires external sulfide, low-potential reductants dithionite or Ti(III) citrate, and high temperature, and proceeds both under non-turnover (Fig. 1, A and C, Fig. 3A, and fig. S4A) and catalytic turnover (fig. S4B) conditions (see supporting text). Under non-turnover conditions, the activity of CODH_as-isol. with 60% occupancy of $\mu_2\text{S}$ position rised from 11,700 to 16,400 units mg^{-1} upon incubation at 70°C under N_2 with Na_2S or dithionite as the source of sulfide (Das and Kanatzidis 1995; Wahl and Rajagopalan 1982) (Figs. 1C and 3A). Under turnover conditions, the activity of CODH_react.Ti rised in the presence of Na_2S by more than 40% to the level of activated state (fig. S4B). Na_2S does not activate or inhibit CO oxidation in NiS₄-form of the enzyme, e.g. in activated CODH_act. (Fig. 1A and fig. S4B) or in the previously described as-isolated CODH_{Ch} (Ha et al. 2007). The sulfide-dependent activation is obviously caused by the displacement of the product CO_2 by $\mu_2\text{S}$ forming

the Ni-(μ_2 S)-Fe1 bridge. We suggest that in the reaction of CO oxidation the displaced μ_2 S ligand stays as sulfide in a cavity in vicinity of cluster C and/or in the substrate and water channel which ends directly above the Ni ion (Dobbek et al. 2001) and permanently rebinds to displace CO₂. The high rate of CO oxidation (k_{cat} of 31,000 s⁻¹ and k_{cat}/K_m of $1.7 \cdot 10^9$ M⁻¹ s⁻¹ at 70°C, Svetlitchnyi et al. 2001) and subsequent μ_2 S rebinding would prevent the release of this ion from the protein by diffusion-controlled process (10^8 to 10^9 M⁻¹ s⁻¹), as it is the case in KCN-inhibited state.

In contrast, sulfide and the bridging μ_2 S inhibit the reduction of CO₂ to CO (Fig. 3B, fig. S4, C and D, and supporting text). This reaction typical for NiFe CODHs (Ragsdale 2004) is non-physiological for CODHIII_{Ch}. CO₂ reduction activities of μ_2 S-depleted CODH_{react.Ti} and μ_2 S-containing CODH_{as-isol.} were 36.6 and 23.5 μ mol CO formed min⁻¹mg⁻¹ (units mg⁻¹), respectively, when measured at 25°C with Ti(III) citrate as electron donor, methyl viologen as electron mediator, NaHCO₃ as CO₂-source, and ferrous hemoglobin as CO trap. Added Na₂S strongly inhibited CO₂ reduction in hemoglobin-independent CO evolution assay (Fig. 3B) as well as in the carboxyhemoglobin-based assay (fig. S4, C and D). Thus, the inhibition of CO₂ reduction by sulfide is caused by its incorporation as μ_2 S, which complicates the binding of CO₂.

For the cluster conformation in the process of CO₂ reduction, crystals of CODH_{act.} were washed with Ti(III) citrate to remove unbound sulfide and soaked with NaHCO₃ in the absence of methyl viologen, generating CODH_{CO2} state (table S1). Cluster displays the “iron out” [Ni-4Fe-5S]-conformation with ~ 50% of μ_2 S displaced by carboxylic acid group bridging the Ni and Fe1 ions (Fig. 2 D). The C atom of carboxylate is bound to the Ni ion and O atoms establish hydrogen bonds to His⁹³ and Lys⁵⁶³ as it was found in recombinant CODHIII_{Ch} (Jeoung 2007). There was no bound CO₂ when the crystals of CODH_{act.} were soaked with NaHCO₃ without removal of unbound sulfide, which agrees with strong inhibition of CO₂ reduction by sulfide. The affinity of cluster C for CO (K_m 18 μ M, Svetlitchnyi et al. 2001) is significantly higher than for CO₂ (K_m 160 μ M, this work). Therefore, in CO oxidation CO easily displaces μ_2 S, whereas in CO₂ reduction μ_2 S retards the binding of CO₂. In the absence of unbound sulfide, the displaced μ_2 S can escape from the protein by diffusion, because CO₂ reduction is slow (0.5 units mg⁻¹, k_{cat} of 1.1 s⁻¹ in the absence

of methyl viologen). It allows the visualization of Ni-bound CO₂ in crystals soaked with Ti(III) citrate and NaHCO₃ (Fig. 2 D).

We conclude from this study that the [Ni-4Fe-5S]-form of cluster C is the biologically relevant species in CODHII_{Ch}. The bridging μ_2 S has two functions which are of physiological importance for the life of *C. hydrogenoformans* on CO. Firstly, it stabilizes the cluster at high growth temperature of the bacteria. Stabilization prevents inactivation via removal of Ni and decomposition of the cluster as observed in several crystal structures (Dobbek et al. 2004, Jeoung 2007) and is essential at 70°C (Fig. 1A and C), whereas at 25°C the NiS₄- and the NiS₃-forms of CODHII_{Ch} are equally stable. Sulfide significantly improves stability by maintenance of the Ni-(μ_2 S)-Fe1 bridge. Since *C. hydrogenoformans* grows in the presence of 2-3 mM sulfide, produces H₂S (Henstra and Stams 2004), and lives in volcanic vents with millimolar concentrations of sulfide (Stetter 1999; Kelley et al. 2002), the stabilization by μ_2 S is physiologically relevant. Secondly, μ_2 S controls the catalytic activity of CODHII_{Ch}. It accelerates the physiologically relevant CO oxidation, prevents the inhibition by the product CO₂, and inhibits the non-physiological CO₂ reduction. This function is especially important under highly reducing, CO-limited and CO₂-rich conditions in volcanic environments (Svetlitchnyi et al. 1991 a,b; Stetter 1999; Kelley et al. 2002), which would favour the CO₂ reduction activity of the enzyme.

This study substantiates our recently proposed mechanism of CO oxidation at the [Ni-4Fe-5S] cluster C of native CODHII_{Ch} (Ha et al. 2007). It shows how CO and CO₂ bind, considers the reactivity with cyanide and sulfide, and discloses the functions of the bridging μ_2 S. The reaction starts from the highly stable resting state of the cluster in the “iron out” [Ni-4Fe-5S]-conformation (CODH_{act}) which preserves the functional enzyme in the absence of CO (Fig. 4A). CO molecule comes in through the substrate/water channel (Fig. 4A). One scenario assumes its binding to the vacant apical position of the Ni ion coordinated by 4 S ligands. The μ_2 S ligand is labilized by the binding of CO, dissociates as sulfide, and stays in a cavity or in the channel in the vicinity of Ni. A simultaneous rearrangement leads to a transient “iron in” [Ni-4Fe-4S]-conformation of square-planar Ni with three S and one CO ligands (CODH_{CN}) (Fig. 4B). Such rearrangement agrees with the conversion of CO by a nickel to sulfur rebound mechanism studied with model compounds containing four-coordinate Ni

(Sellmann et al. 2000, Fan and Hall 2004). The second scenario assumes direct displacement of $\mu_2\text{S}$ by CO resulting in planar Ni-carbonyl (CODH_CN) (Fig. 4B). A water molecule binds as OH^- to Fe1 as proposed previously (DeRose et al. 1998) and identified in recombinant CODH_{Ch} (Jeoung 2007). This re-establishes the “iron out” [Ni-4Fe-5S]-conformation with covalently bound CO and transiently bound OH^- in place of the bridging $\mu_2\text{S}$ (Fig. 4 C). The Ni-bound CO undergoes a nucleophilic attack by the Fe1-bound OH^- with the formation of a Ni- and Fe1-bridging carboxylic acid group (CODH_CO2) (Fig. 4 D), which is subsequently deprotonated by the neighboring residues (His⁹³, Lys⁵⁶³) forming a proton transfer network (Kim et al. 2004). The sulfide ion displaces the preformed CO_2 and reconstitutes the Ni-($\mu_2\text{S}$)-Fe1 bridge (Fig. 4 A), converting unstable NiS_3 -conformation to stable NiS_4 -conformation, and a new reaction cycle can proceed. Dissociation of CO_2 generates two electrons that are transferred through [3Fe-4S] subcluster, clusters B, and D to the external electron acceptor (Dobbek et al. 2001).

References and notes

1. Svetlichny VA, Sokolova TG, Gerhardt M, Kostrikina NA, Zavarzin GA (1991) *Microb Ecol* 21:1-10-
2. Svetlichny VA, Sokolova TG, Gerhardt M, Ringpfeil M, Kostrikina NA, Zavarzin GA (1991) *Syst Appl Microbiol* 14:254-260.
3. Stetter KO (1999) *FEBS Letters* 452:22-25.
4. Kelley DS, Baross JA, Delaney JR (2002) *Annu Rev Earth Plant Sci* 30:385-491.
5. Svetlitchnyi V, Peschel C, Acker G, Meyer O (2001) *J Bacteriol* 183:5134-5144.
6. Soboh B, Linder D, Hedderich R (2002) *Eur J Biochem* 269:5712-5721.
7. Dobbek H, Svetlitchnyi V, Gremer L, Huber R, Meyer O (2001) *Science* 293:1281-1285.
8. Dobbek H, Svetlitchnyi V, Liss J, Meyer O (2004) *J Am Chem Soc* 126:5382-5387.
9. Ha S-W, Korbas M, Klepsch M, Meyer-Klaucke W, Meyer O, Svetlitchnyi V (2007) *J Biol Chem* 282:10639-10646.
10. Gu W, Seravalli J, Ragsdale SW, Cramer SP (2004) *Biochemistry* 43:9029-9035.

11. Drennan CL, Heo J, Sintchak MD, Schreiter E, Ludden PW (2001) *Proc Natl Acad Sci USA* 98:11973-11978.
12. Doukov TI, Iverson TM, Seravalli J, Ragsdale SW, Drennan CL (2002) *Science* 298:567-672.
13. Darnault C, Volbeda A, Kim EJ, Legrand P, Vernede X, Lindahl PA, Fontecilla-Camps JC (2003) *Nat Struct Biol* 10:271-279.
14. Jeoung J-H, Dobbek H (2007) *Science* 318:1461-1464.
15. Feng J, Lindahl PA (2004) *J Am Chem Soc* 126:9094-9100.
16. Ragsdale SW (2004) *Crit Rev Biochem Mol Biol* 39:165-195.
17. Wahl RC, Rajagopalan KV (1982) *J Biol Chem* 257:1354-1359.
18. Das BK, Kanatzidis MG (1995) *Inorg Chem* 34:6505-6508.
19. Ragsdale SW (2007) *J Inorg Biochem* 101:1657-1666.
20. Sellmann D, Geipel F, Heinemann FW (2000) *Chem Eur J* 6:4279-4284.
21. Fan Y, Hall MB (2004) *Chem Eur J* 10:1805-1814.
22. DeRose VJ, Telser J, Anderson ME, Lindahl PE, Hoffman BM (1998) *J Am Chem Soc* 120:8767-8776.
23. Kim EJ, Feng J, Bramlett MR, Lindahl PA (2004) *Biochemistry* 43:5728-5734.
24. Henstra AM, Stams AJM (2004) *Appl Environ Microbiol* 70:7236-7240.
25. We acknowledge financial support from the Deutsche Forschungsgemeinschaft (grants SV10/1-1 and SV10/1-2). Coordinates and structure factors have been deposited in the Protein Data Bank (www.pdb.org) as entries

Figure legends

Fig. 1. Stability and generation of NiS₄- and NiS₃-forms of CODH_{Ch}. (A) Stability at 70°C and (B) stability at 25°C of the NiS₄-form (●,○) and of the NiS₃-form (▲,△) of the enzyme (0.11 μg ml⁻¹) incubated under N₂ with 4 mM Ti(III) citrate in the presence of 1.5 mM Na₂S (closed symbols) and in the absence of Na₂S (open symbols). 100% of CO oxidation activity corresponds to 16,400 and 10,700 units mg⁻¹ for NiS₄- and NiS₃-forms, respectively. (C) Effect of sulfide on reactivation and stability of cyanide-inhibited CODH_{Ch}. CODH_{as-isol.} (0.5 mg ml⁻¹) was activated to CODH_{act.} state at 70°C under N₂ in the presence of 4 mM dithionite as reductant and source of sulfide (■). CODH_{act.} was inhibited by 250 μM KCN at 23°C under N₂ generating CODH_{CN} state (∇). CODH_{CN} was reactivated at 70°C under N₂ in the presence of 4 mM dithionite (●, yields CODH_{react.DT} state), 4 mM Ti(III) citrate + 1 mM Na₂S (○), or 4 mM Ti(III) citrate (▲, yields CODH_{react.Ti} state). 100% of CO oxidation activity corresponds to 11,700 units mg⁻¹.

Fig. 2. Structure of cluster C in different states of CODH_{Ch}. (A) As-isolated **CODH_{as-isol.}** state. An $F_{\text{obs}}-F_{\text{calc}}$ omit electron density map is depicted in blue. The model presents the [Ni-4Fe-5S]-conformation with 60% occupancy (large balls) and the [Ni-4Fe-4S]-conformation with 40% occupancy (small balls). The position of bound cyanide taken from cyanide-inhibited **CODH_{CN}** structure is shown as small balls. (B) Activated **CODH_{act.}** state. An $F_{\text{obs}}-F_{\text{calc}}$ omit electron density map is depicted in blue. The model presents the [Ni-4Fe-5S]-conformation with 85% occupancy for the activated structure (large balls) and the traces of [Ni-4Fe-4S]-conformation (small balls). The position of bound cyanide taken from cyanide-inhibited **CODH_{CN}** structure is shown as small balls. (C) Cyanide-inhibited **CODH_{CN}** state. An $F_{\text{obs}}-F_{\text{calc}}$ omit electron density map is contoured at 5σ level. The model presents a complex with cyanide (large balls). Superimposed is the structure in **CODH_{act.}** state (small balls). (D) Cluster C in **CODH_{CO2}** state with bound CO₂.

Fig. 3. Sulfide-dependent activation of CO oxidation (A) and inhibition of CO₂ reduction (B) in CODHII_{Ch}. (A) CODHII_{Ch} in as-isolated CODH_as-isol. state (0.1 μg ml⁻¹) was incubated under N₂ with 4 mM dithionite + 2 mM dithiothreitol (DTT) + 1 mM Na₂S (●), 4 mM dithionite + 2 mM DTT (Δ), 2 mM Ti(III) citrate + 1 mM Na₂S (∇), 2 mM Ti(III) citrate (▲), 1 mM Na₂S (○), or without reductants and sulfide source (▼) at 70°C. 100% of CO oxidation activity corresponds to 11,700 units mg⁻¹. (D) Headspace analysis of CO₂ reduction to CO. As-isolated CODHII_{Ch} in CODH_as-isol. state (8 μg) was incubated in the presence of 0 (●), 0.5 (■), 1 (▲), or 2 (◆) mM Na₂S at 25°C. CO was quantified by gas chromatography.

Fig. 4. Scheme showing the oxidation of CO to CO₂ and the function of the bridging μ₂S in the [Ni-4Fe-5S] cluster of CODHII_{Ch} from CO grown *C. hydrogenoformans*.

Fig. 1

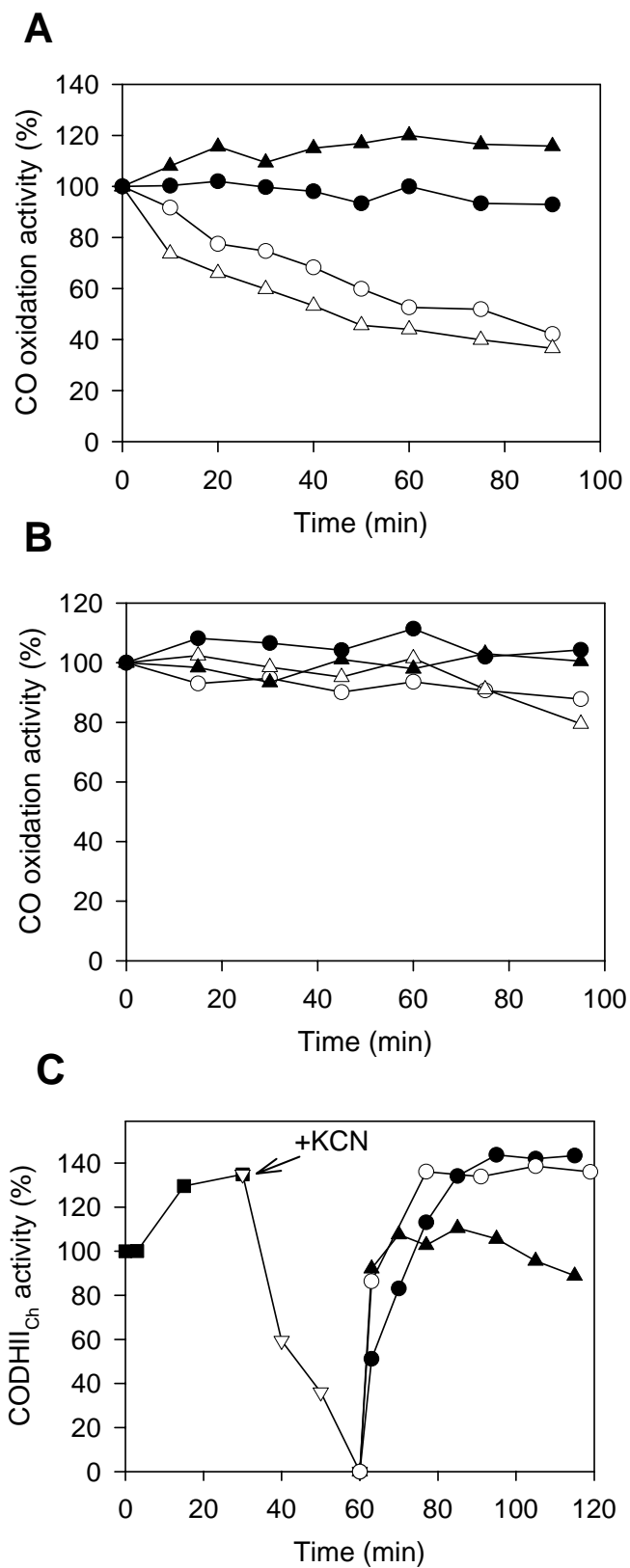


Fig. 2

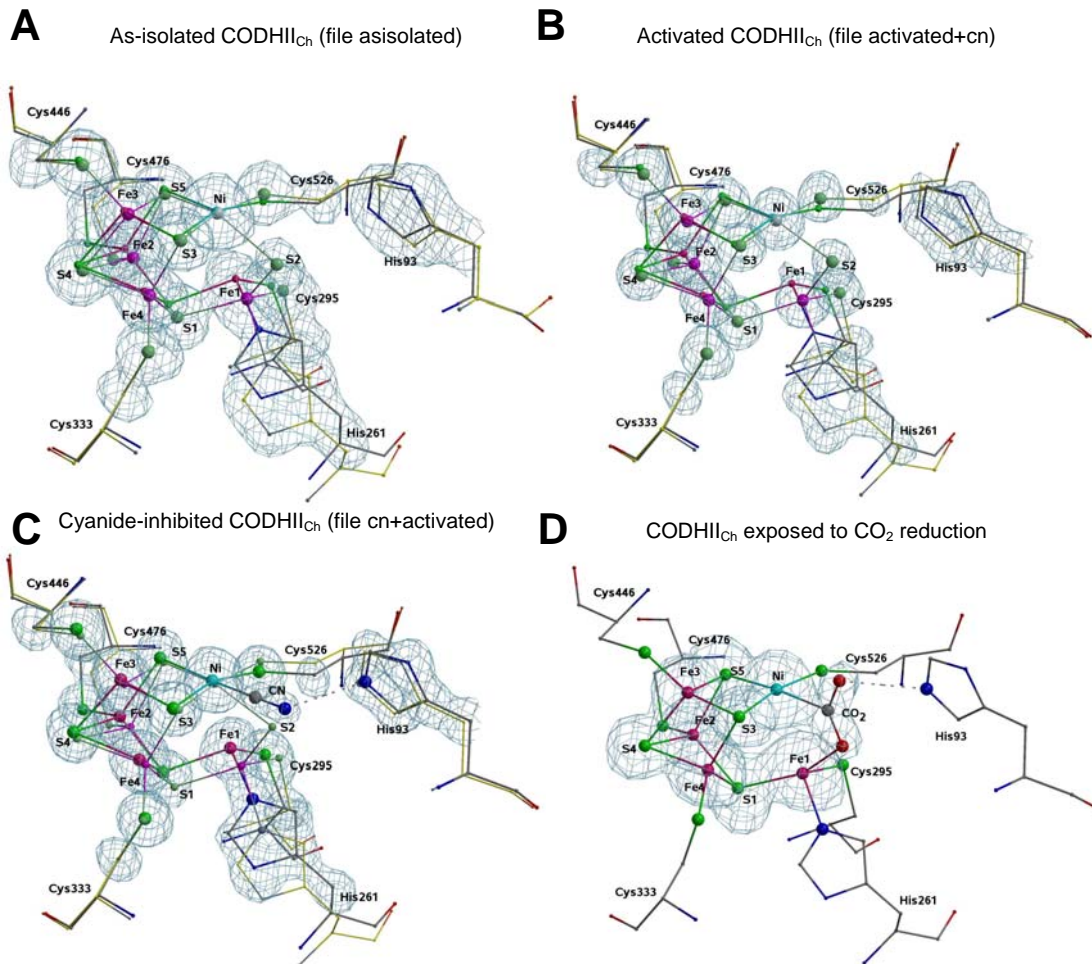


Fig. 3

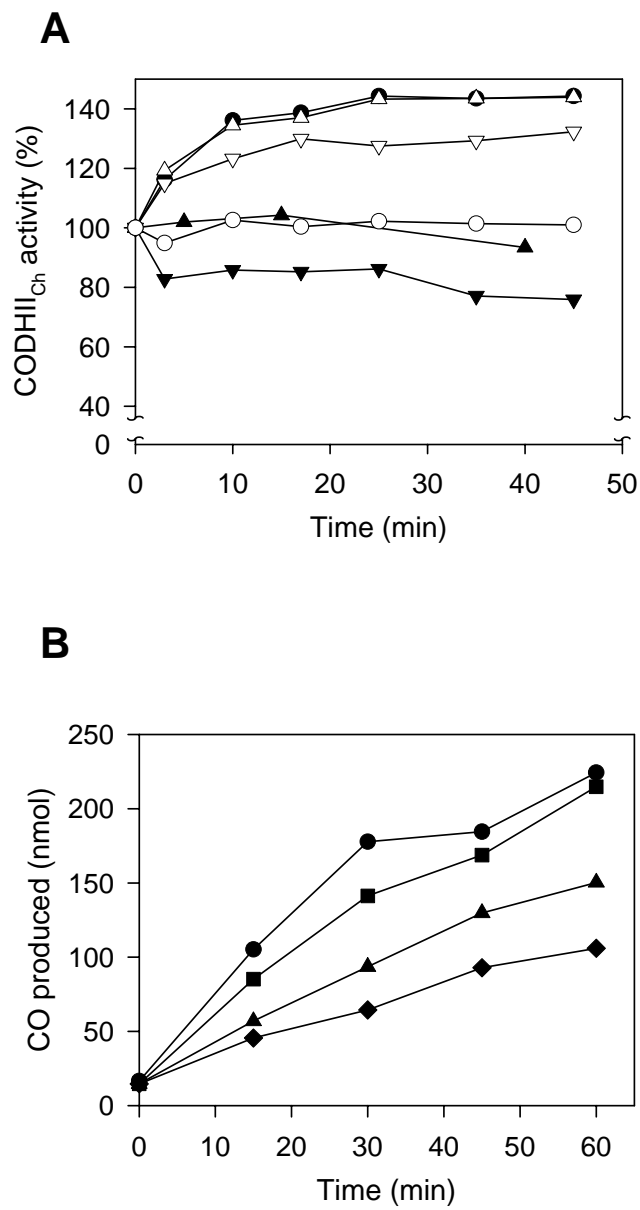
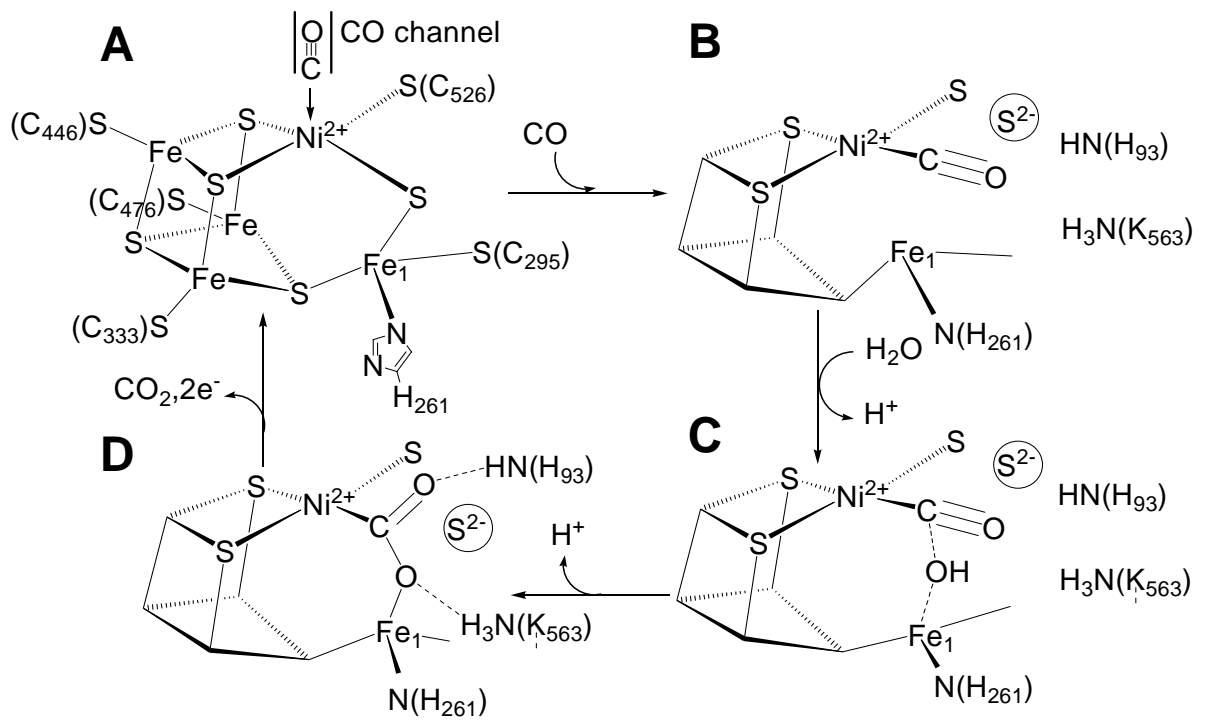


Fig. 4



Supporting online material

Materials and Methods

Purification and assays of CODHII_{Ch}. Growth of *C. hydrogenoformans* Z-2901 (DSM 6008) on CO and purification of the native CODHII_{Ch} were carried out under strict anoxic conditions as detailed (Svetlitchnyi et al. 2001; Svetlitchnyi et al. 2004). Protein estimation employed conventional methods with BSA as a standard (Bradford 1976). CO oxidation activity of CODHII_{Ch} was assayed at 70°C by following the CO-dependent reduction of oxidized methyl viologen as described (Svetlitchnyi et al. 2001). One unit of CO oxidation activity is defined as 1 μmol of CO oxidized per min. Purified as-isolated CODHII_{Ch} (CODH_as-isol.) displayed CO oxidation activity of 11,700 units mg^{-1} and had a protein concentration of 14.3 mg ml^{-1} .

CO₂ reduction activity of CODHII_{Ch} was assayed by following the production of CO which was quantified with ferrous hemoglobin (Bonam et al., 1984) and by direct headspace analysis of CO evolution. The assays with hemoglobin were performed at 25°C and 50°C and the formation of carboxyhemoglobin was monitored at 433 nm. For the assays, 1-ml volumes containing 2 mM Na-dithionite or 2 mM Ti(III) citrate as electron donor, 0.2 mM methyl viologen as electron carrier, 10 mM NaHCO₃ as CO₂ source, 0.2 mg hemoglobin, and 0.9% NaCl in anoxic 100 mM HEPES/NaOH (pH 7.5) were flushed with N₂ in screw-cap cuvettes sealed with a rubber septum. Reactions were initiated by injecting 10 μl of as-isolated or $\mu_2\text{S}$ -depleted (CODH_react.Ti) CODHII_{Ch} with 10 $\mu\text{g ml}^{-1}$. For the headspace analysis of CO evolution, assays were carried out at 25°C in 37-ml serum-stoppered vials which were kept shaken at 150 rpm. Assays were composed of 4 ml of anoxic 50 mM HEPES/NaOH (pH 8.0) (buffer A), 2 mM dithionite, 0.1 mM methyl viologen, and 20 mM NaHCO₃ under a gas atmosphere of N₂. Reactions were performed with 2.0, 4.0, and 8.0 μg of as-isolated CODHII_{Ch}. The gas chromatograph for CO assay (model GC-8A, Shimadzu) was equipped with a reduction gas detector (model RGD2, Trace Analytical) and a molecular sieve 13X column. The temperatures (in °C) were 60 (oven), 25 (injection port), and 280 (detector), respectively. The carrier gas was He at

a flow rate of 30 ml min⁻¹. One unit of CO₂ reduction activity is defined as 1 μmol of CO produced per min.

Activation of as-isolated CODHII_{Ch}. Assays (1 ml) were performed at 23, 50 and 70°C and contained as-isolated (CODH_{as-isol.}) CODHII_{Ch} (0.1 μg ml⁻¹) in buffer A supplemented with 4 mM dithionite + 2 mM dithiothreitol (DTT) + 1 mM Na₂S, 4 mM dithionite + 2 mM DTT, 2 mM Ti(III) citrate + 1 mM Na₂S, 2 mM Ti(III) citrate, 1 mM Na₂S or without reductants and sulfide source under an atmosphere of CO or N₂. Aliquots were removed with time and analyzed for CO oxidation activity.

Inhibition of CODHII_{Ch} by potassium cyanide and reactivation. Inhibition and reactivation were performed as detailed before (Ha et al. 2007). Assays (1.5 ml) were carried out at 23°C and contained activated (CODH_{act.}) CODHII_{Ch} (0.48 mg ml⁻¹) in buffer A supplemented with 4 mM dithionite and 2 mM DTT under an atmosphere of N₂. Inhibition was initiated by the addition of 250 μM KCN. The inhibited sample was then diluted 5,000-fold in N₂-saturated buffer A containing 4 mM dithionite + 2 mM DTT, 4 mM Ti(III) citrate + 1 mM Na₂S, or 4 mM Ti(III) citrate, and the assays were incubated at 70°C under N₂ for reactivation. Aliquots were removed with time and analyzed for CO oxidation activity.

Effect of sodium sulfide on CODHII_{Ch}. Na₂S was added from anoxic solutions in 10 mM NaOH to CO oxidation and CO₂ reduction assays under turnover conditions, to the activation assays of as-isolated CODHII_{Ch}, and to the reactivation assays of cyanide-inhibited reduced CODHII_{Ch} under non-turnover conditions.

Preparation of samples for X-ray crystallography. As-isolated CODHII_{Ch} (CODH_{as-isol.}, 11,700 units mg⁻¹) was used for crystallization without any treatment. For activated CODHII_{Ch} (CODH_{act.}, 16,400 units mg⁻¹), the as-isolated enzyme was diluted to 0.5 mg ml⁻¹ under N₂ with buffer A containing 4 mM dithionite and 2 mM DTT and incubated at 70°C under N₂ for 30 min. Activated CODHII_{Ch} was concentrated under N₂ to 12 mg ml⁻¹, yielding sample CODH_{act.}

For CODHII_{Ch} reversibly inhibited by cyanide (CODH_CN, 1.500 units mg⁻¹), activated CODH_act. was diluted to 0.5 mg ml⁻¹ under N₂ in buffer A containing 4 mM dithionite, 2 mM DTT, and 250 μM KCN. After 30 min incubation at 23°C the activity was completely inhibited. Inhibited CODHII_{Ch} was concentrated under N₂ to 12 mg ml⁻¹, yielding sample CODH_CN. The enzyme was reversibly inhibited since it could be reactivated to 16,400 units mg⁻¹ upon incubation at 70°C under N₂ in buffer A containing 4 mM dithionite and 2 mM DTT.

For CODHII_{Ch} reversibly inhibited by cyanide and then reactivated in the presence of dithionite (CODH_react.DT, 16,000 units mg⁻¹), concentrated cyanide-inhibited CODH_CN was applied. For the reactivation, CODH_CN (200 μl) was dissolved in 6 ml of buffer A with 4 mM dithionite and 2 mM DTT to 0.4 mg ml⁻¹ and incubated at 70°C under N₂ for 30 min. Reactivated CODHII_{Ch} was concentrated under N₂ to 12 mg ml⁻¹, yielding sample CODH_react.DT.

Preparation of samples for XAS. For CODHII_{Ch} reversibly inhibited by cyanide and then reactivated in the presence of Ti(III) citrate (CODH_react.Ti, 10,700 units mg⁻¹), concentrated cyanide-inhibited CODH_CN was applied. To remove dithionite from CODH_CN and exclude its effect as a source of external sulfide, CODH_CN (150 μl) was dissolved in 0.5 ml of buffer A under N₂ containing 4 mM Ti(III) citrate and concentrated to 25 μl by ultrafiltration under N₂. The procedure was repeated three times. For reactivation, the concentrated dithionite-free enzyme (25 μl) was dissolved in 6 ml of buffer A with 4 mM Ti(III) citrate to 0.3 mg ml⁻¹ and incubated at 70°C under N₂ for 30 min. Reactivated CODHII_{Ch} was concentrated under N₂ to 64 mg ml⁻¹, yielding sample CODH_react.Ti.

Sample CODH_turnov.DT, which was exposed to CO oxidation in the presence of CO, electron acceptor methyl viologen, and traces of dithionite as reductant, was produced from activated CODH_act.1 sample prepared as CODH_act. By three times repeated ultrafiltration the protein was transferred to buffer A with 1 mM dithionite and diluted to 2.1 mg ml⁻¹. To establish turnover conditions, 1 ml of the sample was injected to a 110 ml flask containing CO gas phase and 40 ml of vigorously stirred (300 rpm) CO-saturated buffer A supplemented with 20 mM of oxidized methyl viologen. Oxidation of CO was indicated by the appearance of blue color of reduced

methyl viologen. After 30 min of incubation at 23°C with stirring, the protein was concentrated under N₂ to 65 mg ml⁻¹.

Sample CODH_turnov.Ti exposed to CO oxidation with CO, methyl viologen, and traces of Ti(III) citrate as reductant was produced from CODH_act.1 and concentrated to 65 mg ml⁻¹ as described for CODH_turnov.DT, except that the protein was in buffer A supplemented with 2 mM Ti(III) citrate.

Sample CODH_CO exposed to CO under non-turnover conditions was produced from CODH_act.1 and concentrated to 65 mg ml⁻¹ as described for CODH_turnov.DT, except that methyl viologen was omitted.

Stability assays. NiS₄-form of CODHII_{Ch} was prepared generally as CODH_act. by activation of as-isolated enzyme (1.23 mg ml⁻¹) at 70 °C under N₂ in the presence of 4 mM dithionite, 2 mM DTT, and 1 mM Na₂S. To remove the excess of sulfide and dithionite, the activated enzyme was dissolved in 0.6 ml of buffer A under N₂ containing 4 mM Ti(III) citrate and concentrated to 50 µl by ultrafiltration under N₂. The procedure was repeated three times. The rinsed enzyme was diluted 2.5×10⁵-fold in buffer A containing either 4 mM Ti(III) citrate or 4 mM Ti(III) citrate plus 1.5 mM Na₂S.

NiS₃-form of CODHII_{Ch} was prepared as generally as CODH_react. Ti by reactivation of cyanide-inhibited activated enzyme. Before reactivation, unbound cyanide and excess of dithionite were removed by 3 times repeated concentration and washing with buffer A containing 4 mM Ti(III) citrate under N₂. Reactivation was performed at 70 °C under N₂ in the presence of 4 mM Ti(III) citrate. The reactivated enzyme (0.5 µg ml⁻¹) was diluted 2.9×10⁴-fold in buffer A containing either 4 mM Ti(III) citrate or 4 mM Ti(III) citrate plus 1.5 mM Na₂S.

For stability assay, the samples were incubated at 70°C or 25°C under an atmosphere of N₂ or CO. Aliquots were removed with time and analyzed for CO oxidation activity.

Analysis of H₂S release from CODHII_{Ch}. The release of H₂S from CODHII_{Ch}, induced by the reversible inhibition of reduced enzyme by KCN cyanide as well as by the exposure of the enzyme to turnover conditions in the presence of CO and methyl

viologen, was estimated colorimetrically employing the methylene blue method (Fogo and Popowsky 1949). CODHII_{Ch} which was not subjected to any treatment was used as the control for the release of H₂S.

For the assays of H₂S release, activated CODH_act. was applied. By three times repeated ultrafiltration dithionite was removed, the enzyme was transferred to buffer A with 4 mM Ti(III) citrate, and diluted to 13,0 mg ml⁻¹. For the reversible inhibition by KCN, 0.5 ml of the enzyme sample was injected to a 110 ml flask containing N₂ gas phase and 40 ml of N₂-saturated buffer A supplemented with 250 μM KCN and 4 mM Ti(III) citrate. After 30 min of incubation at 23°C with gentle stirring the activity was completely inhibited and the enzyme solution was subjected to ultrafiltration to separate the released sulfide from the protein. The control assay was performed as described for cyanide-inhibition, except that KCN was omitted. For the turnover conditions, 0.5 ml of the enzyme sample was injected to a 110 ml flask containing 40 ml of vigorously stirred (300 rpm) CO-saturated buffer A supplemented with 20 mM of oxidized methyl viologen under CO. Oxidation of CO was indicated by the appearance of blue color of reduced methyl viologen. After 30 min of incubation at 23°C with stirring the enzyme solution was subjected to ultrafiltration.

To bind the released H₂S, ultrafiltrates were collected anaerobically in 5.5% (w/v) N₂-saturated zinc acetate solution in water. The white precipitate containing zinc sulfide was recovered by centrifugation. After the dissolution of the pellets in *N,N*-dimethyl-*p*-phenylenediamine/HCl and addition of FeCl₃ the presence of sulfide in the pellets was obvious from the formation of methylene blue, which displayed a characteristic absorption peak with a maximum at 670 nm (Fogo and Popowsky 1949). The calibration curve was established with Na₂S under the conditions of the assays except that CODHII_{Ch} was omitted.

Crystallization. Crystallization of CODHII_{Ch} samples CODH_as-isol., CODH_act., CODH_CN, and CODH_react.DT was performed at 23°C in anaerobic chamber filled with oxygen-free N₂ as described previously (Dobbek et al. 2004). Crystals were obtained with PEG as precipitant at a pH of 7.5 in the presence of 2 mM Na-dithionite and 2 mM DTT. For CODH_CN the crystallization solution contained 300 μM KCN. Crystals appeared within 2 to 4 days. They were shock frozen in

reservoir solution supplemented with 10 % (v/v) glycerol and stored frozen in liquid N₂. At the time of harvesting, part of the crystals was dissolved in buffer A and used for analysis of CO oxidation activity and reactivation.

For the structure of CODHII_{Ch} exposed to CO₂ reduction (CODH_CO2 state), single crystals of CODH_act. were washed four times in dithionite-free crystallization solution supplemented with 5 mM Ti(III) citrate. The washed crystals were soaked for 90 min in crystallization solution containing 5 mM Ti(III) citrate, 50 mM NaHCO₃, and 10 % (v/v) glycerol. After soaking they were shock frozen yielding CODH_CO2 state.

Structure determination and refinement. The diffraction data were collected on the EMBL beamline X13 or MPG-GBF beamline BW6 on DORIS storage ring (DESY, Hamburg, Germany). All data were collected at 100K using MarCCD detector at wavelengths of 0.81 Å and 1.05 Å at X13 and BW6 respectively. Data were indexed, integrated and scaled using HKL program package (Otwinowsky and Minor, 1997). The structures were refined with REFMAC (Murshudov, Vagin and Dodson, 1996) using individual atomic anisotropic displacement parameters. Model building has been carried out using COOT (Emsley and Cowtan, 2004).

Ni-K edge XAS measurements. For XAS measurements, 25 µl of samples CODH_react.Ti, CODH_act.1, CODH_turnov.DT, CODH_turnov.Ti, and CODH_CO were filled into plastic cells covered with Kapton foil. Cells were sealed and kept in liquid N₂. The Ni K-edge XAS data, 8.2 to 9.2 keV, were collected in fluorescence mode with a Si(111) monochromator at the EMBL beamline D2 (DESY, Hamburg, Germany). Harmonic rejection was achieved by a focusing mirror (cut-off energy 20.5 KeV) and a monochromator detuning to 70% of its peak intensity. The sample cells were kept at ~20 K in a two-stage Displex cryostat. Automated data reduction, such as normalization and extraction of the fine structure, was performed with KEMP (Korbas et al. 2006) assuming an energy threshold $E_{0,Ni}=8333$ eV. Sample integrity during exposure to synchrotron radiation was checked by monitoring the position and shape of the absorption edge on sequential scans. No change in redox state or metal environment was detectable.

Extended X-ray absorption fine structure (EXAFS) analysis. The extracted Ni K-edge (20–700 eV) EXAFS were converted to photoelectron wave vector k -space and weighted by k^3 . The spectra were analyzed with EXCURV98 (Binsted et al. 1992), refining the theoretical EXAFS for defined structural models based on the curved-wave theory. Parameters of each structural model, namely the atomic distances (R), the Debye-Waller factors ($2\sigma^2$), a residual shift of the energy origin (EF) were optimized, minimizing the Fit Index (Φ) while keeping the number of free parameters below those of the independent points (Binsted et al. 1992; Stern 1993). Throughout the data analysis the amplitude reduction factor (AFAC) was kept at 1.0.

Supporting text

Sulfide-dependent activation of CO oxidation in CODH_{Ch}

The rate of sulfide-dependent activation strongly decreased with the decrease of incubation temperature from 70°C, which is the optimum growth temperature of *C. hydrogenoformans*, to 50°C and further to 23°C. A mechanism related to CO-dependent or reductive activation, as it was demonstrated for CODH_{Rt} (Heo et al. 2000; Heo et al. 2001), is apparently not applicable for CODH_{as-isol.} since there was no increase of activity upon incubation with CO or Ti(III) citrate in the absence of sulfide (Fig. S4A). The requirement of sulfide-induced activation for low redox potential and high temperature indicates an efficient interaction of sulfide with highly reduced cluster C at elevated temperatures, which is similar to the interaction of cluster C with cyanide and CO (Ha et al. 2007). Incubation of CODH_{as-isol.} at 70°C under CO with a source of sulfide and low-potential reductants resulted in a mild activation (20%) followed by gradual decrease of activity (Fig. S4A). The low level of activation indicates that sulfide and CO share a common binding site at the reduced cluster C. The decrease of activity under CO compared to the preservation of activity under N₂ which was also documented in stability assays (Fig. S1A) is obviously caused by CO-induced decomposition of cluster C as reported before (Dobbek et al. 2004).

Sulfide-dependent inhibition of CO₂ reduction in CODHII_{Ch}

The rate of CO₂ reduction in hemoglobin-based assay strongly depended on the presence of methyl viologen (apparent K_m of 0.055 mM methyl viologen).

Na₂S strongly inhibits CO₂ reduction activity of CODHII_{Ch} (**Fig. S4, C and D**). Inhibition in hemoglobin-dependent assay is not due to any interaction of sulfide with hemoglobin under the assay conditions, because sulfide had no effect on carboxyhemoglobin absorption spectra upon binding of CO and inhibited CO₂ reduction by as-isolated CODHII_{Ch} in hemoglobin-independent CO evolution assay. CO₂ reduction activity in the absence of hemoglobin was low (0.67 units mg⁻¹), indicating inhibition by accumulated CO.

Our suggestion that the bridging μ_2 S in cluster C inhibits CO₂ reduction is supported by observed activities. In hemoglobin-dependent assays with Ti(III) citrate as electron donor the μ_2 S-depleted CODHII_{Ch} (**CODH_react.Ti**) displayed CO₂ reduction activity of 36,6 units mg⁻¹, which is 56 % higher than of the μ_2 S-containing as-isolated enzyme in **CODH_as-isol.** state (23.5 units mg⁻¹). With sodium dithionite as electron donor the activity of CODH_as-isol. was 73 % (17.11 units mg⁻¹) from the activity with Ti(III) citrate indicating inhibition by dithionite-derived sulfide.

Table S1. Refinement statistics

Data set	As-isolated	Activated	CN inhibited	Reactivated	CO ₂
Resolution range, Å overall (outer shell)	12-1.4 (1.44-1.40)	10-1.20 (1.23-1.20)	10-1.10 (1.13-1.10)	10-1.10 (1.13-1.10)	19-1.60 (1.64-1.60)
Unique reflections	101498 (7335)	156141 (8286)	193312 (13842)	190285 (13058)	63563 (3613)
Multiplicity	2.3 (2.1)	2.1 (1.6)	3.1 (2.6)	3.6 (3.0)	2.3 (1.8)
Completeness, %	99.6 (98.7)	97.3 (99.3)	93.8 (91.9)	90.3 (84.9)	90.9 (70.8)
R _{merge}	0.086 (0.520)	0.071 (0.364)	0.062 (0.55)		0.053 (0.46)
<I/σ _I >	15 (1.9)	21 (3.5)	22 (1.8)	22 (3.2)	18 (2.6)
R-factor	0.14 (0.25)	0.13 (0.17)	0.14 (0.226)	0.13 (0.22)	0.13 (0.18)
R _{free}	0.17 (0.27)	0.16 (0.20)	0.16 (0.24)	0.17 (0.27)	0.18 (0.26)
rmsd bond length, Å	0.018	0.016	0.021	0.022	0.021
rmsd bond angles, degrees	1.74	1.74	1.847	2.023	1.821

Table S2. EXAFS refinement parameters for CODH_{Ch} exposed to reactivation and turnover conditions

N	Ni ... L	R (Å)	2σ ² (Å ²)	EF (eV)	Φ·10 ³
CODH_react.Ti					
3	Ni ... S	2.256 (5)	0.0125 (8)	-12.8 (8)	0.4102
1	Ni ... Fe	2.753 (8)	0.010 (2)		
CODH_act.1					
3.7(2)	Ni ... S	2.219 (3)	0.0088 (7)		
1	Ni ... Fe	2.64 (1)	0.018 (2) *		
1	Ni ... Fe	2.97 (2)	0.018 (2) *		
CODH_turnov.DT					
3.7 (1)	Ni ... S	2.219 (2)	0.0087 (6)	-9.4 (4)	0.1213
1	Ni ... Fe	2.64 (1)	0.017 (2) *		
1	Ni ... Fe	2.96 (1)	0.017 (2) *		
CODH_turnov.Ti					
3.8 (2)	Ni ... S	2.209 (3)	0.0107 (8)	-7.2 (5)	0.1855
1	Ni ... Fe	2.63 (1)	0.021 (2) *		
1	Ni ... Fe	2.97 (2)	0.021 (2) *		
CODH_CO					
3.7 (1)	Ni ... S	2.218 (2)	0.0073 (5)	-9.9 (4)	0.1133
1	Ni ... Fe	2.644 (9)	0.015 (1) *		
1	Ni ... Fe	2.96 (1)	0.015 (1) *		

The numbers (N) of ligand atoms (L), their distance to the nickel ion (R), the respective Debye-Waller factor (2σ²), the C–N bond length (R_{CN}), the Fermi energy for all shells (EF), and the Fit Index (Φ), indicating the quality of the fit are shown. Values in parentheses represent statistical errors (2·SD, SD – standard deviation) of the least square refinement. The * indicates the joint refinement of parameters. For sample labels see text.

Figure S1

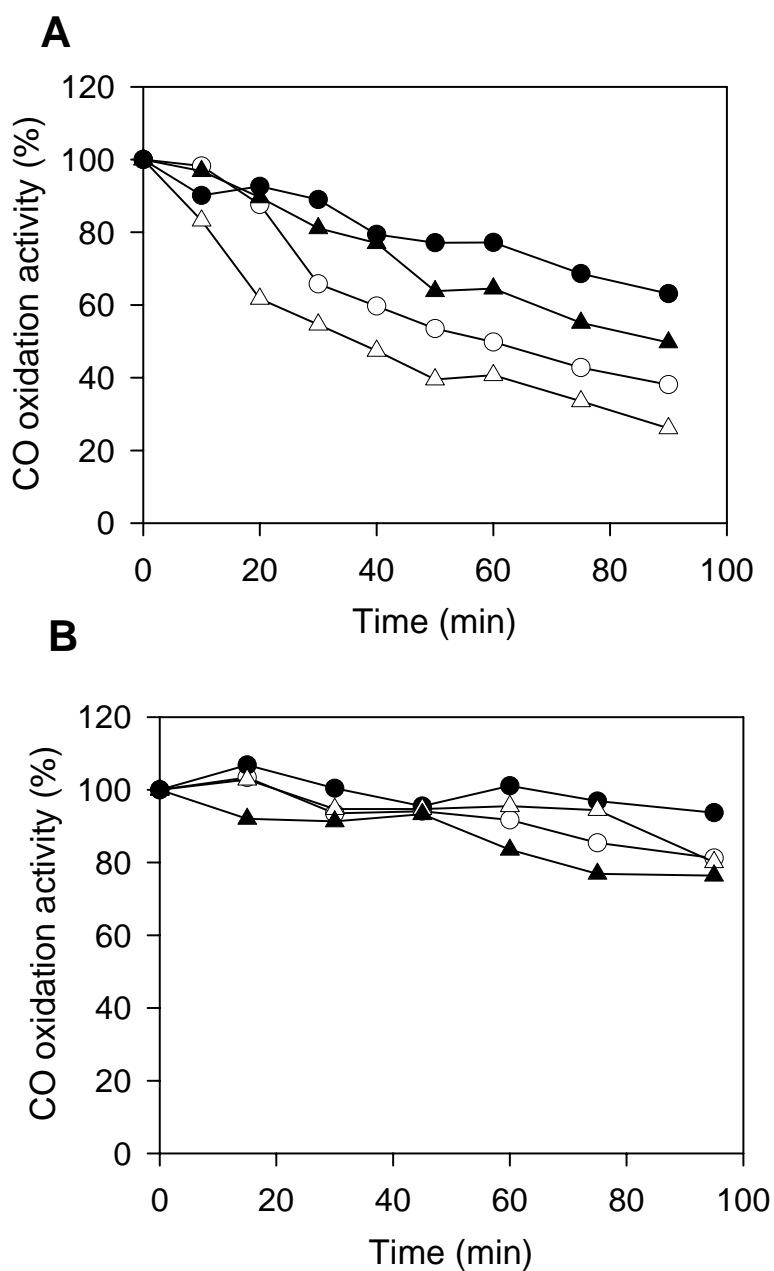


Figure S1. Stability of NiS₄- and NiS₃-forms of CODHII_{Ch} under CO. (A) Stability at 70°C and (B) stability at 25°C of the NiS₄-form (●,○) and of the NiS₃-form (▲,△) of the enzyme (0.11 μg ml⁻¹) incubated under CO with 4 mM Ti(III) citrate in the presence of 1.5 mM Na₂S (closed symbols) and in the absence of Na₂S (open symbols). 100% of CO oxidation activity corresponds to 16,400 and 10,700 units mg⁻¹ for NiS₄- and NiS₃-forms, respectively.

Figure S2

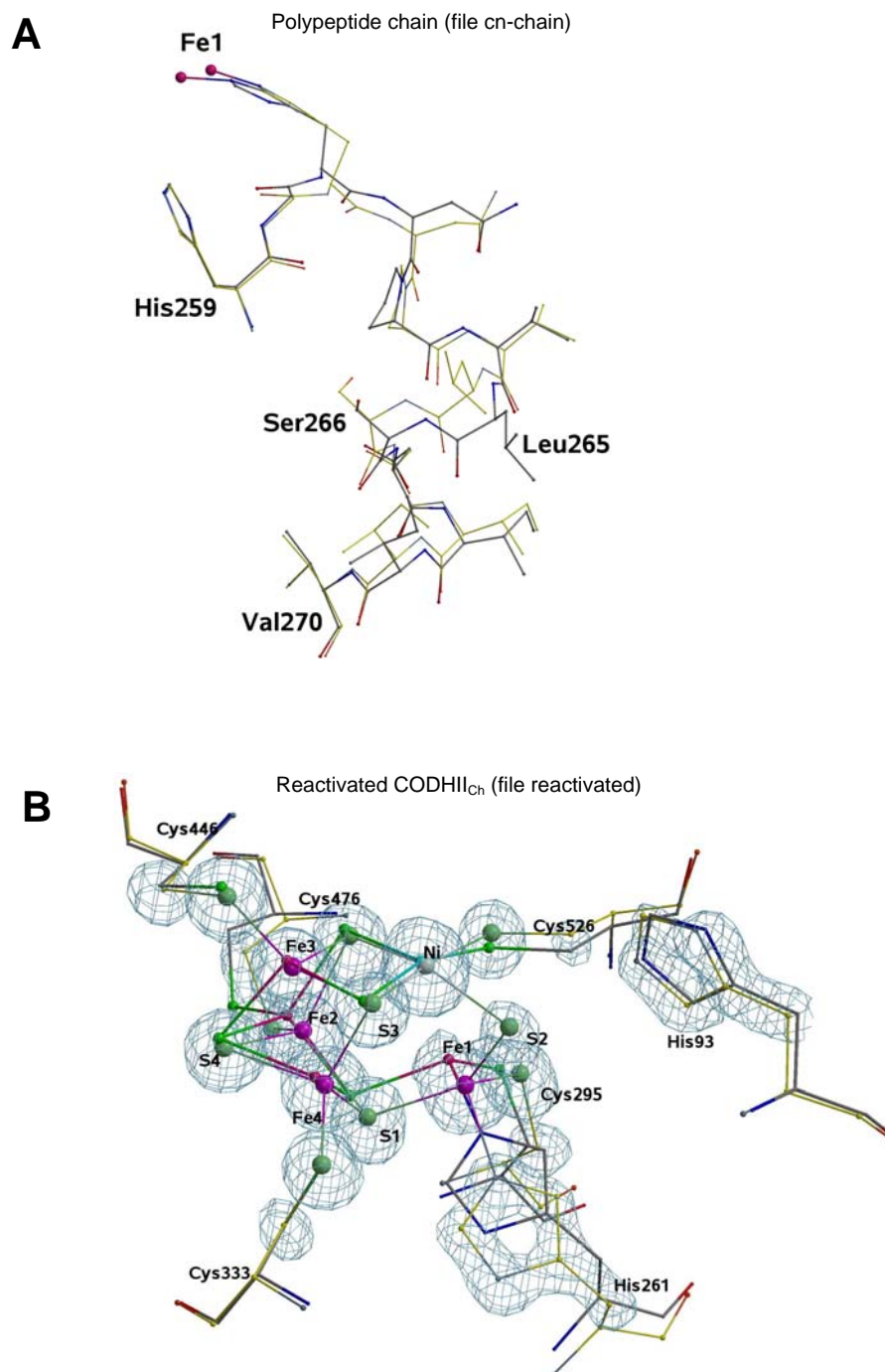


Figure S2. Conformational change of protein environment due to the interconversion of NiS₃- and NiS₄-forms of cluster C and the structure of cluster C in reactivated CODH_{Ch}. (A) Superposition of the polypeptide chain fragments His²⁵⁹-Val²⁷⁰ in the NiS₃-form of cyanide-inhibited CODH_CN state (yellow sticks) and the NiS₄-form of activated CODH_act. state (grey sticks). (B) Cluster C in NiS₄-form of reactivated CODH_react.DT (large balls). Cyanide-inhibited CODH_CN was reactivated in the presence of dithionite as reductant and source of sulfide. The structure is identical to the activated CODH_act. state. Cyanide is not present in the structure. The position of bound cyanide taken from cyanide-inhibited CODH_CN structure is shown as small balls.

Figure S3

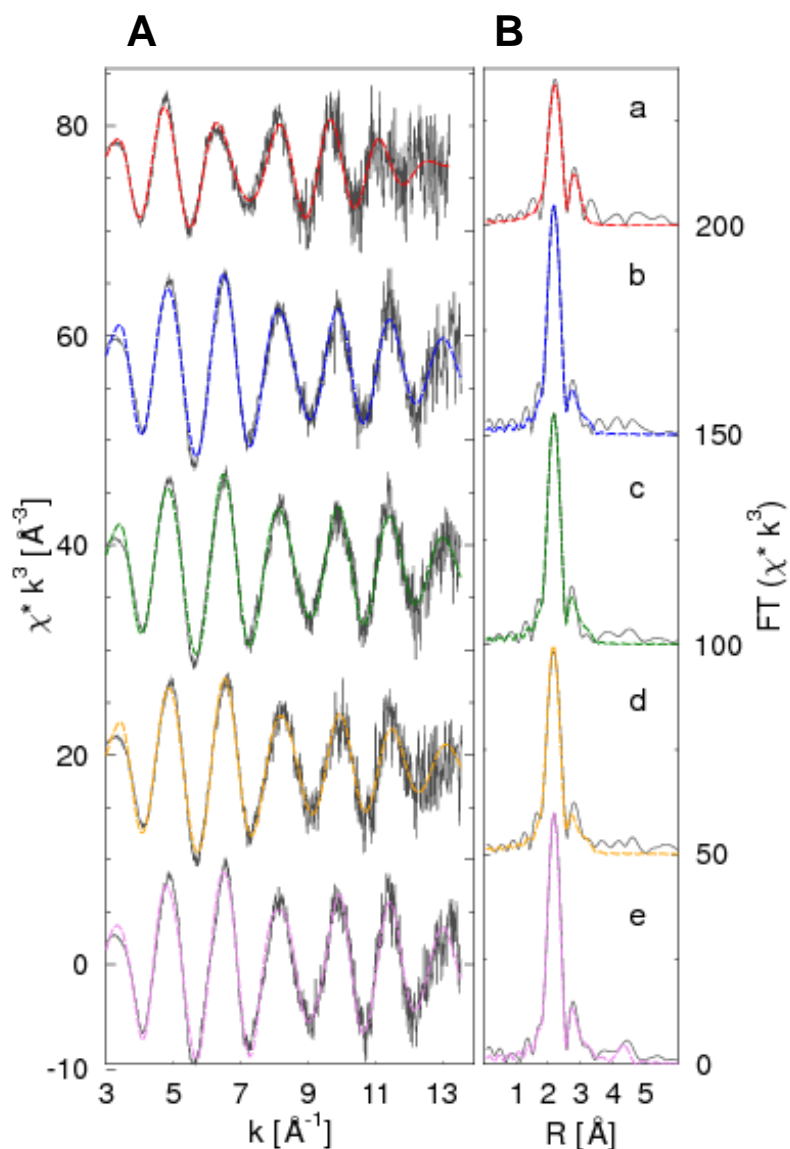


Figure S3. Ni K-edge k^3 -weighted EXAFS spectra (A) and Fourier transforms of EXAFS spectra (B) of different CODHII_{Ch} samples. Samples are as follows: CODH_react.Ti (trace a), CODH_act.1 (trace b), CODH_turnov.DT (trace c), CODH_turnov.Ti (trace d), and CODH_CO (trace e). Calculated spectra are shown by black lines; experimental spectra based on the model given in Table 2 are represented by colored curves. The abbreviations are: χ , EXAFS signal; k , photoelectron wavenumber; R , interatomic distance; FT, Fourier transform (modulus). The Fourier transform is phase-corrected for the shortest metal ligand contribution, and therefore, the peaks do not appear at the refined metal neighbor distances.

Figure S4

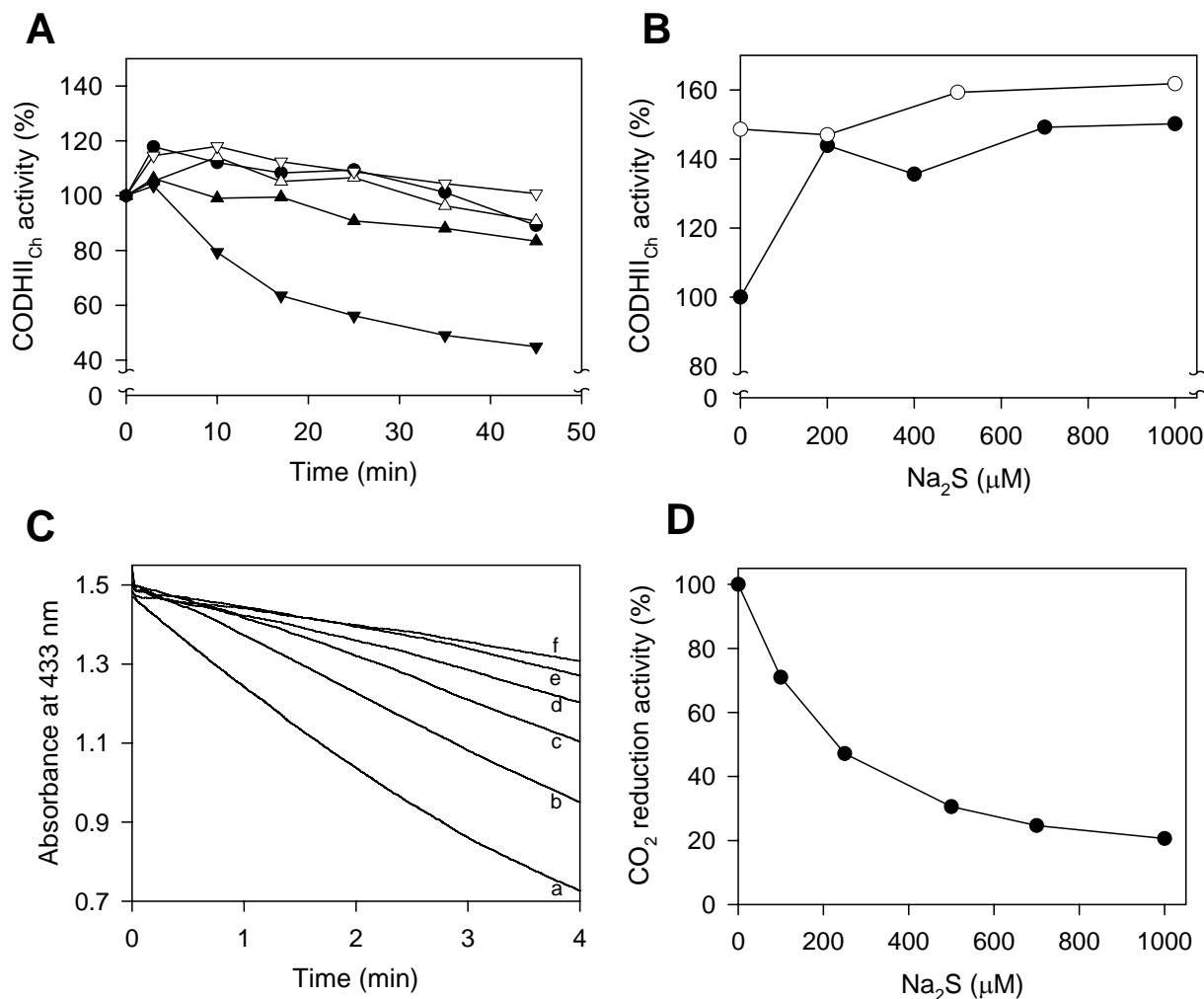


Figure S4. Sulfide-dependent activation of CO oxidation (A and B) and inhibition of CO₂ reduction (C and D) in the native CODHII_{Ch}. (A) Activation of CO oxidation under non-turnover conditions with CO gas phase. Native CODHII_{Ch} in as-isolated CODH_{as-isol.} state (0.1 μg ml⁻¹) was incubated in the presence of 4 mM dithionite + 2 mM DTT + 1 mM Na₂S (●), 4 mM dithionite + 2 mM DTT (△), 2 mM Ti(III) citrate + 1 mM Na₂S (▽), 2 mM Ti(III) citrate (▲), or without reducing agents and sulfide source (▼) at 70°C. 100% of CO oxidation activity corresponds to 11,700 units mg⁻¹. (B) Activation of CO oxidation under turnover conditions in the presence of CO and methyl viologen at 70°C. Na₂S was added to serum-stoppered cuvettes for the assay of CO oxidation activity containing 1.0 ng ml⁻¹ CODHII_{Ch} in reactivated CODH_{react.Ti} state with NiS₃-coordination (●) and in activated CODH_{act.} state with NiS₄-coordination (○). 100% activity corresponds to 10,700 units mg⁻¹. (C) Sulfide-dependent inhibition of CO₂ reduction in hemoglobin-based assay. The decrease in absorbance at 433 nm due to formation of carboxyhemoglobin is plotted vs. time. Assays contained 0.1 μg ml⁻¹ of μ₂S-depleted CODHII_{Ch} in CODH_{react.Ti} state and the following Na₂S concentrations: 0 (trace a), 100 (trace b), 250 (trace c), 500 (trace d), 700 (trace e), and 1,000 μM (trace f). (D) CO₂ reduction activity from (C) is plotted vs. concentration of Na₂S. 100 % of activity corresponds to 36.6 units mg⁻¹.

Figure S5

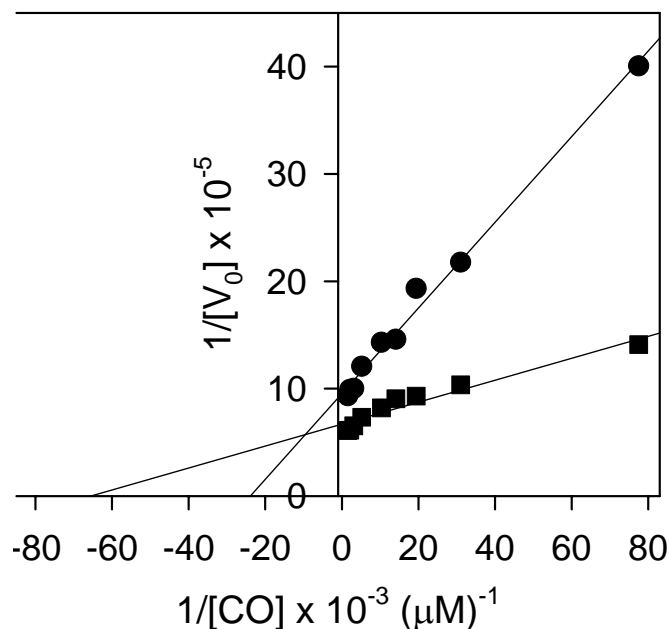


Figure S5. Comparison of catalytic efficiency on CO oxidation between NiS₄ (■) and NiS₃-form (●) of CODHII_{Ch}. NiS₄-form of CODHII_{Ch} was prepared by activation at 70 °C in the presence of 4 mM dithionite and 2 mM DTT with 1 mM Na₂S. To generate NiS₃-form of CODHII_{Ch}, reversibly inhibited enzyme by cyanide was treated with Ti(III) citrate at 70 °C in the absence of source of sulfide. Reactions were initiated by the addition of 10 μl of stock enzyme solution (0.1 μg ml⁻¹). The different CO concentrations were established by mixing of CO and N₂-saturated reaction mixture. 100% of CO oxidation activity corresponds to 16,400 and 10,700 units mg⁻¹ for NiS₄ and NiS₃-form of CODHII_{Ch}, respectively.

References (supporting material)

1. Svetlitchnyi V, Peschel C, Acker G, Meyer O (2001) *J Bacteriol* 183:5134-5144.
2. Svetlitchnyi V, Dobbek H, Meyer-Klaucke W, Meins T, Thiele B, Römer P, Huber R, Meyer O (2004) *Proc Natl Acad Sci USA* 101:446-451.
3. Bradford MM (1976) *Anal Biochem* 72:248-254
4. Bonam D, Murrell SA, Ludden PW (1984) *J Bacteriol* 159:693-699.
5. Ha S-W, Korbass M, Klepsch M, Meyer-Klaucke W, Meyer O, Svetlitchnyi V (2007) *J Biol Chem* 282:10639-10646.
6. Fogo JK, Popowsky M (1949) *Anal Chem* 21:732-734.
7. Dobbek H, Svetlitchnyi V, Liss J, Meyer O (2004) *J Am Chem Soc* 126:5382-5387.
8. Otwinowsky Z, Minor W (1997) *Methods in Enzymology*, Volume 276: Macromolecular Crystallography, part A, p. 307-326, C.W. Carter, Jr. and R.M. Sweet, Eds., Academic Press (New York).
9. Murshudov GN, Vagin AA, Dodson EJ, (1997) *Acta Cryst. D*53, 240-255.
10. Emsley P, Cowtan K (2004), *Acta Cryst. D*60, 2126-2132.
11. Korbass M, Fulla Marsa D, Meyer-Klaucke W (2006) *Rev Sci Instrum* 77:063105.
12. Binsted N, Strange RW, Hasnain SS (1992) *Biochemistry* 31:12117-12125.
13. Stern EA (1993) *Phys Rev B* 48:9825-9827.
14. Heo J, Staples CR, Halbleib CM, Ludden PW (2000) *Biochemistry* 39:7956-7963.
15. Heo J, Halbleib CM, Ludden PW (2001) *Proc Natl Acad Sci USA* 98:7690-7693.

7 Cyanide-induced decomposition of the active site [Ni-4Fe-5S] cluster of CO dehydrogenase from *Carboxydotherrnus hydrogenoformans* and its functional reconstitution

Seung-Wook Ha, Ortwin Meyer, and Vitali Svetlitchnyi[§]

Lehrstuhl für Mikrobiologie, Universität Bayreuth, Universitätsstrasse 30, D-95440 Bayreuth, Germany

[§] Corresponding author

Tel.: 49-921-552790, Fax: 49-921-552727

E-mail: vitali.svetlitchnyi@googlemail.com

Present address: Centre “Bioengineering”, The Russian Academy of Sciences, Prosp. 60 let Oktiabria, bld. 7-1, Moscow, 117312 Russian Federation

Manuscript for the submission to the Journal of Biological Chemistry

ABSTRACT

Native NiFe CO dehydrogenase II (CODHII_{Ch}) isolated from CO-grown hydrogenogenic bacterium *Carboxydotherrnus hydrogenoformans* catalyzes the oxidation of CO at the Ni-(μ_2 S)-Fe1 subsite of the [Ni-4Fe-5S] active site cluster C. The Ni ion is coordinated by four sulfur atoms including one labile μ_2 S that bridges Ni and Fe1, two μ_3 S, and a cysteine sulfur. Potassium cyanide inhibits both reduced and oxidized CODHII_{Ch}. The mechanism of inhibition depends of the redox state of the enzyme. In highly reduced state in the presence of strong reductants dithionite or Ti(III) citrate (~ -500 mV), cyanide mimics the substrate CO. It displaces μ_2 S as sulfide and forms a Ni-cyanide in equatorial plane which occupies the binding position of CO. Thiocyanate is not formed, indicating the absence of cyanolyzable sulfane (S⁰) sulfur in reduced CODHII_{Ch}. In oxidized state in the absence of strong reductants, cyanide does not behave as the substrate CO. Inhibition of oxidized CODHII_{Ch} is accompanied by the formation of thiocyanate (SCN⁻) indicating the presence and release of cyanolyzable sulfane sulfur. We conclude that μ_2 S in Ni-(μ_2 S)-Fe1 subsite of cluster C is cyanolyzable, since (i) ~ 2 moles of cyanolyzable sulfur per mole of homodimeric CODHII_{Ch} are liberated as thiocyanate, which correlates with 2 moles of μ_2 S in clusters C and C', (ii) other inorganic sulfur atoms in CODHII_{Ch} are non-cyanolyzable μ_3 S, (iii) the chemically identical μ_2 S in Mo-(μ_2 S)-Cu subsite of [CuSMoO₂] active site from *Oligotropha carboxidovorans* CO dehydrogenase is cyanolyzable in oxidized enzyme. Cyanide-inhibited oxidized CODHII_{Ch} can be completely reactivated only in the presence of sulfide, which suggests the reformation of the Ni-(μ_2 S)-Fe1 bridge and supports our recent data on the involvement of μ_2 S in the catalytic cycle and stabilization of cluster C in the native enzyme. Prolonged incubation of oxidized CODHII_{Ch} with cyanide decreases the maximum level of reactivation and promotes irreversible decomposition of cluster C, which is obvious from the release of nickel and iron.

INTRODUCTION

Carbon monoxide (CO) dehydrogenases (CODHs) play an important role in several microorganisms for utilization of CO as a central metabolic feature. Although the enzymes can be classified in two categories according to their metal compositions (NiFe- and MoCu-CODHs), they intrinsically catalyze the oxidation of CO in the reaction: $\text{CO} + \text{H}_2\text{O} \rightarrow \text{CO}_2 + 2\text{H}^+ + 2\text{e}^-$ (Ragsdale 2004). In the CO-dependent hydrogenogenic anaerobic bacterium *Carboxydotherrnus hydrogenoformans*, the reaction is mainly catalyzed by two homologous NiFe CO dehydrogenases, CODHI_{Ch} and CODHII_{Ch} (Svetlitchnyi et al. 2001). The homodimeric CODHII_{Ch} contains two active site clusters C and C' and three electron-transferring cubane-type [4Fe-4S] clusters B, B', and D. Crystal structure of the native CODHII_{Ch} in highly active state revealed a functional active center as the [Ni-4Fe-5S] clusters C and C' (Dobbek et al. 2001, 2004; Ha et al. manuscript in preparation). The integral Ni ion in cluster C of CODHII_{Ch} is coordinated by four sulfur ligands: one inorganic $\mu_2\text{S}$, two inorganic $\mu_3\text{S}$, and one thiolate sulfur from cysteine residue. The $\mu_2\text{S}$ bridges the Ni and Fe1 ions of the cluster forming a Ni-($\mu_2\text{S}$)-Fe1 subsite. The coordination of the Ni ion by four sulfur ligands has been substantiated by X-ray absorption spectroscopy (XAS) on CODHII_{Ch} (Gu et al. 2004, Ha et al. 2007).

To identify the binding position of the substrate CO in cluster C of CODHII_{Ch} we have employed potassium cyanide which is an analogue of CO under highly reducing conditions (Ha et al. 2007). Cyanide inhibits CO oxidation activity of CODHII_{Ch} under reducing conditions in the presence of low potential reductants dithionite or Ti(III) citrate (redox potential ~ -500 mV) as well as under more oxidized conditions with a weak reductant dithiothreitol (~ -330 mV) or in the absence of reductants. Micromolar and millimolar concentrations of cyanide are required for inhibition of reduced and oxidized CODHII_{Ch}, respectively, suggesting different mode of cyanide action.

Under reducing conditions, which are required for the interaction of the substrate CO with the active site, the inhibition by cyanide is competitive with respect to CO and is prevented in the presence of CO indicating that cyanide and the substrate CO interact with cluster C in a similar fashion (Ha et al. 2007). Inhibition of reduced

CODHII_{Ch} is fully reversible because initial activity can be restored upon removal of bound-cyanide. Complete reactivation in the presence of Ti(III) citrate and external sulfide (Ha et al. in preparation) alone indicates that cyanide does not decompose the active site chemically. A formation of nickel-cyanide complex in the equatorial plane was identified by X-ray absorption spectroscopy and crystallography in reduced CODHII_{Ch} upon inhibition by cyanide (Ha et al. 2007; Ha et al. in preparation). Thereby one of the four square-planar sulfur ligands of Ni, identified by crystallography as the labile $\mu_2\text{S}$, is replaced. Based on reformation of the Ni-($\mu_2\text{S}$)-Fe1 subsite after reactivation in the presence of dithionite, it has been presumed that the bridging sulfur remains bound to Fe1 as S^{2-} , which functions as a catalytic base in deprotonation of Ni-bound carboxylic group (Ha et al. 2007).

Under oxidizing conditions, inhibition of CODHII_{Ch} by cyanide is not prevented in the presence of CO indicating that cyanide does not behave similar to the substrate CO (Ha et al. 2007). CODH_{Oc} from aerobic bacterium *Oligotropha carboxidovorans* contains in the [Cu-S-MoO₂] active site a Mo-($\mu_2\text{S}$)-Cu subsite at which CO is oxidized. Copper and molybdenum are bridged by a cyanolyzable sulfane $\mu_2\text{S}^0$ which reacts with cyanide yielding thiocyanate (SCN^-) (Gnida et al. 2003, Meyer et al. 2000). Oxidized CODH_{Oc} is inactivated when $\mu_2\text{S}$ is removed by cyanide and can be reactivated upon reinsertion of $\mu_2\text{S}$ (Resch et al. 2005). The bimetallic Ni-($\mu_2\text{S}$)-Fe1 subsite in CODHII_{Ch} resembles the Mo-($\mu_2\text{S}$)-Cu subsite in CODH_{Oc} suggesting that cyanide can remove the bridging $\mu_2\text{S}$ from oxidized cluster C. This would explain the decrease of CO oxidation activity, since the $\mu_2\text{S}$ ligand is involved in stabilization of cluster C and catalysis in the native CODHII_{Ch} (Dobbek et al. 2004; Ha et al. in preparation).

Here we have studied the reactivity of oxidized CODHII_{Ch} with potassium cyanide and provide a strong evidence for the presence of cyanolyzable sulfane sulfur in oxidized CODHII_{Ch} as well as for its participation in the catalysis. We show that under oxidizing conditions decrease of CO oxidation activity is caused by removal of cyanolyzable sulfur. The fully functional state of the enzyme can be recovered in the presence of sulfide, suggesting the reinsertion of the cyanolyzable sulfur into the active site. The data on the reactivity of oxidized and reduced cluster C with cyanide strongly indicate that the $\mu_2\text{S}$ in the Ni-($\mu_2\text{S}$)-Fe1 bridge is cyanolyzable.

EXPERIMENTAL PROCEDURES

Preparation and assay of CODHII_{Ch}

Native CODHII_{Ch} was obtained from *C. hydrogenoformans* Z-2901 (DSM 6008) grown lithoautotrophically in 50-liter fermentors (Biostat U; Braun Biotech, Melsungen, Germany) with CO as the energy and carbon source according to the procedure described before (Svetlitchnyi et al. 2001). Due to the oxygen sensitivity of CODHII_{Ch}, all experiments were carried out under strictly anoxic conditions (Svetlitchnyi et al. 2001). All buffers used for purification of CODHII_{Ch} were prepared by repeated evacuation and flushing with N₂ and supplemented with 3 mM sodium dithionite. N₂ (99.999%) and CO (99.9%) were purchased from Riessner-Gase (Lichtenfels, Germany) and subjected to additional purification by passage over a heated copper catalyst. The purified CODHII_{Ch} (15 mg ml⁻¹) was frozen in liquid N₂ and kept at -80°C under N₂. Protein estimation employed conventional methods with bovine serum albumin (BSA) as a standard (Bradford 1971). For CO oxidation assays, 1-ml volume of CO-saturated reaction mixture composed of anoxic 50 mM HEPES/NaOH, pH 8.0 (buffer A) with 20 mM methyl viologen as electron acceptor was introduced into screw-capped cuvette sealed with a rubber septum under CO, the reaction mixture was slightly prereduced with Ti(III) citrate, and reaction was initiated by adding 10 µl of diluted enzyme solution (approx. 0.1 µg ml⁻¹). The assays were performed at 70 °C. One unit of CO oxidation activity is defined as 1 µmol of CO oxidized min⁻¹.

The purified as isolated CODHII_{Ch} displayed CO oxidation activity of 10,400 units mg⁻¹ of protein at 70°C. Because the position of the bridging µ₂S in cluster C of as isolated CODHII_{Ch} is usually not completely occupied (Ha et. al. manuscript in preparation), the enzyme was exposed to activation in the presence of 2 mM sodium dithionite and 2 mM sodium sulfide at 70°C according to described procedure (Ha et. al. manuscript in preparation). Such activation of as isolated enzyme results in significant increase of activity and complete occupancy of the µ₂S position. Activated CODHII_{Ch} displayed CO oxidation activity of 14,200 units mg⁻¹ and was employed for further experiments.

Inhibition of oxidized and reduced CODHII_{Ch} by potassium cyanide and reactivation

To establish oxidizing conditions, activated CODHII_{Ch} samples were subjected to gel filtration on Sephadex G-25 in reductant-free anoxic buffer A under N₂ to remove dithionite and sulfide, and the enzyme fractions were collected in N₂-flushed tubes fitted with butyl rubber stoppers. Subsequently, the desalted enzyme solution was diluted with anoxic reductant-free buffer A to 2.2 mg ml⁻¹. The oxidized state of enzyme was verified by visible spectroscopy. Since chemical formation of thiocyanate was detected in reaction mixtures containing dithionite and cyanide, Ti(III) citrate instead of dithionite was used as a reductant in this study. To reduce the oxidized enzyme, Ti(III) citrate (83 mM stock solution (Seefeldt and Ensign 1994)) was added to the enzyme preparations to a final concentration of 4 mM. To initiate the inhibition of CODHII_{Ch}, a stock solution of cyanide (0.5 M) prepared in 10 mM anoxic NaOH under N₂, was added to 6 ml of enzyme solutions to the final cyanide concentrations of 5 mM and 1 mM for oxidized and reduced enzyme, respectively.

The incubation of CODHII_{Ch} with cyanide was performed closed tubes in anaerobic glove box filled with oxygen-free N₂ at 25 °C with gentle stirring at 100 rpm. For assay, 10 µl aliquots were taken during the incubation and CO oxidation activity was assayed at 70 °C.

For reactivation, cyanide-treated enzyme preparations were first diluted 202-fold in buffer A in the presence of 1 mM dithiothreitol (DTT). Such dilution prevents fast and reversible inhibition of CODHII_{Ch} by cyanide after addition of reductant (Ha et al. 2007). For the reactivation, 10 µl of the diluted samples were injected into 1 ml of buffer A with 4 mM Ti(III) citrate or 4 mM Ti(III) citrate plus 2 mM sodium sulfide under N₂ gas phase followed by incubation at 70°C. Aliquots were taken with time and assayed for CO oxidation activity during the reactivation.

Determination of thiocyanate

Cyanolyzable sulfane sulfur in CODHII_{Ch} was analyzed after treatment of oxidized or reduced enzyme with cyanide. Formation of thiocyanate in protein-free ultrafiltrates was colorimetrically quantified as Fe(SCN)₃ at 460 nm (Westley 1981).. The protein-free samples (500 µl sample volume for each measurement) were obtained

by ultrafiltration using centrifugal membrane filters (Vivaspin 500 concentrator 30 KDa cutoff, Vivasciences, Stonehouse, Great Britain).

UV-visible absorption spectroscopy and metal analysis

Approximate number of 4Fe clusters in CODHII_{Ch} was estimated employing the following extinction coefficients (ϵ_{419} , per millimolar per centimeter) which were previously reported for the enzyme carrying five 4Fe clusters: $\epsilon_{419} = 83.8$ (oxidized state of CODHII_{Ch}) and $\epsilon_{419} = 42.8$ (reduced state of CODHII_{Ch}) (Svetlitchnyi et al. 2001). For visible absorption spectroscopy, 130 μ l samples of the enzyme solution (2.2 mg protein ml⁻¹) were taken before addition of cyanide and after 24 h incubation in the presence of 5 mM or 50 mM cyanide and mixed with 1 ml of anoxic buffer A under N₂ in gas tight cuvettes. Oxidized CODHII_{Ch} was reduced with 4 mM dithionite under N₂ at 23°C or with CO at 50 °C (5 min incubation).

The amounts of Ni and Fe released from the oxidized and reduced CODHII_{Ch} after incubation with cyanide were estimated in protein-free ultrafiltrates employing inductively coupled plasma mass spectrometry (model VG Plasmaquad PQ2 turbo plus; Fisons Instruments/VG elemental, Wiesbaden, Germany).

RESULTS

Inhibition of native oxidized CODHII_{Ch} by potassium cyanide

Potassium cyanide inhibits CO oxidation activity of reduced as well as oxidized CODHII_{Ch} under non-turnover conditions in the absence of CO and electron acceptor methyl viologen (Ha et al. 2007). Inhibition in reduced state is reversible and is prevented by CO whereas in the oxidized state much higher concentrations of cyanide are required for the same level of inhibition and CO does not have a protective function (Ha et al. 2007).

To explain the observed differences in inhibition patterns, we have compared the effect of the enzyme's redox state on the inhibition by cyanide and on the formation of thiocyanate under non-turnover conditions. The inhibitory effect of cyanide on CODHII_{Ch} applied in a concentration of 2.2 mg ml⁻¹ (17.1 μ M) strongly

depends on the redox state of the enzyme (Fig. 1). Oxidized CODHII_{Ch} is slowly inhibited by 5 mM cyanide (half-life 13 h, complete inhibition after 46.5 h) (Fig. 1A). On the other hand, reduced enzyme in the presence of 4 mM Ti(III) citrate undergoes fast inhibition already by 1 mM cyanide (half-life 2 h) (Fig. 1B).

Oxidized CODHII_{Ch} contains cyanolyzable sulfur

To make the analysis of cyanolyzable sulfur and the measurement of thiocyanate formed possible, high concentration of oxidized CODHII_{Ch} was applied (2.2 mg ml⁻¹, 17 μM). At this protein concentration, 5 mM cyanide was employed to ensure the inhibition in a time frame of 2 days (Fig. 1A). At higher cyanide concentrations (10 to 50 mM) the activity was inhibited faster, but irreversible inactivation and fast decomposition of metal clusters occurred (data not shown). Decrease of CO oxidation activity during the incubation of oxidized CODHII_{Ch} with cyanide paralleled with the formation of thiocyanate (Fig. 1A). This indicates that oxidized CODHII_{Ch} contains cyanolyzable sulfane sulfur in the oxidation state 0 (S⁰) which can react with cyanide yielding thiocyanate (Meyer et al. 2000; Iciek and Wlodek 2001; Resch et al. 2005; Wood 1987).

After 9 h of incubation the activity decreases to 55% of the initial level and approximately 1.4 mol of thiocyanate per mol of homodimeric enzyme is formed (Fig. 1A). In this period thiocyanate was formed with the highest rate (3 μM SCN⁻ h⁻¹) and no nickel or iron were released from the protein (Table 1) indicating that besides the liberation of sulfane sulfur, the metal clusters of CODHII_{Ch} remained intact. During further incubation the rate of thiocyanate formation decreases. Complete inhibition after 46.5 h coincides with the formation of 38 μM thiocyanate which corresponds to approx. 2 mol of thiocyanate per mol of CODHII_{Ch}. This indicates the presence of 1 mol of readily releasable cyanolyzable sulfur per active site cluster C and is in agreement with the presence of one μ₂S per [Ni-4Fe-5S] cluster. The sulfane sulfur in CODHII_{Ch} which reacts with cyanide is apparently the bridging μ₂S in the Ni-(μ₂S)-Fe1 subsite. It is in the oxidation state 2- in reduced enzyme (Ha et al. 2007) and appears to be in the oxidation state 0 in oxidized enzyme.

In addition, nickel and iron are gradually released from the enzyme after 18 h of

incubation (Table 1) reflecting cyanide-induced decomposition of metal clusters. The inhibition of oxidized CODHII_{Ch} is definitely caused by the effect of cyanide and not by oxidative damage since the activity does not decrease when the enzyme is incubated in the absence of cyanide (not shown).

Cyanide-induced decomposition of metal clusters in oxidized CODHII_{Ch}

Cyanide induces decomposition of metal clusters in oxidized CODHII_{Ch}. The decomposition correlates with deprivation of activity and starts with the release of the labile cyanolyzable sulfur (Fig. 1A), which is followed by the release of nickel and iron (Table 1).

The visible spectra of CODHII_{Ch} (Svetlitchnyi et al. 2001) before (Fig. 2A, sample 0 h from Fig. 1A, 14,200 units mg⁻¹) and after 24 h (Fig. 2B, sample 24 h from Fig. 1A, 4,540 units mg⁻¹) incubation with cyanide substantiate that the metal clusters in oxidized enzyme remain relatively intact during the first 24 h of incubation with 5 mM cyanide. Both samples in oxidized state exhibit identical FeS-like shoulder centered around 419 nm (Fig. 2A and B, traces a). The extinction coefficients of oxidized CODHII_{Ch} at 419 nm were 84.5 and 79.9 mM⁻¹cm⁻¹ for the enzyme before and after 24 h incubation with 5 mM cyanide, respectively. Assuming the extinction coefficient of about 4 per mM per Fe in a 4Fe cluster, the calculated approximate number of 4Fe clusters is 5.28 and 4.99, respectively (Svetlitchnyi et al. 2001). These values correspond to the presence of five 4Fe clusters in both samples. After 24 h with 5 mM cyanide, the enzyme lost 27.2 % of Ni and 2.2% of Fe (Table 1) indicating significant decomposition of the Ni-site in cluster C. However, reduction with CO and with dithionite cause identical bleaching of the shoulder in both samples supporting the presence of five 4Fe clusters (Fig. 2A and B, traces b and c). The complete reduction of all clusters by CO indicates that electrons produced by functional population of the enzyme can reduce the metal clusters in catalytically non-functional and/or inhibited enzyme fraction.

After 24 h incubation with 50 mM cyanide CODHII_{Ch} does not show any CO oxidation activity and the metal clusters appear to be significantly decomposed (Fig. 2C). The shoulder at 419 nm in oxidized enzyme is lowered (Fig. 2C, trace a) and

displays an extinction coefficient of $55.3 \text{ mM}^{-1}\text{cm}^{-1}$ corresponding to an approximate number of 4Fe clusters of 3.5. Treatment with dithionite results in a very weak bleaching of the shoulder which is consistent with a considerable decomposition of FeS clusters (Fig. 2C, trace c). The shoulder at 419 nm is not bleached upon incubation with CO (Fig. 2C, trace b) indicating non-functional state of cluster C.

Reactivation of oxidized CODHII_{Ch} treated with cyanide

The oxidized CODHII_{Ch} inhibited by 5 mM cyanide (samples from Fig. 1A) could be reactivated under low redox-potential conditions in the presence of sodium sulfide (Fig. 3A). However, the maximum level of reactivation depends on the integrity of metal clusters which correlates with the incubation time with cyanide (Fig. 2 and Table 1). The enzyme sample after 9 h of incubation, which lost 45% of the activity and 1.4 mol of cyanolyzable sulfur per mol of protein (Fig. 1A) and did not lost Ni or Fe (Table 1), can be completely reactivated under N₂ in the presence of sodium sulfide plus Ti(III) citrate (Fig. 3A). The level of reactivation with Ti(III) citrate alone is 35% lower than the reactivation with sulfide (Fig. 3A). These data provide a strong evidence that reincorporation of the cyanolyzable sulfur is required for complete reactivation. Prolonged incubation time gradually decreases the level of maximum reactivation indicating irreversible decomposition of cluster C which was obvious from the release of nickel and iron (Table 1). However, in these samples (24 h and 46.5 h) the level of reactivation in the presence of sulfide was significantly higher as well (Fig. 3A).

Reduced CODHII_{Ch} does not contain cyanolyzable sulfur

Complete inhibition of CO oxidation activity during the incubation of reduced CODHII_{Ch} (2.2 mg ml^{-1}) with 1 mM potassium cyanide is not followed by the formation of thiocyanate (Fig. 1B) indicating the absence of cyanolyzable sulfur in reduced enzyme. This substantiates the 2- oxidation state of the bridging sulfur in the Ni-(μ_2 S)-Fe1 subsite of reduced cluster C and agrees with the release of μ_2 S as H₂S upon inhibition of reduced CODHII_{Ch} by cyanide (Ha et al. 2007; Ha et al. manuscript

in preparation). Cyanide treatment of reduced CODHII_{Ch} did not destroy the metal clusters since no nickel or iron were released (Table 1) and the enzyme could be completely reactivated in the presence of sulfide and Ti(III) citrate (Fig. 3B). The reactivation levels in the presence of sulfide and Ti(III) citrate were significantly higher compared to the levels in the presence of Ti(III) citrate and the absence of sulfide. This supports our previous data on the involvement of $\mu_2\text{S}$ in catalysis and stabilization of cluster C (Ha et al. manuscript in preparation).

DISCUSSION

Depending on the redox state of CODHII_{Ch}, potassium cyanide has two different modes of interaction with cluster C. Strongly reducing conditions at potentials of ~ -500 mV are required for the interaction of the substrate CO with cluster C during the oxidation of CO (Ha et al. 2007). At such potentials cyanide behaves as a competitive inhibitor with respect to CO and a linear Ni-CN complex in cyanide-inhibited CODHII_{Ch} was identified by X-ray absorption spectroscopy (Ha et al. 2007). Based on the evidence that cyanide mimics CO, the inhibition is caused by the occupation of the CO binding position at Ni ion by cyanide which prevents the binding of the substrate CO (Ha et al. 2007). On the other hand, oxidizing conditions do not support the interaction of the substrate CO with cluster C of CODHII_{Ch} and cyanide does not mimic the substrate.

Treatment of oxidized CODHII_{Ch} with cyanide in millimolar concentrations diminishes CO oxidation activity and the loss of activity coincides with the release of thiocyanate (Fig. 1A). This indicates that the oxidized enzyme contains cyanolyzable sulfane sulfur in the oxidation state 0 (S^0) which can react with cyanide with the formation of thiocyanate (Meyer et al. 2000; Iciek and Wlodek 2001; Resch et al. 2005; Wood 1987) and which is obviously the labile bridging $\mu_2\text{S}$ in the Ni-($\mu_2\text{S}$)-Fe1 subsite of cluster C. The suggestion that the readily cyanolyzable sulfur in *C. hydrogeniformans* CODHII_{Ch} is the bridging $\mu_2\text{S}$ is based on the reactivity patterns of reduced and oxidized enzyme with cyanide (Figs. 1 and 3), lability of the $\mu_2\text{S}$ in [Ni-4Fe-5S] cluster (Dobbek et al. 2004), and cyanolyzability of $\mu_2\text{S}$ in oxidized Mo-

($\mu_2\text{S}$)-Cu subsite of $[\text{CuSMoO}_2]$ active site in CODH from *Oligotropha carboxidovorans* (Meyer et al. 2000; Resch et al. 2005). Moreover, approximately 2 mol of cyanolyzable sulfur per mol of enzyme are liberated, which corresponds to the content of the bridging $\mu_2\text{S}$ in the native CODHII_{Ch} (Fig. 1A). Other inorganic $\mu_3\text{S}$ cannot be cyanolyzable in intact clusters C, B, and D since they are in the oxidation state 2-. Displacement of the bridging sulfur provokes a chemical decomposition of cluster C in oxidized CODHII_{Ch} (Fig. 2 C and Table 1). This is indicated by the decrease of reversibility of inhibition (Fig. 3A) and is apparently caused by better accessibility of Ni and Fe ions for cyanide. Indeed, Ni and Fe are gradually released in the time-course of cyanide-treatment (Table 1).

In contrast to oxidizing conditions, cyanide does not cause chemical decomposition of metal clusters in reduced CODHII_{Ch} since complete inhibition is fully reversible (Fig. 3A) and metals are not liberated (Table 1). However, the bridging $\mu_2\text{S}$ was removed as H_2S from the reduced cluster C during reversible inhibition by cyanide and the generation of $\mu_2\text{S}$ -depleted $[\text{Ni-4Fe-4S}]$ -form of cluster C was confirmed by X-ray absorption spectroscopy after partial reactivation under reducing conditions in the absence of external sulfide (Ha et al. manuscript in preparation). This form of cluster C in native CODHII_{Ch} can be represented by the recombinant CODHII_{Ch} expressed in *Escherichia coli* (Jeoung and Dobbek 2007). As NiFe CODHs from *Moorella thermoacetica* and *Rhodospirillum rubrum* as well as recombinant CODHII_{Ch}, all of which lack the $\mu_2\text{S}$ (Drennan et al. 2001; Doukov et al. 2002; Darnault et al. 2003; Jeoung and Dobbek 2007), the native CODHII_{Ch} lacking $\mu_2\text{S}$ displays CO oxidation activity. However, $[\text{Ni-4Fe-4S}]$ -form has definitely lower CO oxidation activity and efficiency (k_{cat}/K_m) and is less thermostable than $\mu_2\text{S}$ -containing native enzyme (Ha et al. 2007; Ha et al. manuscript in preparation).

Complete reactivation of cyanide-treated oxidized CODHII_{Ch} upon release of sulfane $\mu_2\text{S}$ occurs only in the presence of sulfide and low potential reductants (Fig. 3A). Apparently, the activity is recovered to the highest level by the reincorporation of sulfur in the form of S^{2-} reestablishing the Ni-($\mu_2\text{S}$)-Fe1 bridge. Release of Ni and Fe from the enzyme implies decrement of maximum reversibility. Indeed, oxidized CODHII_{Ch} treated with cyanide for 24 h lost 27% of Ni and could recover only 80% of

initial activity (Table 1 and Fig. 3A).

Low redox potential and external sulfide required for the reactivation of cyanide-treated oxidized CODHII_{Ch} indicate that the reincorporation of sulfur occurs only with highly reduced cluster C and that the bridging $\mu_2\text{S}$ in functional cluster C is in the 2- oxidation state. Positive effect of sulfide on reactivation of inhibited reduced enzyme (Fig. 3B) can be explained by higher CO oxidation activity and stability of the enzyme with [Ni-4Fe-5S]-form of cluster C compared to [Ni-4Fe-4S]-form (Ha et al. manuscript in preparation). The absence of thiocyanate (this work) and liberation of H_2S (Ha et al. manuscript in preparation) from cyanide-treated reduced CODHII_{Ch} indicate that all inorganic sulfur atoms in the reduced enzyme including the bridging $\mu_2\text{S}$ are in the oxidation state 2-. In contrast, in the absence of reductants under oxidizing conditions the $\mu_2\text{S}^{2-}$ is readily oxidized to sulfane $\mu_2\text{S}^0$ which is cyanolyzable.

The scenario describing the effect of cyanide on oxidized CODHII_{Ch} includes two steps. In the first step, cyanide attacks the bridging $\mu_2\text{S}$ in S^0 state and removes it from cluster C as thiocyanate which gradually converts the [Ni-4Fe-5S]-form into the [Ni-4Fe-4S]-form and parallels with the decrease of CO oxidation activity. This step corresponds to the enzyme sample incubated with cyanide for 9 h (Fig. 1A). The activity decreases only partially (45% inhibition at 70% release of $\mu_2\text{S}$ after 9 h in Fig. 1A) because $\mu_2\text{S}$, which presence in the active site stimulates CO oxidation by acceleration of CO_2 displacement, is not obligately required for catalysis (Ha et al. manuscript in preparation; Jeoung and Dobbek 2007). At this step no extensive decomposition of metal cluster occurs since the activity can be completely restored to the initial level by reincorporation of $\mu_2\text{S}$ upon incubation with sulfide (Fig. 3A) and metals are not liberated (Table 1). Partial reactivation in the absence of sulfide can be explained by release of cyanide, bound non-specifically to Ni and Fe.

In the second step, cyanide attacks and removes the Ni and Fe1 ions in cluster C destabilized by the release of $\mu_2\text{S}$. This provides accessibility to other inorganic $\mu_3\text{S}$ of the cluster. Under oxidizing conditions they undergo oxidation to S^0 state, react with cyanide and leave the cluster. At this step cluster C is completely decomposed, as it is

apparent from low reversibility of inhibition in the presence of sulfide (sample 46.5 h in Fig. 3A), from the release of Ni and Fe (Table 1), as well as from UV-visible spectra indicating reduction of the number of the clusters in the enzyme (Fig. 2C). The decomposition of clusters B and D upon prolonged incubation with cyanide cannot be excluded.

ACKNOWLEDGMENTS

We gratefully acknowledge financial support from the Deutsche Forschungsgemeinschaft (grants SV 10/1-1 and SV 10/1-2). This research has employed equipment financed by the Freistaat Bayern and the Fonds der Chemischen Industrie.

REFERENCES

1. Ragsdale, S. W. (2004) *Crit. Rev. Biochem. Mol. Biol.* **39**, 165-195
2. Svetlitchnyi, V., Peschel, C., Acker, G., and Meyer, O. (2001) *J. Bacteriol.* **183**, 5134-5144
3. Dobbek H, Svetlitchnyi V, Gremer L, Huber R, Meyer O (2001) *Science* 293:1281-1285
4. Dobbek, H., Svetlitchnyi, V., Liss, J., Meyer, O. (2004) *J. Am. Chem. Soc.* **126**, 5382-5387.
5. Ha, S.-W., Bourenkov, G., Meyer-Klaucke, W., Meyer, O., and Svetlitchnyi, V. (Manuscript in preparation)
6. Gu, W., Seravalli, J., Ragsdale, S. W., and Cramer, S. P. (2004) *Biochemistry* **43**, 9029-9035

7. Ha, S.-W., Korbas, M., Klepsch, M., Meyer-Klaucke, W., Meyer, O., and Svetlitchnyi, V. (2007) *J. Biol. Chem.* **282**, 10639-10646
8. Gnida, M., Ferner, R., Gremer, L., Meyer, O., and Meyer-Klaucke, W. (2003) *Biochemistry* **42**, 222-230
9. Meyer, O., Gremer, L., Ferner, R., Ferner, M., Dobbek, H., Gnida, M., Meyer-Klaucke, W., and Huber, R. (2000) *Biol. Chem.* **381**, 865-876
10. Resch, M., Dobbek, H., and Meyer, O. (2005) *J. Biol. Inorg. Chem.* **10**, 518-528.
11. Bradford, M. M. (1976) *Anal. Biochem.* **72**, 248-254
12. Seefeld, L. C. and Ensign, S. A. (1994) *Analy. Biochem.* **221**, 379-386
13. Westley, J. (1981) *Methods Enzymol.* **77**, 285-291
14. Iciek, M. and Wlodek, L. (2001) *Pol. J. Pharmacol.* **53**, 215-225
15. Wood, J. (1987) *Method. Enzymol.* **143**, 25-29
16. Jeoung, J. and Dobbek, H. (2007) *Science* **318**, 1461-1464
17. Drennan, C. L., Heo, J., Sintchak, M. D., Schreiter, E., and Ludden, P. W. (2001) *Proc. Natl. Acad. Sci. USA* **98**, 11973-11978
18. Doukov, T. I., Iverson, T. M., Seravalli, J., Ragsdale, S. W., Drennan, C. L. (2002) *Science* **298**, 567-672
19. Darnault, C., Volbeda, A., Kim, E. J., Legrand, P., Vernede, X., Lindahl, P. A., and Fontecilla-Camps, J. C. (2003) *Nat. Struct. Biol.* **10**, 271-279

Figure legends

Fig. 1. Inhibition of CO oxidation activity and formation of thiocyanate during incubation of oxidized (A) and reduced (B) CODHII_{Ch} with potassium cyanide. Oxidized enzyme (2.2 mg ml⁻¹, 17 μM) in reductant-free anoxic 50 mM HEPES/NaOH (pH 8.0) under N₂ with 5 mM cyanide and reduced enzyme (2.2 mg ml⁻¹, 17 μM) in anoxic 50 mM HEPES/NaOH (pH 8.0) under N₂ with 4 mM Ti(III) citrate and 1 mM cyanide were incubated at 23 °C. Aliquots were removed with time and assayed for CO oxidation activity at 70 °C (closed symbols) and formation of thiocyanate (open symbols). 100 % of activity corresponds to 14,200 units mg⁻¹.

Fig. 2. UV-visible absorption spectra of oxidized CODHII_{Ch} before incubation with cyanide (A) and after 24 h incubation with 5 mM (B) or 50 mM (C) cyanide. (A) Sample 0 h from Fig. 1 A with 14,200 units mg⁻¹. (B) Sample 24 h from Fig. 1 A with 4,540 units mg⁻¹. (C) Sample with no activity. The enzyme samples (0.25 mg ml⁻¹) were in 50 mM HEPES/NaOH (pH 8.0). Conditions for each curve: a, under N₂; b, reduced with CO; c, reduced with 4 mM dithionite under N₂. Insets: difference spectra of condition a minus condition b (solid line) and condition a minus condition c (dashed line).

Fig. 3. Sulfide-dependent reactivation of cyanide-inhibited oxidized (A) and reduced (B) CODHII_{Ch}. Samples of oxidized CODHII_{Ch} incubated with 5 mM cyanide were taken in the experiment described in Fig. 1A. Samples of reduced CODHII_{Ch} incubated with 1 mM cyanide were taken in the experiment described in Fig. 1B. The incubation time with cyanide was 9 h (circles), 24 h (squares), and 46.5 h (triangles). For reactivation, the samples were incubated at 70 °C under N₂ gas phase in the presence of 4 mM Ti(III) citrate plus 2 mM sodium sulfide (closed symbols) and in the presence of Ti(III) citrate without sulfide (open symbols). Aliquots were removed with time and assayed at 70 °C. 100 % of activity corresponds to 14,200 units mg⁻¹.

Tables

Table 1. Analysis of metals released from oxidized CODHII_{Ch} during cyanide treatment^a.

Time (h)	Incubation without KCN		Incubation with 5 mM KCN	
	mol of Ni per mol of CODHII _{Ch} (% ^b)	mol of Fe per mol of CODHII _{Ch} (% ^b)	mol of Ni per mol of CODHII _{Ch} (% ^b)	mol of Fe per mol of CODHII _{Ch} (% ^b)
0.5	ND ^c (0)	ND (0)	ND (0)	ND (0)
9	ND (0)	ND (0)	ND (0)	ND (0)
18	ND (0)	ND (0)	0.315 (15.8)	0.408 (2.0)
24	ND (0)	ND (0)	0.544 (27.2)	0.544 (2.2)

^a Released metals from CODHII_{Ch} were analyzed by ICP-MS as described in Materials and Methods.

^b Percentage of released nickel and iron under the indicated incubation conditions relative to the total amount of metal per CODHII_{Ch} dimer. 100 % correspond to 2 Ni- and 20 Fe/dimer of CODHII_{Ch}.

^c ND - amount of metals in the samples were under the detection level of ICP-MS.

Fig. 1

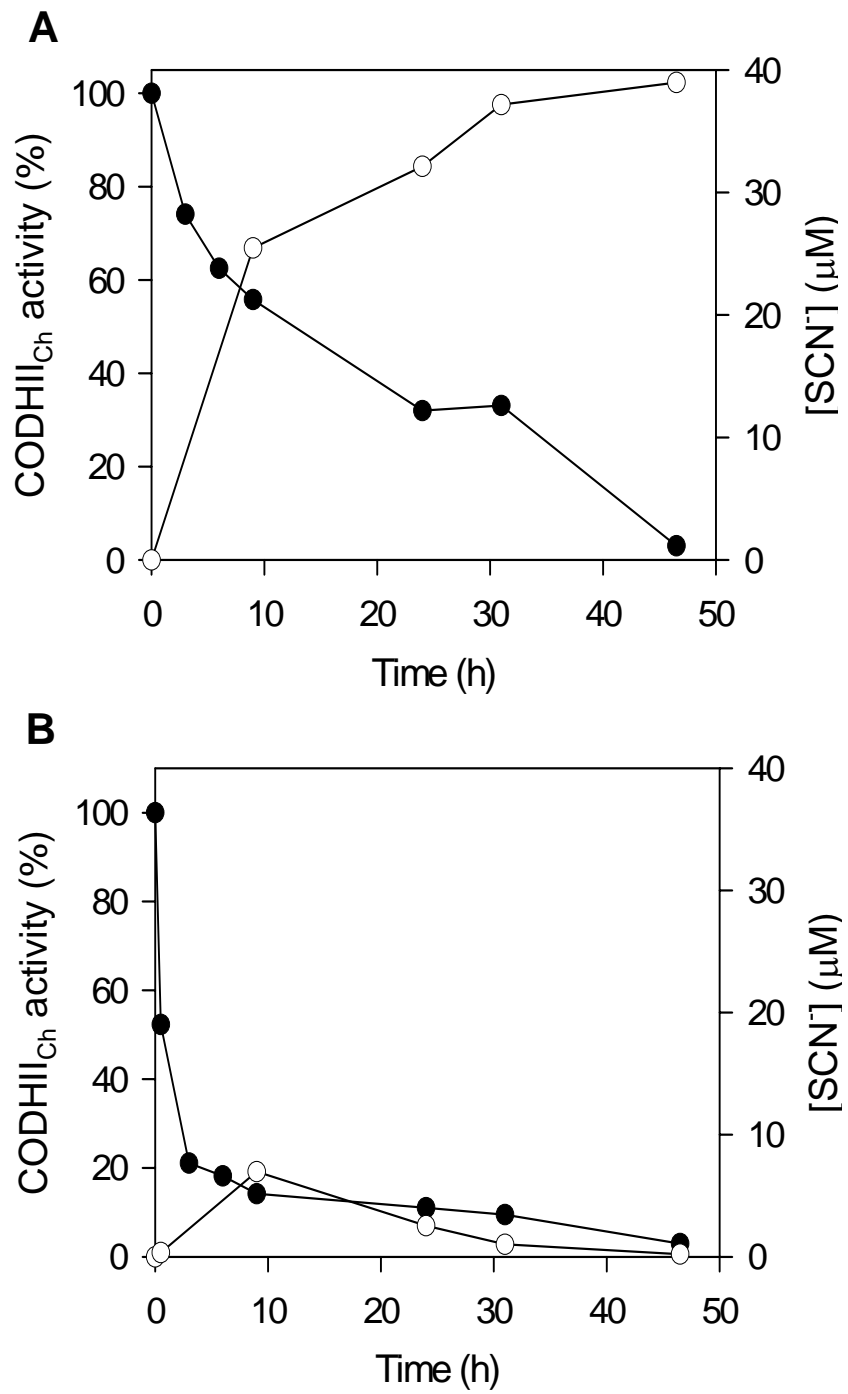


Fig. 2

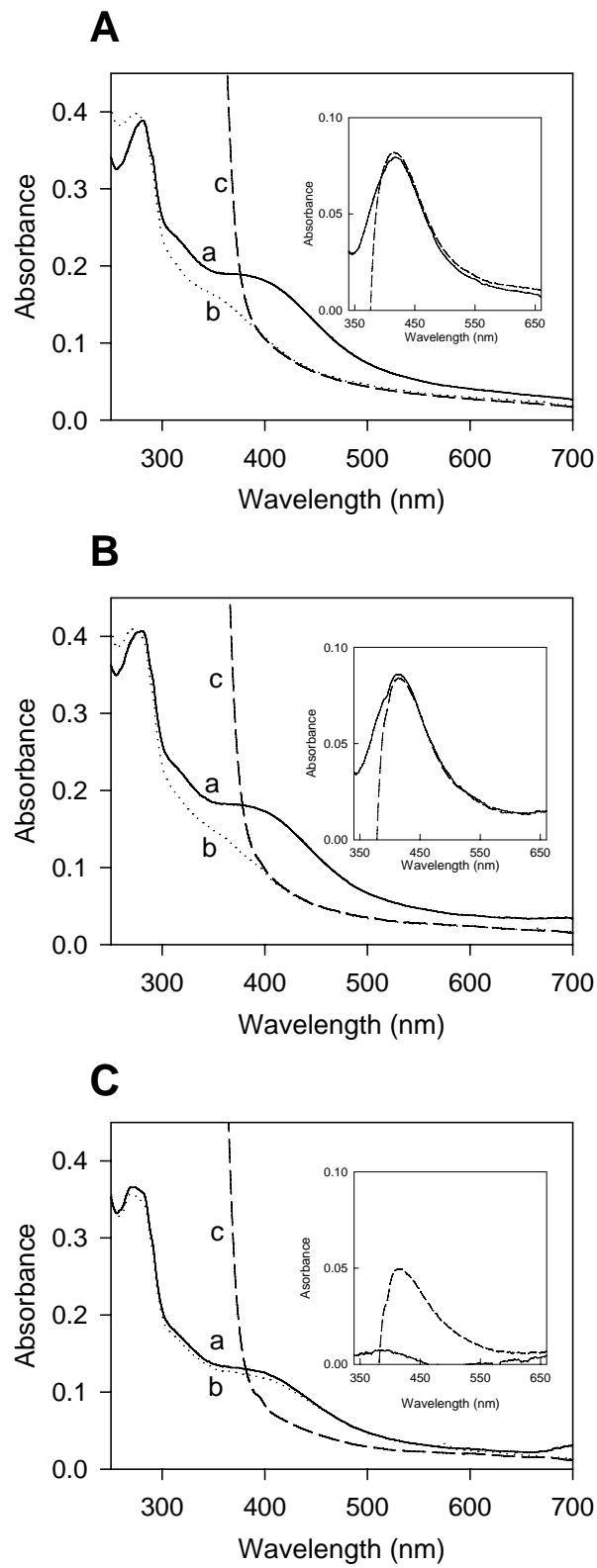
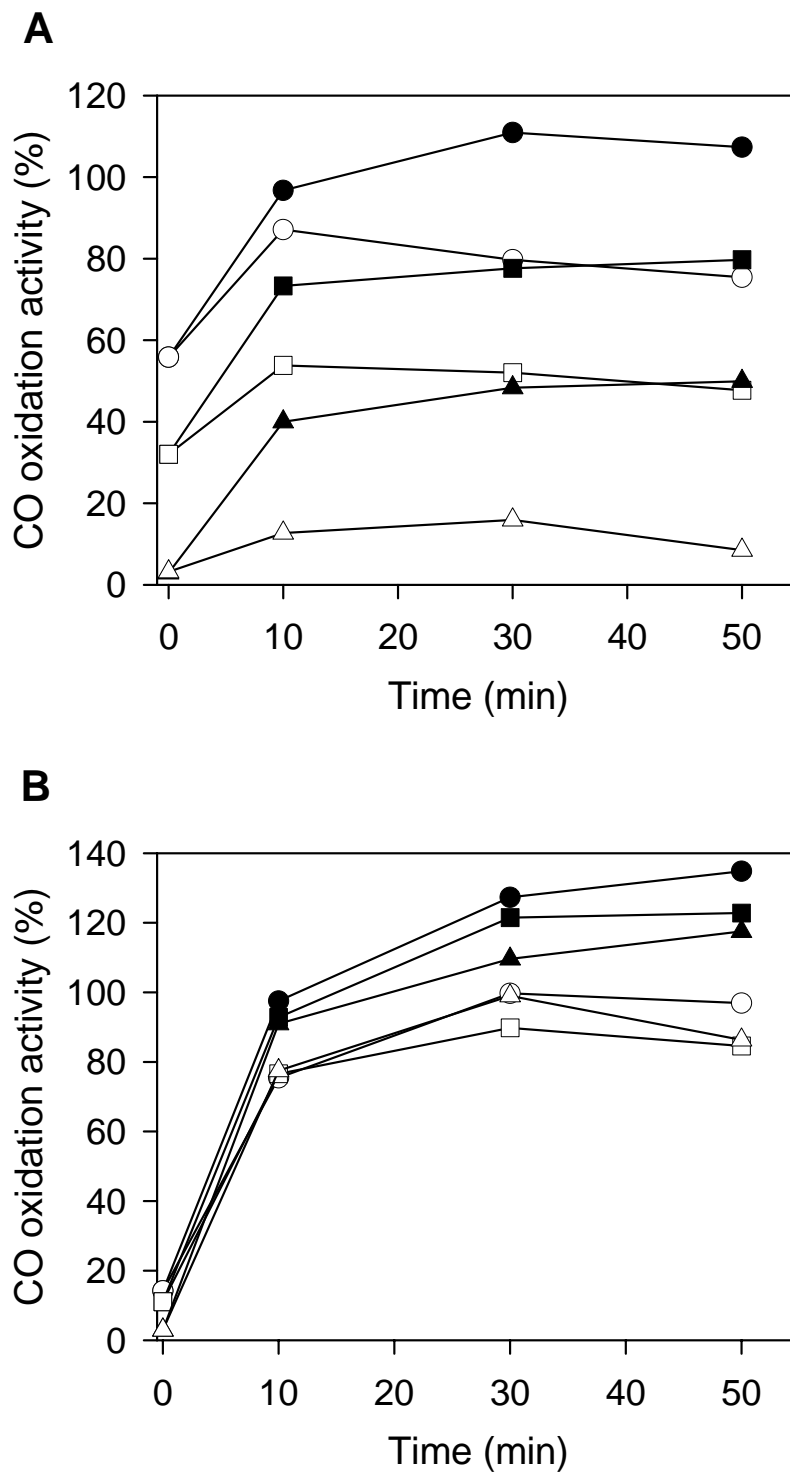


Fig. 3



8 Erklärung

Hiermit erkläre ich, dass ich die Arbeit selbständig verfasst und keine anderen als die von mir angegebenen Quellen und Hilfsmittel benutzt habe.

Ferner erkläre ich, dass ich anderweitig mit oder ohne Erfolg nicht versucht habe, diese Dissertation einzureichen. Ich habe keine gleichartige Doktorprüfung an einer anderen Hochschule endgültig nicht bestanden.

Bayreuth, den 28. Oktober 2008

(Seung-Wook Ha)